LARGE-SCALE OPTIMIZATION FOR GREEN LOGISTICS AND STOCHASTIC RESOURCE ALLOCATION FOR FOOD SECURITY

A Dissertation

Presented to the Faculty of the Graduate School

of Cornell University

in Partial Fulfillment of the Requirements for the Degree of

Doctor of Philosophy

by

Faisal M. M. Alkhannan Alkaabneh

May 2020

LARGE-SCALE OPTIMIZATION FOR GREEN LOGISTICS AND STOCHASTIC RESOURCE ALLOCATION FOR FOOD SECURITY

Faisal M. M. Alkhannan Alkaabneh, Ph.D.

Cornell University 2020

We studied several important management and policy analysis problems in food supply chain systems utilizing large-scale optimization, stochastic resource allocation, and data-analytics methodologies. We focused on three main research questions: 1) How can retailers build green, efficient last-mile logistics system when the objective is to maximize their profit and minimize the costs due to fuel consumption, inventory holding, and greenhouse gas emissions (Chapter 2); 2) what is the best environmental intervention policy to reduce the environmental externalities associated with the production of fruits and vegetables considering environmental and economic dimensions simultaneously (Chapter 3); and (3) How can food banks better manage food supplies distribution to combat food insecurity of underserved population (Chapters 4 & 5). Specifically, we have explored the following four dimensions in food supply chains 1) Benders decomposition for the inventory vehicle routing problem with perishable products and environmental costs. We consider the problem of inventory routing in the context of perishable products and find near-optimal replenishment scheduling and vehicle routes. To solve the problem efficiently, we develop an exact method based on Benders decomposition to find high-quality solutions in reasonable time and a two-stage meta-heuristic. 2) A systems approach to carbon policy for fruit supply chains: carbon tax, technology innovation, or land sparing? Reducing carbon emissions of food supply chains has

increasingly received attention from businesses and policymakers. In order to propose sound policies aimed at lowering such emissions, policy makers favor tools that are informative in the economic and environmental dimensions simultaneously. In this study we offer a systems-based approach which is intended to do just that by developing a spatially and temporally disaggregated price equilibrium mathematical model for a food production and distribution system and applying it to the U.S. apple supply chain. We find that R&D which leads to storage technologies with lower carbon emission rates has the greatest potential for emission reduction. 3) Unified framework for efficient, effective, and fair resource allocation by food banks based on Approximate Dynamic Programming. The evidence linking food insecurity, poor nutrition, and increased risk of chronic health problems, combined with the high cost of health-care systems to treat food insecurity, poses significant health threats and presents challenges to the food bank system. We develop a framework for optimizing resource allocation by food banks using a dynamic programming model. To deal with the high-dimensional state space in the dynamic program, we construct approximations to the value function that are parameterized by a small number of parameters. Computational experiments using real-world data obtained from one of the food banks in New York State demonstrate the performance of the approach. Specifically, when compared against the policy currently implemented in practice, our algorithm demonstrates a 7.73% improvement in total utility. 4) Predicting demand patterns at mobile food pantries using interpretable analytics. In a food bank environment under limited budget and supplies, predicting demand patterns can help food bank better serve needy people and improve the efficiency of its operations. We use data from 80 mobile food pantry programs served by one of the food banks in New York state to build guidelines for food

bank personnel to better forecast the demand at these programs. We construct a data-driven representation of programs and apply a broad class of analytics methods to predict several aspects of demand. Our study demonstrates that powerful data-analytics techniques combined with data-visualization models can be used to understand and interpret the variability in demand at mobile food pantry programs.

BIOGRAPHICAL SKETCH

Faisal Alkaabneh was born and raised in Amman, Jordan. He received a B.S. in Industrial Engineering from the University of Jordan in Amman, Jordan in 2012, and M.S in Engineering Systems and Management from Masdar Institute of Science and Technology in Abu Dhabi, United Arab Emirates in 2014. Faisal then attended graduate school at Cornell University in Summer 2015.

This dissertation is dedicated to my mother (Suhad Alkaabneh), father (Mohammad Alkaabneh), and brothers (Zaid, Hamzah, and Hashem) for their support and patience during my studies.

ACKNOWLEDGEMENTS

During my Ph.D. at Cornell I worked and interacted with so many people I wish to thank for their amazing role and friendship in my Ph.D. journey. I would like to thank my advisor Prof. H. Oliver Gao for his advice and mentorship over my Ph.D. studies. I would also like to thank the other members of my Ph.D. committee, Prof. Miguel Gómez and Prof. Sid Banerjee for their patience, support, insight, and feedback. I cannot express enough how much I have learned from them about being a better researcher and teacher. I would like to thank Prof. Al Goerge for his dedication and support for the Systems Engineering program at Cornell, his dedication and support is very inspiring for us as the next generation systems engineering educators. I would like to thank other systems engineering field members Prof. Fengqi You and Prof. Jamol Pender for their support to me while I was in the academic job market.

And finally I would like to thank my friends and colleagues in the Systems Engineering, CS, CEE, and ORIE departments.

TABLE OF CONTENTS

LIST OF TABLES

LIST OF FIGURES

CHAPTER 1

INTRODUCTION

Food supply chains are continuously evolving and adapting systems of organizations, people, activities, information, and resources involved in moving food products or services from suppliers to customer. Optimizing the performance of a food supply chain by focusing on a single performance measure and ignoring the critical interactions between different components is not well suited to effectively manage and optimize the performance of the food supply chain system as a whole. For example, last-mile food delivery systems that are responsible for moving food products from a supermarket, retailer, shopping center, or distribution hub to the final delivery destination – consumer home – are complex systems with complicated interactions between different parts. The main parts within the last-mile food delivery systems are: the consumer who considers delivery time as a key factor of satisfaction, the supplier who wants to maximize their profits, and the society who is concerned about the impact of last-mile delivery systems on the environment due to the transportation activities. In order to guide decision makers to develop efficient and effective last-mile food delivery systems, decision makers should utilize tools that take into account the evolving and adapting behavior of the last-mile food delivery system.

Compared to traditional engineering and operations management modeling approaches systems engineering, on the other hand, recognizes that any system has a number of parts that together produce the behavior and performance of the system. Simon Ramo [57] defines systems engineering as "a branch of engineering which concentrates on the design and application of the whole as dis-

tinct from the parts, looking at a problem in its entirety, taking account of all the facets and all the variables and linking the social to the technological." Hence, a systems engineer seeking to optimize a performance of a system must look at the systems' and the interactions between these parts to achieve the maximum capability of each part. Going back to the example of last-mile food delivery system, a systems engineering approach to optimize the performance of the system should consider the profit of the supplier, the delivery time for the customers, and environmental impact of the system according to weighted objectives.

Whereas early systems engineering applications focused on military and space exploration projects, the increase in complexities of systems, advancement in technologies, and the urgent need to build reliable robust systems have made it inevitable to utilize systems engineering concepts in building and developing systems for projects within the commercial and public sectors. Furthermore, systems engineering concepts such as multi-objective optimization provides important insights to decision makers to analyze economic, environmental, and social tradeoffs of any system design. Multi-objective optimization, for instance, is now used to design and build systems for different application, water management [50, 55, 11], power generation [76], logistics [133, 127], and supply chain [96, 134], to name a few.

A major challenge in building and designing food systems relative to other systems is the complex interactions between the different parts within the food supply chain. Such challenges are best exemplified in food bank organizations. Food banks receive most of their supplies through donations. Donations are

highly unpredictable, and food banks have no control over the items and quantities they receive. At the same time, the mission of food banks is to combat food insecurity and to provide healthy food for needy people. The evidence linking food insecurity, poor nutrition and increased risk of chronic diseases necessarily implies that food banks should consider the nutrition dimension of served populations. My PhD dissertation is centered around systems thinking to develop analytical tools for improving decision making in environments that involve uncertainty and complex objectives. My work adopts an interdisciplinary approach, that combines stochastic modeling and leverages optimization techniques.

In Chapter 2, we consider the problem of inventory routing in the context of perishable products and find near-optimal replenishment scheduling and vehicle routes when the objective is to maximize the supplier's profit and minimize the costs due to fuel consumption, inventory holding, and greenhouse gas emissions. In Chapter 3, our work deals with a fundamental environmental intervention question in food supply chains: what is the best policy to reduce the environmental externalities associated with the production of fruits and vegetables considering environmental and economic dimensions simultaneously? We offered a systems-based approach by developing a spatially and temporally disaggregated price equilibrium mathematical model. In Chapter 4, we develop a framework for optimizing resource allocation by food banks among the agencies they serve. Our framework explicitly considers the effectiveness and efficiency measures of the resource allocation problem faced by food banks and implicitly considers the equity performance measure. In Chapter 5, we apply a broad class of analytics methods to predict several aspects of demand at Mobile

Food Pantry Programs. Our study demonstrates that powerful data-analytics techniques combined with data-visualization models can be used to understand and interpret the variability in demand at mobile food pantry programs.

CHAPTER 2

BENDERS DECOMPOSITION FOR THE INVENTORY VEHICLE ROUTING PROBLEM WITH PERISHABLE PRODUCTS AND ENVIRONMENTAL COSTS

The material of this chapter is published at Computers & Operations Research journal Alkaabneh et al. [4].

2.1 Introduction

A supply chain is a system of organizations, people, activities, information, and resources involved in moving a product or service from supplier to customer. Supply chains for perishable products constitute an important subclass of supply chains globally, though they have distinct features and characteristics that differentiate them from other supply chains. Essentially, the fundamental difference between perishable and non-perishable products is the continuous and significant change in the quality of perishable products throughout the entire supply chain until the point of final consumption [135, 3]. Common perishable goods include food products, flowers, live animals, ready-mixed concrete, packaged fresh produce, fruit juice, pharmaceuticals, and frozen products. They are characterized as perishable because their quality worsens over time and their value declines as a result.

Among the most critical and important logistics decisions companies face at the operational level are inventory management, vehicle routing, and schedul-

ing of vehicles for delivery. Efficient management of vehicle routes for delivery of products from a supplier to a set of customers can result in significant savings in both operational cost and greenhouse gas (GHG) emissions [13]. Likewise, inventory control constitutes an important logistics operation, especially when products have a limited shelf life [30]. The integration of routing, inventory, and replenishment scheduling decisions yields a new logistics problem called the Inventory Routing Problem (IRP). In the context of IRP, the supplier manages inventory replenishment on behalf of the customers. Once the customer provides the supplier with its demand for each time period during a certain planning horizon, the supplier is responsible for maintaining the desired level of inventory of products at the customer site. The application of an IRP system leads to an overall reduction in logistics costs and is often described as a win—win situation [75].

Given the considerable body of scientific evidence linking global warming with the increase in GHG emissions [113], companies and organizations worldwide are stepping up their efforts to reduce their GHG emissions [66]. For instance, Walmart set out in earnest to find a more sustainable approach to their retail business and set long-term goals to operate with 100 percent renewable energy, to create zero waste in their own operations, and to sell products that sustain people and the environment. Among the areas where Walmart is making progress toward this goal is their supply chain operations. The company improved the way it loads, routes, and drives its trucks,[1] and Walmart claims that it will realize savings of $1 billion a year as a result. Likewise, other companies, such as Amazon.com, are pursuing innovative plans to improve their

[1]https://www.theguardian.com/sustainable-business/2015/nov/18/walmart-climate-change-carbon-emissions-renewabe-energy-environment

sustainability measures toward an environment in which logistics plays a major role.[2] Hence it is important for companies seeking better environmental sustainability measures to accurately estimate their GHG emissions due to logistics operations. Given the importance and large scale of perishable products supply chains, this study is motivated by the importance of reducing GHG emissions within the perishable products supply chain industry in IRP settings.

2.1.1 Related Work and Contributions

Bell et al. [14] introduced the formal definition of IRP in a seminal paper dealing with IRP at Air Products, a producer of industrial gases. Since then, a great deal of work has been added to the IRP literature. Studies that have contributed to this literature can essentially be classified as one of two main types: studies that have developed algorithms to solve IRP models efficiently, and studies that have extended previously published IRP models to account for practical considerations and to relax some assumptions found in previous models. However, some studies have made algorithmic and modeling contributions simultaneously. For an extensive review of the IRP literature, the interested reader is referred to [27].

Within the IRP literature, there are studies that have succeeded in developing efficient algorithms to solve IRP models. For instance, Archetti, Bertazzi, Laporte, and Speranza [8] developed a branch-and-cut algorithm for a single-vehicle IRP, while Solyalı and Süral [115] developed a branch-and-cut algorithm enhanced with an upper bound heuristic to solve a single-vehicle IRP. Among the algorithms developed to solve IRP with multiple vehicles, Coelho and La-

[2]https://www.amazon.com/p/feature/wnsdvqqghme982o

porte [29] proposed a branch-and-cut algorithm, Adulyasak, Cordeau, and Jans [1] developed a heuristic based on the adaptive large neighborhood search (ALNS) technique combined with branch-and-cut, and Desaulniers, Rakke, and Coelho [42] developed a branch-price-and-cut algorithm. Other studies have developed meta-heuristics to solve IRP models efficiently. For instance, Archetti, Boland, and Speranza [9] developed a meta-heuristic that combines tabu search and mathematical programming formulations to solve IRP for the case of multiple vehicles. However, it should be noted that these studies are dedicated to the classical IRP setting, where there is a single supplier, a single product, multiple customers, and a finite planning horizon.

Apart from studies that have focused on developing efficient algorithms to solve IRP models, several studies in the IRP literature have aimed to extend traditional IRP models to solve IRP instances with some new or unique characteristic that traditional IRP models fail to accommodate. Among these extensions are the multi-product IRP [117], stochasticity in demand [100], infinite planning time horizon [88] and many-suppliers-to-many-customers distribution systems [26]. Yet another interesting practical extension of the classical IRP models is extending IRP models of supply chain systems to perishable products.

Incorporating characteristics of perishable products adds complexity to the IRP, which is already quite complex; hence relatively few studies have addressed the perishable inventory routing problem (PIRP). Generally speaking, perishable products can be classified into two general categories, based on how their quality changes over time. The first category contains products such as

drugs and milk products that are considered fit for consumption until their stated expiration date, while the second category contains products whose quality changes over time, possibly in a non-monotone fashion. Here we provide a brief review of some of the studies that considered PIRP. Custódio and Oliveira [37] described a real-world application of IRP for the distribution of frozen products in Portugal and used a heuristic to solve the developed model. Hemmelmayr, Doerner, Hartl, and Savelsbergh [60] developed a mathematical model to plan delivery routes for the supply of blood products to hospitals by a blood bank given fixed routes and stochastic demand. Nagurney, Masoumi, and Yu [90] developed a supply chain network optimization model for the management of human blood, while Le, Diabat, Richard, and Yih [73] developed a column generation algorithm for PIRP. Coelho and Laporte [30] presented a mathematical model for PIRP and proposed a branch-and-cut algorithm to solve the developed model; this study was the first to consider the impact of product age on its quality. Their mathematical model incorporates the fact that the revenue from– and inventory holding costs surrounding—–perishable products are functions of their age and this information is not necessarily flat as suggested in earlier studies.

It has been suggested by a number of studies in the vehicle routing literature that there are opportunities for reducing GHG emissions by extending the traditional vehicle routing problem (VRP) objectives to account for environmental and social impacts other than just the economic costs [109]. To this end, several researchers have extended traditional VRP models to account for environmental and social factors. For instance, Bektaş and Laporte [13] developed a VRP mathematical model that minimizes the distance traveled, greenhouse gas emissions,

fuel consumption, and travel times and their costs. Greenhouse gas emissions were modeled as a function of fuel consumption, which is itself a function of vehicle load, speed, and distance traveled. They showed that there is great potential for realizing savings in the total cost of routing and GHG emissions when fuel consumption is modeled as a function of vehicle speed, load, and distance traveled. Thus, there is strong evidence from the VRP literature that using different models to calculate the fuel cost yields different routing decisions.

The only study in the IRP literature that utilized accurate estimation of the fuel cost is that by Soysal, Bloemhof-Ruwaard, Haijema, and van der Vorst [116]. They considered PIRP in the case of multiple products, a many-to-many distribution system, and accurate estimation of the fuel cost, and they included the cost of greenhouse gas emissions in the objective function. They were interested in analyzing the value of horizontal collaboration between suppliers within the context of PIRP and found that such collaboration leads to reductions in emissions, driving time, inventory, and costs of waste given an uncertain demand. They were able to solve small instances with 5 customers using a commercial mixed integer programming (MIP) solver, but they did not provide an algorithm or heuristic for solving large-scale instances of their model.

We summarize the aforementioned prior work on PIRP in Table 2.1. The first column of the table shows the article/study considered for discussion. The second column indicates whether the model presented in each study considered revenue and holding costs as a function of product age. The third through fifth columns indicate which factors were considered when calculating the fuel

(transportation) cost in each study. The sixth column represents demand uncertainty and indicates whether the demand was assumed to be stochastic or deterministic. Lastly, the seventh column indicates the methodology developed in each study.

Table 2.1: Literature on PIRP

Study	Aging Effects	Fuel Cost Function: Distance Traveled	Fuel Cost Function: Vehicle Load	Fuel Cost Function: Vehicle Speed	Stoch. Demand	Approach
[37]	-	✔	-	-	-	Heuristic
[60]	-	✔	-	-	✔	Heuristic
[90]	-	✔	-	-	✔	Heuristic
[73]	-	✔	-	-	-	Column gen.
[30]	✔	✔	-	-	-	Branch-and-cut
[116]	✔	✔	✔	✔	✔	Solver
This work	✔	✔	✔	✔	-	Benders decomp.

To the best of our knowledge, solving large-scale instances of PIRP with GHG emissions costs and accurate estimation of the fuel cost has not been addressed before. Our study makes four main contributions. First, we introduce the perishable inventory routing problem in conjunction with accurate estimation of the fuel cost and GHG emissions mathematical model. Second, we propose a Benders decomposition algorithm with several computational enhancements: valid inequalities, warm-up start, and Pareto-optimal cuts. Third, we develop an effective meta-heuristic to obtain good-quality solutions based on solving a mixed integer programming (MIP) formulation and a greedy random adaptive search procedure (GRASP). Fourth, we demonstrate the benefits of utilizing a model that accurately that estimates fuel consumption levels as a function of vehicle load, speed and distance traveled in the context of PIRP, as opposed to traditional models that rely on distance traveled as the sole measure

of fuel consumption. The overall benefits can be summarized as savings in the fuel cost and lower GHG emissions.

2.2 Problem Description and Mathematical Formulation

We now formally introduce the perishable inventory routing problem (PIRP). For the sake of convenience and consistency, we use the conventional notation for IRP that is found in the literature. Our IRP model is presented as a directed graph $\mathcal{G} = (\mathcal{V}, \mathcal{A})$, where $\mathcal{V} = \{0, ..., n\}$ is the vertex set and $\mathcal{A}$ is the edge set. The vertex 0 is the supplier node, and the vertices in the set $\mathcal{V}' = \mathcal{V} \backslash \{0\}$ are the customer nodes. There is a routing cost c_{ij} associated with edge $(i, j) \in \mathcal{A}$. This cost c_{ij} can be viewed as the cost of traveling along edge (i, j) when the vehicle is not loaded. Our model assumes that the edge length matrix is symmetric (i.e., $c_{ij} = c_{ji}$).

Given the nature of perishable products, the age of a product is equal to some element of the discrete, finite set $\mathcal{S} = \{0, 1, 2, ..., s\}$. For a product that becomes spoiled after s time periods, at age $s + 1$ it is deemed to be spoiled and not suitable for consumption, and hence it vanishes from the inventory. The revenue from an item depends on its age g and is denoted by u^g. An inventory holding cost is incurred for every product in the inventory of the supplier and every product in the inventory of a customer. This cost depends on the age of the product, g, and is denoted by h_i^g. The inventory capacity of customer i is known and is denoted by C_i; this holding capacity cannot be exceeded at any time.

The set of time periods is $\mathcal{T} = \{1, ..., p\}$, where p is the planning horizon. In each time period, the quantity of items made available at the supplier is r^t. We assume that the supplier always acquires the freshest products—an assumption that is consistent with that presented in [30]. Let d_i^t be the demand of customer i in each time period t. As in the model presented in [30], we assume that customers do not require the supplier to supply them with the freshest items, and that in any time period, the supplier has the choice of delivering products of any age to customers; nevertheless, the revenue of the supplier depends on the age of the products delivered. As in other studies in the literature on IRP, we assume that the supplier has enough inventory to satisfy the demands of all the customers during the planning horizon. Furthermore, neither the supplier nor the customers are allowed to have a negative inventory in any time period. We decompose the demand d_i^t of customer i in time period t as $\sum_{g \in \mathcal{S}} d_i^{gt}$, since the demand can be satisfied by products of any age g, so long as the products are not spoiled. Lastly, a fleet of vehicles is available at the supplier site to deliver products to the customers. We denote the set of vehicles by $\mathcal{K}$ and the capacity of vehicle k by Q_k.

When the supplier decides to replenish a customer's inventory, the following constraints are imposed:

- The customer's inventory level can never exceed its capacity.
- Inventory levels are not allowed to be negative.
- Each of the supplier's vehicles must start its delivery task at the supplier site and return there at the end of the delivery task.

- The vehicle capacities cannot be exceeded.

The solution to the PIRP provides the following information to the supplier: (1) when to supply each customer during the planning horizon, (2) the quantities and ages of the products to be delivered to each customer, and (3) how to combine visits to different customers into vehicle routes.

We define a binary variable x_{ij}^{kt} that is equal to 1 if and only if vehicle k travels along edge (i, j) in time period t, and we define a binary variable y_i^{kt} that is equal to 1 if and only if node i (the supplier or a customer) is visited by vehicle k in time period t. Let I_i^t denote the inventory level at node i at the end of time period t. Just as with the demand d_i^t we decompose the inventory level decision variable I_i^t by the ages of the items; hence $I_i^t = \sum_{g \in \mathcal{S}} I_i^{gt}$, where I_i^{gt} is the quantity of product of age g in the inventory at node i at the end of time period t. We denote by q_i^{gkt} the quantity of product of age g that is delivered in vehicle k to customer i in time period t. The problem can then be formulated as follows, which is adapted from [30]:

$$\min_{I,d,q,y,x} \quad -\sum_{i\in\mathcal{V}'}\sum_{g\in\mathcal{S}}\sum_{t\in\mathcal{T}} u^g d_i^{gt} + \sum_{i\in\mathcal{V}}\sum_{g\in\mathcal{S}}\sum_{t\in\mathcal{T}} h_i^g I_i^{gt} + \sum_{(i,j)\in\mathcal{A}}\sum_{k\in\mathcal{K}}\sum_{t\in\mathcal{T}} c_{ij} x_{ij}^{kt} \tag{2.1}$$

$$\text{s.t.} \quad I_0^{gt} = I_0^{g-1,t-1} - \sum_{i\in\mathcal{V}'}\sum_{k\in\mathcal{K}} q_i^{gkt} \quad \text{for all } g\in\mathcal{S}\backslash\{0\}, t\in\mathcal{T} \tag{2.2}$$

$$I_0^{0t} = r^t \quad \text{for all } t\in\mathcal{T} \tag{2.3}$$

$$I_i^{gt} = I_i^{g-1,t-1} + \sum_{k\in\mathcal{K}} q_i^{gkt} - d_i^{gt} \text{ for all } i\in\mathcal{V}', g\in\mathcal{S}\backslash\{0\}, t\in\mathcal{T} \tag{2.4}$$

$$I_i^{0t} = \sum_{k\in\mathcal{K}} q_i^{0kt} - d_i^{0t} \quad \text{for all } i\in\mathcal{V}', t\in\mathcal{T} \tag{2.5}$$

$$\sum_{g\in\mathcal{S}} I_i^{gt} \le C_i \quad \text{for all } i\in\mathcal{V}', t\in\mathcal{T} \tag{2.6}$$

$$d_i^t = \sum_{g\in\mathcal{S}} d_i^{gt} \quad \text{for all } i\in\mathcal{V}', t\in\mathcal{T} \tag{2.7}$$

$$\sum_{g\in\mathcal{S}}\sum_{k\in\mathcal{K}} q_i^{gkt} \le C_i - \sum_{g\in\mathcal{S}} I_i^{g,t-1} \quad \text{for all } i\in\mathcal{V}', t\in\mathcal{T} \tag{2.8}$$

$$q_i^{gkt} \le C_i y_i^{kt} \quad \text{for all } i\in\mathcal{V}', g\in\mathcal{S}, k\in\mathcal{K}, t\in\mathcal{T} \tag{2.9}$$

$$\sum_{i\in\mathcal{V}'}\sum_{g\in\mathcal{S}} q_i^{gkt} \le Q_k y_0^{kt} \quad \text{for all } k\in\mathcal{K}, t\in\mathcal{T} \tag{2.10}$$

$$\sum_{j\in\mathcal{V}:j\neq i} x_{ij}^{kt} + \sum_{j\in\mathcal{V}:j\neq i} x_{ji}^{kt} = 2y_i^{kt} \quad \text{for all } i\in\mathcal{V}, k\in\mathcal{K}, t\in\mathcal{T} \tag{2.11}$$

$$\sum_{i\in\mathcal{ST}}\sum_{j\in\mathcal{ST}} x_{ij}^{kt} \le \sum_{i\in\mathcal{ST}} y_i^{kt} - y_m^{kt} \quad \text{for all } \mathcal{ST}\subseteq\mathcal{V}', k\in\mathcal{K}, \; t\in\mathcal{T} \text{ and some } m\in\mathcal{ST} \tag{2.12}$$

$$\sum_{k\in\mathcal{K}} y_i^{kt} \le 1 \quad \text{for all } i\in\mathcal{V}', t\in\mathcal{T} \tag{2.13}$$

$$I_i^{gt}, d_i^{gt}, q_i^{gkt} \ge 0 \quad \text{for all } i\in\mathcal{V}', k\in\mathcal{K}, t\in\mathcal{T} \tag{2.14}$$

$$x_{ij}^{kt} \in \{0,1\} \quad \text{for all } (i,j)\in\mathcal{A}, k\in\mathcal{K}, t\in\mathcal{T} \tag{2.15}$$

$$y_i^{kt} \in \{0,1\} \quad \text{for all } i\in\mathcal{V}, k\in\mathcal{K}, t\in\mathcal{T}. \tag{2.16}$$

The objective function (2.1) maximizes the total sales revenue minus the total cost of inventory and routing; for the sake of convenience, it is expressed

in terms of minimization. Constraints (2.2) define the supplier's inventory levels and the aging of the products by one unit in each time period. Constraints (2.3) ensure that the supplier always receives the freshest products. Constraints (2.4) and (2.5) define the customers' inventory levels and the aging of the products they hold. Constraints (2.6) ensure that the inventory capacities of the customers are respected. Constraints (2.7) require the demand of each customer in each period to be the sum of the quantities of products of different ages. Note that spoiled products cannot be used to satisfy the demand, and hence are eliminated from the inventory. Constraints (2.8) and (2.9) ensure that each vehicle delivers products only to those customers that the vehicle has been assigned to. Constraints (2.10) ensure that the vehicle capacities are not exceeded. Constraints (2.11) ensure that each vertex on a route has exactly one incoming edge and one outgoing edge, while Constraints (2.12) eliminate sub-tours ($\mathcal{ST}$ denotes the set of sub-tours). Inequalities (2.13) prohibit split deliveries, by ensuring that each customer is served by at most one vehicle in each time period. Constraints (2.14) require the continuous decision variables to be non-negative and Constraints (2.15)–(2.16) require the integer decision variables to be binary.

2.2.1 Calculating GHG Emissions

Calculating fuel consumption of a vehicle during routing is a critical step in accurately estimating GHG emissions and operational costs associated with routing. Recently, there has been growing interest in providing simulation models that accurately predict fuel consumption of vehicles in different settings and for different values of parameters. For instance, the United States Environmental

Protection Agency (USEPA) developed a simulator, called the MOtor Vehicle Emissions Simulator (MOVES), to estimate emissions of mobile sources at the national, county, and project levels [89]. Likewise, several studies in the scientific literature have proposed models for the estimation of GHG emissions of moving vehicles based on different factors. One such study, by Bektaş and Laporte [13], presented a mathematical model for the optimization of vehicle routes that takes fuel consumption into account. In their model, vehicle speed and load were among the factors considered in estimating GHG emissions of vehicles during routing. In this paper, we adopt their model to estimate fuel consumed by a vehicle during routing.

Bektaş and Laporte's model is a comprehensive emissions model in which the rate of fuel consumption is a function of engine characteristics, road conditions, vehicle speed, and vehicle load. For further information on the comprehensive model used to calculate fuel consumption levels and hence GHG emissions, the interested reader is referred to [13]. To simplify the presentation in this paper and to keep the discussion concise, we introduce a parameter α_{ij} to represent the effective value of all the parameters associated with fuel consumption due to vehicle load; this parameter is defined as the cost associated with traveling 1 meter when the vehicle load is 1 kg. That parameter will be multiplied by the vehicle load to calculate the fuel cost per meter. Also, we introduce a new decision variable f_{ij}^{kt} to represent the load (in kg) of vehicle k when traveling along edge (i, j) in time period t. Thus the routing cost is $\sum_{(i,j)\in\mathcal{A}} \sum_{k\in\mathcal{K}} \sum_{t\in\mathcal{T}} (c_{ij} x_{ij}^{kt} + \alpha_{ij} f_{ij}^{kt})$. While our work explicitly considers vehicle speed in the calculation of greenhouse gas emissions, vehicle speed in our model is an exogenous parameter and to be set by the decision maker.

To calculate the value of f_{ij}^{kt} for edge (i, j), we need to impose the following constraints:

$$\sum_{j \in \mathcal{V}} f_{ij}^{kt} - \sum_{j \in \mathcal{V}} f_{ji}^{kt} = \sum_{g \in \mathcal{S}} q_i^{gkt} \quad \text{for all } i \in \mathcal{V}, k \in \mathcal{K}, t \in \mathcal{T} \tag{2.17}$$

$$\sum_{g \in \mathcal{S}} q_j^{gkt} x_{ij}^{kt} \leq f_{ij}^{kt} \quad \text{for all } j \in \mathcal{V}, (i, j) \in \mathcal{A}, k \in \mathcal{K}, t \in \mathcal{T} \tag{2.18}$$

$$f_{ij}^{kt} \leq (Q_k - \sum_{g \in \mathcal{S}} q_i^{gkt}) x_{ij}^{kt} \quad \text{for all } i \in \mathcal{V}, (i, j) \in \mathcal{A}, k \in \mathcal{K}, t \in \mathcal{T} \tag{2.19}$$

$$f_{ij}^{kt} \geq 0 \quad \text{for all } (i, j) \in \mathcal{A}, k \in \mathcal{K}, t \in \mathcal{T}. \tag{2.20}$$

Constraints (2.18) and (2.19) are non-linear, because they each involve a product of two decision variables; however, these constraints can be linearized simply and effectively using the big M technique, resulting in the following set of linear constraints:

$$\sum_{g \in \mathcal{S}} q_j^{gkt} - f_{ij}^{kt} \leq M(1 - x_{ij}^{kt}) \quad \text{for all } j \in \mathcal{V}, (i, j) \in \mathcal{A}, k \in \mathcal{K}, t \in \mathcal{T} \tag{2.21}$$

$$-M x_{ij}^{kt} \leq f_{ij}^{kt} \quad \text{for all } (i, j) \in \mathcal{A}, k \in \mathcal{K}, t \in \mathcal{T} \tag{2.22}$$

$$f_{ij}^{kt} \leq Q_k x_{ij}^{kt} - \sum_{g \in \mathcal{S}} q_i^{gkt} + M(1 - x_{ij}^{kt}) \quad \text{for all } i \in \mathcal{V}, (i, j) \in \mathcal{A}, k \in \mathcal{K}, t \in \mathcal{T} \tag{2.23}$$

$$f_{ij}^{kt} \leq Q_k x_{ij}^{kt} + M x_{ij}^{kt} \quad \text{for all } (i, j) \in \mathcal{A}, k \in \mathcal{K}, t \in \mathcal{T}. \tag{2.24}$$

We restate the PIRP formulation for convenience:

$$\min_{I,d,q,f,y,x} \quad -\sum_{i\in\mathcal{V}}\sum_{g\in\mathcal{S}}\sum_{t\in\mathcal{T}} u_i^g d_i^{gt} + \sum_{i\in\mathcal{V}}\sum_{g\in\mathcal{S}}\sum_{t\in\mathcal{T}} h_i^g I_i^{gt}$$

$$+ \sum_{(i,j)\in\mathcal{A}}\sum_{k\in\mathcal{K}}\sum_{t\in\mathcal{T}} c_{ij} x_{ij}^{kt} + \sum_{(i,j)\in\mathcal{A}}\sum_{k\in\mathcal{K}}\sum_{t\in\mathcal{T}} \alpha_{ij} f_{ij}^{kt} \tag{2.25}$$

$$\text{s.t.} \quad (2.2) - (2.16), (2.17), (2.20) - (2.24). \tag{2.26}$$

2.3 Benders Decomposition

In 1962, Benders [16] proposed a decomposition strategy for solving a large-scale optimization problem based on partitioning the problem into two simpler problems: a master problem (MP) and a subproblem (SP). Benders' algorithm works by solving the MP, which is a simpler version of the original problem, and passing the values of the MP solution to the SP. The algorithm solves each of the two simpler problems iteratively, one at a time. In each iteration, a new constraint, known as a Benders cut, is added to the MP. The algorithm keeps iterating until a pre-defined stopping criterion is met.

Several studies in the literature have reported the success of implementing Benders decomposition to solve difficult combinatorial problems [34, 63, 32, 35]. In the context of logistics, Adulyasak, Cordeau, and Jans [2] implemented Benders decomposition to solve the production inventory routing problem with stochastic demand, which is a more general problem than the IRP, since it considers decision variables for both production quantities and production scheduling. However, the authors did not incorporate environmental considerations and considered only non-perishable products.

2.3.1 Benders Reformulation

If the decision variables for visit scheduling and vehicle routing are held fixed, the PIRP reduces to a simple problem that aims to determine the quantities to be delivered to each customer on each visit and the ages of those products delivered. Thus we define variables $\bar{y}$ and $\bar{x}$ to represent the fixed, complicating variables. Once the values of the decision variables y and x are fixed, the Ben-

ders SP is obtained:

$$\min_{I,d,q,f} \quad -\sum_{i\in\mathcal{V}'}\sum_{g\in\mathcal{S}}\sum_{t\in\mathcal{T}} u^g d_i^{gt} + \sum_{i\in\mathcal{V}}\sum_{g\in\mathcal{S}}\sum_{t\in\mathcal{T}} h_i^g I_i^{gt} + \sum_{(i,j)\in\mathcal{A}}\sum_{k\in\mathcal{K}}\sum_{t\in\mathcal{T}} \alpha_{ij} f_{ij}^{kt} \tag{2.27}$$

$$\text{s.t.} \quad I_0^{gt} = I_0^{g-1,t-1} - \sum_{k\in\mathcal{K}}\sum_{i\in\mathcal{V}'} q_i^{gkt} \quad \text{for all } g\in\mathcal{S}\backslash\{0\}, t\in\mathcal{T} \tag{2.28}$$

$$I_0^{0t} = r^t \quad \text{for all } t\in\mathcal{T} \tag{2.29}$$

$$I_i^{gt} = I_i^{g-1,t-1} + \sum_{k\in\mathcal{K}} q_i^{gkt}$$

$$-d_i^{gt} \quad \text{for all } i\in\mathcal{V}', g\in\mathcal{S}\backslash\{0\}, t\in\mathcal{T} \tag{2.30}$$

$$I_i^{0t} = \sum_{k\in\mathcal{K}} q_i^{0kt} - d_i^{0t} \quad \text{for all } i\in\mathcal{V}', t\in\mathcal{T} \tag{2.31}$$

$$\sum_{g\in\mathcal{S}} I_i^{gt} \le C_i \quad \text{for all } i\in\mathcal{V}', t\in\mathcal{T} \tag{2.32}$$

$$d_i^t = \sum_{g\in\mathcal{S}} d_i^{gt} \quad \text{for all } i\in\mathcal{V}', t\in\mathcal{T} \tag{2.33}$$

$$\sum_{g\in\mathcal{S}}\sum_{k\in\mathcal{K}} q_i^{gkt} \le C_i - \sum_{g\in\mathcal{S}} I_i^{g,t-1} \quad \text{for all } i\in\mathcal{V}', t\in\mathcal{T} \tag{2.34}$$

$$q_i^{gkt} \le C_i \bar{y}_i^{kt} \quad \text{for all } i\in\mathcal{V}', g\in\mathcal{S}, k\in\mathcal{K}, t\in\mathcal{T} \tag{2.35}$$

$$\sum_{i\in\mathcal{V}'}\sum_{g\in\mathcal{S}} q_i^{gkt} \le Q_k \bar{y}_0^{kt} \quad \text{for all } k\in\mathcal{K}, t\in\mathcal{T} \tag{2.36}$$

$$\sum_{g\in\mathcal{S}} q_j^{gkt} - f_{ij}^{kt} \le$$

$$M(1-\bar{x}_{ij}^{kt}) \quad \text{for all } j\in\mathcal{V}', (i,j)\in\mathcal{A}, k\in\mathcal{K}, t\in\mathcal{T} \tag{2.37}$$

$$-M\bar{x}_{ij}^{kt} \le f_{ij}^{kt} \quad \text{for all } (i,j)\in\mathcal{A}, k\in\mathcal{K}, t\in\mathcal{T} \tag{2.38}$$

$$f_{ij}^{kt} \le Q_k \bar{x}_{ij}^{kt} - \sum_{g\in\mathcal{S}} q_i^{gkt}$$

$$+M(1-\bar{x}_{ij}^{kt}) \quad \text{for all } i\in\mathcal{V}', (i,j)\in\mathcal{A}, k\in\mathcal{K}, t\in\mathcal{T} \tag{2.39}$$

$$f_{ij}^{kt} \le Q_k \bar{x}_{ij}^{kt} + M\bar{x}_{ij}^{kt} \quad \text{for all } (i,j)\in\mathcal{A}, k\in\mathcal{K}, t\in\mathcal{T} \tag{2.40}$$

$$I_i^{gt}, d_i^{gt}, q_i^{gkt}, f_{ij}^{kt} \ge 0 \quad \text{for all } i\in\mathcal{V}, k\in\mathcal{K}, k\in\mathcal{K}, t\in\mathcal{T}. \tag{2.41}$$

However, SP(I, d, q, f) might be infeasible if the quantity of items supplied to some customer during the planning horizon falls short of that customer's demand. This problem can be addressed by introducing a continuous variable to represent the amount of the shortage. To this end, we introduce a variable s_i^t to represent the amount by which the product supplied to customer i in time period t falls short of that customer's demand. This positive variable is added to constraints (2.33) to serve as an artificial quantity of product provided by the supplier to a customer to prevent having unmet demand. In addition, a large penalty is associated with this variable to prevent having any shortage in the optimal solution of the PIRP. Therefore, (2.33) is replaced by the following constraint:

$$d_i^t = \sum_{g \in \mathcal{S}} d_i^{gt} + s_i^t \qquad \text{for all } i \in \mathcal{V}', t \in \mathcal{T}. \tag{2.42}$$

The coefficient of the decision variable s_i^t in the objective function, σ_i, which is the cost of the unmet demand of customer i, is set to a very large number. The objective function of SP(I, d, q, f, s) is

$$\begin{aligned} \min_{I,d,q,f,s} \quad & -\sum_{i \in \mathcal{V}'} \sum_{g \in \mathcal{S}} \sum_{t \in \mathcal{T}} u^g d_i^{gt} + \sum_{i \in \mathcal{V}} \sum_{g \in \mathcal{S}} \sum_{t \in \mathcal{T}} h_i^g I_i^{gt} + \sum_{(i,j) \in \mathcal{A}} \sum_{k \in \mathcal{K}} \sum_{t \in \mathcal{T}} \alpha_{ij} f_{ij}^{kt} \\ & + \sum_{i \in \mathcal{V}'} \sum_{t \in \mathcal{T}} \sigma_i s_i^t. \end{aligned} \tag{2.43}$$

Proposition 2.3.1. For any fixed values of the decision variables y and x, SP(I, d, q, f, s) is feasible and bounded.

Proof. The proof follows from the proposition presented in [2]. □

The associated dual variables to constraints (2.28)–(2.32), (2.34)–(2.40), and (2.42) are $\boldsymbol{E} = \{E^{gt} | g \in \mathcal{S} \backslash \{0\}, t \in \mathcal{T}\}$, $\boldsymbol{H} = \{H^t | t \in \mathcal{T}\}$, $\boldsymbol{\Gamma} = \{\Gamma_i^{gt} | i \in \mathcal{V}', g \in \mathcal{S} \backslash \{0\}, t \in \mathcal{T}\}$, $\boldsymbol{\Xi} = \{\Xi_i^t | i \in \mathcal{V}', t \in \mathcal{T}\}$, $\boldsymbol{K} = \{K_i^t \geq 0 | i \in \mathcal{V}', t \in \mathcal{T}\}$, $\boldsymbol{M} = \{M_i^t \geq$

$0|i \in \mathcal{V}', t \in \mathcal{T}\}$, $\boldsymbol{N} = \{N_i^{gkt} \geq 0|i \in \mathcal{V}', k \in \mathcal{K}, g \in \mathcal{S}, t \in \mathcal{T}\}$, $\boldsymbol{\Omega} = \{\Omega^{kt} \geq 0|k \in \mathcal{K}, t \in \mathcal{T}\}$, $\boldsymbol{O} = \{O_{ij}^{kt} \geq 0|(i,j) \in \mathcal{A}, k \in \mathcal{K}, t \in \mathcal{T}\}$, $\boldsymbol{\Phi} = \{\Phi_{ij}^{kt} \geq 0|(i,j) \in \mathcal{A}, k \in \mathcal{K}, t \in \mathcal{T}\}$, $\boldsymbol{\Pi} = \{\Pi_{ij}^{kt} \geq 0|(i,j) \in \mathcal{A}, k \in \mathcal{K}, t \in \mathcal{T}\}$, $\boldsymbol{\Psi} = \{\Psi_{ij}^{kt} \geq 0|(i,j) \in \mathcal{A}, k \in \mathcal{K}, t \in \mathcal{T}\}$, and $\boldsymbol{\Lambda} = \{\Lambda_i^t|i \in \mathcal{V}', t \in \mathcal{T}\}$, respectively. After associating the dual variables, the dual linear Benders subproblem can be written as

$$
\begin{aligned}
\max \quad & -\sum_{t\in\mathcal{T}} r^t H^t - \sum_{i\in\mathcal{V}'}\sum_{t\in\mathcal{T}} C_i K_i^t - \sum_{i\in\mathcal{V}'}\sum_{t\in\mathcal{T}} d_i^t \Lambda_i^t - \sum_{i\in\mathcal{V}'}\sum_{t\in\mathcal{T}} C_i M_i^t \\
& - \sum_{i\in\mathcal{V}'}\sum_{g\in\mathcal{S}}\sum_{k\in\mathcal{K}}\sum_{t\in\mathcal{T}} (C_i \bar{y}_i^{kt}) N_i^{gkt} - \sum_{k\in\mathcal{K}}\sum_{t\in\mathcal{T}} (Q_k \bar{y}_0^{kt}) \Omega^{kt} \\
& - \sum_{(i,j)\in\mathcal{A}}\sum_{k\in\mathcal{K}}\sum_{t\in\mathcal{T}} (M(1-\bar{x}_{ij}^{kt})) O_{ij}^{kt} - \sum_{(i,j)\in\mathcal{A}}\sum_{k\in\mathcal{K}}\sum_{t\in\mathcal{T}} (M\bar{x}_{ij}^{kt}) \Phi_{ij}^{kt} \\
& - \sum_{(i,j)\in\mathcal{A}}\sum_{k\in\mathcal{K}}\sum_{t\in\mathcal{T}} ((Q_k - M)\bar{x}_{ij}^{kt} + M) \Pi_{ij}^{kt} \\
& - \sum_{(i,j)\in\mathcal{A}}\sum_{k\in\mathcal{K}}\sum_{t\in\mathcal{T}} ((Q_k + M)\bar{x}_{ij}^{kt}) \Psi_{ij}^{kt} \qquad (2.44) \\
\text{s.t.} \quad & \boldsymbol{E}, \boldsymbol{H}, \boldsymbol{\Gamma}, \boldsymbol{I}, \boldsymbol{K}, \boldsymbol{\Lambda}, \boldsymbol{M}, \boldsymbol{N}, \boldsymbol{\Omega}, \boldsymbol{O}, \boldsymbol{\Phi}, \boldsymbol{\Pi}, \boldsymbol{\Psi} \in \Upsilon, \qquad (2.45)
\end{aligned}
$$

where Υ is the polyhedron defined by the constraints of the dual problem. Let $\mathcal{P}_{\mp}$ be the set of extreme points defined by Υ. Since SP is feasible and bounded by Proposition 1, strong duality ensures that the dual problem of the primal SP is feasible and bounded as well. Therefore, we can add a Benders cut to the MP:

$$
\begin{aligned}
& \eta + \sum_{i\in\mathcal{V}'}\sum_{g\in\mathcal{S}}\sum_{k\in\mathcal{K}}\sum_{t\in\mathcal{T}} C_i N_i^{gkt} y_i^{kt} + \sum_{k\in\mathcal{K}}\sum_{t\in\mathcal{T}} Q_k \Omega^{kt} y_0^{kt} \\
& \quad + \sum_{(i,j)\in\mathcal{A}}\sum_{k\in\mathcal{K}}\sum_{t\in\mathcal{T}} \Big(M(O_{ij}^{kt} - \Phi_{ij}^{kt} - \Pi_{ij}^{kt} + \Psi_{ij}^{kt}) + Q_k(\Pi_{ij}^{kt} + \Psi_{ij}^{kt}) \Big) x_{ij}^{kt} \\
& \geq -\sum_{t\in\mathcal{T}} r^t H^t - \sum_{i\in\mathcal{V}'}\sum_{t\in\mathcal{T}} C_i K_i^t - \sum_{i\in\mathcal{V}'}\sum_{t\in\mathcal{T}} d_i^t \Lambda_i^t - \sum_{i\in\mathcal{V}'}\sum_{t\in\mathcal{T}} C_i M_i^t \\
& \quad - \sum_{(i,j)\in\mathcal{A}}\sum_{k\in\mathcal{K}}\sum_{t\in\mathcal{T}} M \Pi_{ij}^{kt}, \qquad (2.46)
\end{aligned}
$$

where η is the underestimation variable for revenue and holding, shortages, and

GHG emissions costs. Let

$$\chi(\boldsymbol{H}, \boldsymbol{K}, \boldsymbol{\Lambda}, \boldsymbol{M}) = -\sum_{t\in\mathcal{T}} r^t E^t - \sum_{i\in\mathcal{V}'}\sum_{t\in\mathcal{T}} C_i K_i^t - \sum_{i\in\mathcal{V}'}\sum_{t\in\mathcal{T}} d_i^t \Lambda_i^t$$
$$- \sum_{i\in\mathcal{V}'}\sum_{t\in\mathcal{T}} C_i M_i^t - \sum_{(i,j)\in\mathcal{A}}\sum_{k\in\mathcal{K}}\sum_{t\in\mathcal{T}} M\Psi_{ij}^{kt}.$$

Then the Benders MP can be written as

$$\max_{y,x,\eta} \quad -\sum_{i\in\mathcal{V}}\sum_{j\in\mathcal{V},i<j}\sum_{k\in\mathcal{K}}\sum_{t\in\mathcal{T}} c_{ij}x_{ij}^{kt} + \eta \tag{2.47}$$

s.t. (2.11)–(2.13) and (2.15)–(2.16) are satisfied and

$$\eta + \sum_{(i,j)\in\mathcal{A}}\sum_{k\in\mathcal{K}}\sum_{t\in\mathcal{T}} (M(O_{ij}^{kt} - \Phi_{ij}^{kt} - \Pi_{ij}^{kt} + \Psi_{ij}^{kt}) + Q_k(\Pi_{ij}^{kt} + \Psi_{ij}^{kt}))x_{ij}^{kt}$$
$$+ \sum_{i\in\mathcal{V}}\sum_{g\in\mathcal{S}}\sum_{k\in\mathcal{K}}\sum_{t\in\mathcal{T}} C_i N_i^{gkt} y_i^{kt} + \sum_{k\in\mathcal{K}}\sum_{t\in\mathcal{T}} Q_k \Omega^{kt} y_0^{kt} \geq \chi(\boldsymbol{H}, \boldsymbol{K}, \boldsymbol{\Lambda}, \boldsymbol{M})$$
$$\text{for all } \boldsymbol{E}, \boldsymbol{H}, \boldsymbol{\Gamma}, \boldsymbol{I}, \boldsymbol{K}, \boldsymbol{\Lambda}, \boldsymbol{M}, \boldsymbol{N}, \boldsymbol{\Omega}, \boldsymbol{O}, \boldsymbol{\Phi}, \boldsymbol{\Pi}, \boldsymbol{\Psi} \in \mathcal{P}_{\mp} \tag{2.48}$$

Note that the Benders MP includes the sub-tour elimination Constraints (2.12), which are too stringent to allow full enumeration within the Benders MP, hence we relax these constraints and add them dynamically once a sub-tour is detected and hence resolve the master problem iteratively within each iteration to ensure that the solution provided by the master problem does not have any sub-tours.

2.3.2 Benders Decomposition Enhancements

Despite the great success of Benders decomposition, the algorithm may require a large number of iterations to converge. To overcome this deficiency in the classical algorithm, several techniques were introduced to accelerate the con-

vergence of the algorithm or reduce the number of iterations. For an extensive review of the literature on the Benders decomposition algorithm, as well as its applications, accelerating techniques, and algorithmic refinements, the interested reader is referred to [101]. In the following subsections, we provide several techniques and strategies to accelerate the convergence or reduce the number of iterations of the Benders decomposition for the PIRP.

Valid Inequalities and Symmetry Breaking

Valid inequalities can be added to the Benders MP to help it find near-optimal solutions by providing it with some information projected out in the SP. The inclusion of valid inequalities strengthens the Benders MP and accelerates its convergence.

In this paper, we consider adding several valid inequalities and symmetry-breaking constraints to the Benders MP. First, we adapt the families of inequalities presented in [28]:

$$x_{0i}^{kt} \leq y_i^{kt}, \quad \text{for all } i \in \mathcal{V}, k \in \mathcal{K}, t \in \mathcal{T} \tag{2.49}$$

$$x_{ij}^{kt} \leq y_i^{kt}, \quad \text{for all } i, j \in \mathcal{V}, k \in \mathcal{K}, t \in \mathcal{T} \tag{2.50}$$

$$y_i^{kt} \leq y_0^{kt}, \quad \text{for all } i \in \mathcal{V}', k \in \mathcal{K}, t \in \mathcal{T} \tag{2.51}$$

$$y_0^{kt} \leq y_0^{k-1,t}, \quad \text{for all } i \in \mathcal{V}, k \in \mathcal{K}\backslash\{1\}, t \in \mathcal{T} \tag{2.52}$$

Inequalities (2.49) and (2.50) impose the condition that if the supplier is the immediate successor of customer i along the route planned for vehicle k in time

period t, then i must be visited by vehicle k in that period. Constraints (2.51) ensure that the supplier is visited if any customer is visited by vehicle k in time period t. Constraints (2.52), which can only be used when the fleet of vehicles is homogeneous, ensure that vehicle k cannot leave the depot if vehicle $k-1$ is not used. Coelho and Laporte [30] used Constraints (2.52) in their work; since the vehicle fleet is homogeneous in all of our test instances, we are able to use these constraints as well.

The total number of visits for customer i during the planning horizon must be at least as large as the ratio of its total demand to the lesser of its storage capacity and the capacity of the vehicle with the maximum capacity. Furthermore, the total number of visits for all customers must be at least as large as the ratio of the sum of their total demands to the capacity of the vehicle with maximum capacity. Thus we have the following set of valid inequalities:

$$\sum_{k\in\mathcal{K}}\sum_{t\in\mathcal{T}} y_i^{kt} \geq \left\lceil \frac{\sum_{t\in\mathcal{T}} d_i^t}{\min\{\max_k Q_k, C_i\}} \right\rceil \quad \text{for all } i \in \mathcal{V}' \tag{2.53}$$

$$\sum_{k\in\mathcal{K}}\sum_{t\in\mathcal{T}} y_0^{kt} \geq \left\lceil \frac{\sum_{i\in\mathcal{V}}\sum_{t\in\mathcal{T}} d_i^t}{\max_k Q_k} \right\rceil \tag{2.54}$$

Lastly, for perishable products, the number of visits for a customer should be at least as large as the number of life cycles of the product (the life cycle is the amount of time elapsed between being fresh and expiring) during the planning horizon. Thus a valid inequality for PIRP can be stated as

$$\sum_{k\in\mathcal{K}}\sum_{t\in\mathcal{T}} y_i^{kt} \geq \left\lceil \frac{|\mathcal{T}|}{|\mathcal{S}|} \right\rceil, \qquad \text{for all } i \in \mathcal{V}' \tag{2.55}$$

Proposition 2.3.2. Constraints (2.55) are valid cuts for PIRP if $d_i^t > 0$ for $i \in \mathcal{V}'$ and $t \in \mathcal{T}$.

Proof. Assume that customer i always receives products that are fresh, and assume without loss of generality that the current time period is 1 and the life cycle of the product is s. Then after s time periods (i.e., at $t = 1 + s$) the inventory level of customer i is zero because of the perishability constraint. Thus there should be a supply to customer i at time $t = 1 + s$, and hence a visit to satisfy the constraint that the entire demand of customer i has to be covered. Since $s \leq |S|$, a lower bound on the number of visits for each customer can be expressed as $\left\lceil \frac{|\mathcal{T}|}{|\mathcal{S}|} \right\rceil$. □

Pareto-Optimal Cuts.

Magnanti and Wong [82] proposed a strategy to accelerate the convergence of the Benders algorithm by adding more stringent, undominated cuts, known as Pareto-optimal cuts. Let $\boldsymbol{Y}$ and $\boldsymbol{X}$ be the set of vectors associated with the decision variables y_i^{kt} and x_{ij}^{kt} obtained after solving the MP. The cut generated from the dual of SP(I, d, q, f, s) from the extreme point

$$(\boldsymbol{E^1}, \boldsymbol{H^1}, \boldsymbol{\Gamma^1}, \boldsymbol{I^1}, \boldsymbol{K^1}, \boldsymbol{\Lambda^1}, \boldsymbol{M^1}, \boldsymbol{N^1}, \boldsymbol{\Omega^1}, \boldsymbol{O^1}, \boldsymbol{\Phi^1}, \boldsymbol{\Pi^1}, \boldsymbol{\Psi^1})$$

dominates the cut generated from the extreme point

$$(\boldsymbol{E^2}, \boldsymbol{H^2}, \boldsymbol{\Gamma^2}, \boldsymbol{I^2}, \boldsymbol{K^2}, \boldsymbol{\Lambda^2}, \boldsymbol{M^2}, \boldsymbol{N^2}, \boldsymbol{\Omega^2}, \boldsymbol{O^2}, \boldsymbol{\Phi^2}, \boldsymbol{\Pi^2}, \boldsymbol{\Psi^2})$$

if and only if the inequality for at least one of these points is strict. Generating Pareto-optimal cuts requires two more steps. The first is to find core points of the convex hull of MP, and the second is to solve an LP problem to find good dual solutions. This extra computational effort is usually compensated for by faster convergence of the Benders algorithm and hence reduces the overall number of iterations. Nevertheless, finding the core points of the convex hull of the

MP is challenging. To circumvent this difficulty, researchers have developed several strategies to find the core points or approximations to them. The second step in finding a Pareto-optimal cut is to solve the following subproblem:

$$
\begin{aligned}
\max \quad & -\sum_{t\in\mathcal{T}} r^t H^t - \sum_{i\in\mathcal{V}'}\sum_{t\in\mathcal{T}} C_i K_i^t - \sum_{i\in\mathcal{V}'}\sum_{t\in\mathcal{T}} d_i^t \Lambda_i^t - \sum_{i\in\mathcal{V}'}\sum_{t\in\mathcal{T}} C_i M_i^t \\
& - \sum_{i\in\mathcal{V}'}\sum_{g\in\mathcal{S}}\sum_{k\in\mathcal{K}}\sum_{t\in\mathcal{T}} (C_i \tilde{y}_i^{kt}) N_i^{gkt} - \sum_{k\in\mathcal{K}}\sum_{t\in\mathcal{T}} (Q_k \tilde{y}_0^{kt}) \Omega^{kt} \\
& - \sum_{(i,j)\in\mathcal{A}}\sum_{k\in\mathcal{K}}\sum_{t\in\mathcal{T}} (M(1-\tilde{x}_{ij}^{kt})) O_{ij}^{kt} - \sum_{(i,j)\in\mathcal{A}}\sum_{k\in\mathcal{K}}\sum_{t\in\mathcal{T}} (M\tilde{x}_{ij}^{kt}) \Phi_{ij}^{kt} \\
& - \sum_{(i,j)\in\mathcal{A}}\sum_{k\in\mathcal{K}}\sum_{t\in\mathcal{T}} ((Q_k - M)\tilde{x}_{ij}^{kt} + M) \Psi_{ij}^{kt} \qquad (2.56) \\
\text{s.t.} \quad & -\sum_{t\in\mathcal{T}} r^t H^t - \sum_{i\in\mathcal{V}'}\sum_{t\in\mathcal{T}} C_i K_i^t - \sum_{i\in\mathcal{V}'}\sum_{t\in\mathcal{T}} d_i^t \Lambda_i^t - \sum_{i\in\mathcal{V}'}\sum_{t\in\mathcal{T}} C_i M_i^t \\
& - \sum_{i\in\mathcal{V}'}\sum_{g\in\mathcal{S}}\sum_{k\in\mathcal{K}}\sum_{t\in\mathcal{T}} (C_i \bar{y}_i^{kt}) N_i^{gkt} - \sum_{k\in\mathcal{K}}\sum_{t\in\mathcal{T}} (Q_k \bar{y}_0^{kt}) \Omega^{kt} \\
& - \sum_{(i,j)\in\mathcal{A}}\sum_{k\in\mathcal{K}}\sum_{t\in\mathcal{T}} (M(1-\bar{x}_{ij}^{kt})) O_{ij}^{kt} - \sum_{(i,j)\in\mathcal{A}}\sum_{k\in\mathcal{K}}\sum_{t\in\mathcal{T}} (M\bar{x}_{ij}^{kt}) \Phi_{ij}^{kt} \\
& - \sum_{(i,j)\in\mathcal{A}}\sum_{k\in\mathcal{K}}\sum_{t\in\mathcal{T}} ((Q_k - M)\bar{x}_{ij}^{kt} + M) \Psi_{ij}^{kt} = z_{SP}^*(\bar{y}, \bar{x}) \qquad (2.57) \\
& \text{and } \boldsymbol{E}, \boldsymbol{H}, \boldsymbol{\Gamma}, \boldsymbol{I}, \boldsymbol{K}, \boldsymbol{\Lambda}, \boldsymbol{M}, \boldsymbol{N}, \boldsymbol{\Omega}, \boldsymbol{O}, \boldsymbol{\Phi}, \boldsymbol{\Pi}, \boldsymbol{\Psi} \in \Upsilon, \qquad (2.58)
\end{aligned}
$$

where $\tilde{y}$ and $\tilde{x}$ are the core points of the MP convex hull. Constraints (2.57) and (2.58) ensure that we select a feasible dual solution that was optimal for the original dual SP objective function (i.e., the objective function (2.44)).

In addition to these acceleration techniques, we implement some of the classical acceleration strategies, such as a trust region and knapsack inequalities, to accelerate the convergence rate of the Benders decomposition. For further information on these techniques, the interested reader is referred to [107]. Note that the original dual subproblem is solved first and then the modified subproblem is solved.

2.4 A Meta-Heuristic for PIRP

The aforementioned acceleration strategies proved to be effective in significantly closing the gap obtained by the Benders decomposition. Nonetheless, that was the case only for PIRP with a single vehicle. In the case of multiple vehicles, the gap would still be large even with a large number of iterations. Understandably, developing an efficient, exact algorithm to solve PIRP with multiple vehicles can be very challenging; however, developing an exact algorithm is still desired.

Our ultimate objective of developing the Benders decomposition framework is to get high-quality solutions of the PIRP with a guarantee of their quality. However, since Benders decomposition is not able to yield good solutions in and of itself, we can still utilize Benders decomposition to evaluate the quality of a solution or — even better — to improve on an existing solution by running the Benders decomposition algorithm for a certain number of iterations before termination. To this end, we develop a powerful heuristic to provide good solutions that will later be evaluated by Benders decomposition and improved upon. Note that combining Benders decomposition with heuristics is not new in the literature; see [129] and [43]. Instead of initially solving the master problem with no Benders cuts, which is the standard implementation of the Benders decomposition algorithm, we start with a feasible solution and generate Benders cuts based on that solution. Specifically, we use the solution generated by a heuristic to generate the initial set of Benders cuts.

The two-stage meta-heuristic we develop is inspired by the meta-heuristic developed by Archetti, Boland, and Speranza [9] to solve the IRP, but with major changes due to the differences between the PIRP with accurate estimation of the fuel cost and the IRP. In the following subsections, we describe the main components of the hybrid two-stage meta-heuristic.

2.4.1 Phase 1: Generation of an Initial Set of Solutions

Even obtaining a feasible solution for PIRP within a reasonable computing time may be a challenging task. The basic idea of Phase 1 is to solve a relaxation of the original PIRP model similar to the meta-heuristic developed by Archetti et al. [9]. To this end, we solve the PIRP model by assuming only a single vehicle, and we relax the integrality requirement of the routing variables (i.e., we allow $x_{ij}^t \in [0,1]$ instead of requiring that $x_{ij}^t \in \{0,1\}$). Also, note that the vehicle index is dropped, since all the vehicles are aggregated under one vehicle that has the capacity of all the vehicles combined. Implementing such a procedure provides only one feasible solution; nonetheless, we can get a set of feasible solutions by adding cuts to the relaxed problem to cut the current schedule of visits and hence obtain a new solution. To this end, after each iteration of Phase 1, we add the following cut to the relaxed PIRP formulation and use it to get a new feasible solution:

$$\left(\sum_{i \in \mathcal{V}, t \in \mathcal{T} | \bar{y}_i^t = 1} (1 - y_i^t) + \sum_{i \in \mathcal{V}, t \in \mathcal{T} | \bar{y}_i^t = 0} y_i^t \right) \geq 1, \tag{2.59}$$

where $\bar{y}_i^t$ is the value of the scheduling variable y_i^t found in the previous iteration. Inequality (2.59) simply implies that each iteration in Phase 1 will provide

a solution different than the previous solution by at least one visit to a customer. Adding the cut (2.59) iteratively provides a set of feasible solutions. In our implementation, we solve the Phase 1 mathematical model $\lfloor 1.5|\mathcal{K}| \rfloor$ times by adding $\lfloor 1.5|\mathcal{K}| \rfloor - 1$ cuts iteratively. Thus at the end of Phase 1, we have a set of $|\mathcal{T}|$ feasible solutions. Since each solution yields a scheduling decision and a routing decision by assuming that there is one vehicle, we actually obtain a feasible solution to the original multi-vehicle problem. Obtaining a feasible solution to the original problem is done simply by running the adaptive large neighborhood search (ALNS) heuristic due to Demir, Bektaş, and Laporte [41] on the vehicle routing problem (VRP) instances generated from each solution. For each solution, a VRP instance is generated based on the values of the variables y_i^t and q_i^{gt}. For each $t \in \mathcal{T}$, we identify the set of customers with $y_i^t = 1$ and use the values of $\sum_{g \in \mathcal{S}} q_i^{gt}$ as the demand of customer i. In this way a VRP instance is generated for each $t \in \mathcal{T}$. Thus the ALNS heuristic generates the values of the decision variables y_i^{kt}, x_{ij}^{kt}, and q_i^{gkt}, and hence a feasible solution for the original PIRP formulation.

2.4.2 Phase 2: GRASP

The greedy randomized adaptive search procedure (GRASP) is an iterative procedure developed in the late 1980s by Feo and Resende [46] in which each iteration consists of two phases. In the construction phase a feasible solution is produced, and in the local search phase a local optimum in the neighborhood of the constructed solution is sought. More information on GRASP can be found in [47].

For the construction phase, we use the set of feasible solutions found at the end of Phase 1, hence we can focus on developing the second phase, with the GRASP algorithm, to get a high-quality solution. We define a set of moves from the current solution to a solution in the neighborhood thereof. In what follows, we provide a brief description of the neighborhood moves inspired by the search procedure used by Archetti et al. [9], which are basically remove, insert, and move operations that change the scheduling of visits to customers.

We now describe the remove operations used in our implementation (i.e., operations that lead to removal of a visit to one customer).

1. **Most visited:** The customers are ranked by the frequency of visits scheduled for each of them (i.e., the ratio of the customer's total number of visits to the number of time periods in the planning horizon). This operator starts with an empty removal list. It fills the removal list of the most visited with the 40% of customers that have the highest visit frequencies. Then the algorithm picks one of the customers in the list at random. The selected customer will get a new schedule of visits similar to the previous schedule but with one visit removed. A removable visit is defined as a visit whose removal maintains the feasible solution with respect to all constraints. In case there is more than one visit that could be removed, one of those visits is picked at random to be removed from the set of scheduled visits.
2. **Routing cost:** This operation removes a visit of a customer that has a high routing cost. The routing cost of each customer is defined as the ratio of the sum of the customer's routing costs for individual time periods to

the number of time periods in the planning horizon. The routing cost of each customer in each time period is calculated as the difference between the total routing cost when the customer visit is scheduled and the total routing cost when the customer visit is removed. Note that the routing cost is a vector with $|\mathcal{T}|*|\mathcal{V}'|$ components. After constructing the routing cost vectors, the routing cost removal list of customers along with their visits is sorted and the 40% of customers with the highest routing costs are selected. Then one of the customers in that list is selected for a change in its schedule by having a visit removed.

3. **Minimum delivered quantity:** For each time period, the two customers with the lowest quantities of product to be delivered are selected and added to the minimum delivered quantity removal list. After constructing that removal list, the heuristic picks one of the customers at random and removes one visit from its schedule. Two customers are selected (rather than one) in order to increase the size of the list.

4. **Random selection:** This operator selects a customer at random and finds a visit that can be removed. The selected visit to be removed is the visit that leads to the greatest improvement in the objective function.

Note that each removal is implemented provided that the new schedule of the selected customer maintains feasibility with respect to all constraints (vehicle capacity, demand satisfaction, and inventory capacity). When a visit is removed, the quantity of product that was to be delivered on that visit has to be delivered on some other visit(s). In our implementation, we first try to move the delivery to the visit preceding the removed visit while respecting all the constraints. Otherwise, we try to split the delivery between the visits preceding

and following the removed visit.

We now describe the insert operations used in our implementation.

1. **Least visited:** The customers are ranked by the frequency of visits scheduled for them (i.e., the ratio of each customer's number of visits to the number of time periods in the planning horizon). This operator starts with an empty insert list. It fills the insert list with the 40% of customers that have the lowest visit frequencies. Then, the algorithm picks one of the customers in the list at random and adds a visit to that customer at random.
2. **Holding cost:** This operator adds visits to customers that have a high inventory cost. The inventory cost of each customer is defined as the ratio of the sum of the customer's holding costs for individual time periods to the number of time periods in the planning horizon. The list of customers is sorted by holding cost, and the 40% of customers with the highest costs are selected. Then one of the customers is selected for a change in its schedule by having a visit added.
3. **Maximum delivered quantity:** For each time period, the two customers with the largest quantities of product to be delivered are selected and added to the list. After constructing the list of customers with the largest quantities of product, the algorithm picks one of them at random and adds one visit to the selected customer.
4. **Random selection:** This operator selects a customer at random and adds a visit to its schedule.

For each of the insert and remove operations, the quantities of product that

are to be delivered to the selected customer on the individual visits have to be updated. In our implementation we solve a small LP problem to decide the quantities delivered to each customer (respecting vehicle capacities, customer inventory capacities, and quantities available at the supplier site). The small LP problem objective function is concerned with holding costs and revenues.

Lastly, the move operation tries to change the schedule for a customer by changing the scheduling of one of its visits (i.e., changing a visit from the original time period t' to some time period t for which no visit to that customer was originally scheduled). The move operator is implemented in the same fashion as in [9]: Select a customer i, and time periods t' and t; then remove the visit to i in time period t', and add a visit to i in time period t.

For insert and move operations, routing decisions are updated by inserting the new visit to the selected customer in the selected time period by choosing a route and a position within that route which is based on the minimum cost. After calculating the value of the objective function for each of the selected remove, insert, and move operations, the one with the best value of the objective function is selected and the current solution is updated accordingly.

We define a counter (called COUNT) as the number of times a solution found by GRASP so far was better than the best solution found before that, and we set an upper limit on the value of COUNT. Once the number of times the best solution found so far is equal to the maximum value we set, we run the ALNS heuristic due to Demir et al. [41] to find near-optimal routing decisions for each

time period and update the routing decisions and the value of the objective function accordingly. In our implementation, we set the upper limit on COUNT to 8. Whenever the actual value of COUNT hits 8, we reset it to 0 and run the ALNS heuristic. As to the termination criteria of GRASP, we set an upper limit on the number of iterations of GRASP to be performed when there is no improvement over the best value of the objective function found so far. We set the maximum number of iterations to $15 * |\mathcal{V}|$. Another termination criterion we use is based on the total time spent by the meta-heuristic: If the total time exceeds three hours, the search is terminated.

2.5 Computational Study

In this section, we present computational test and analysis results with an emphasis on:

- Testing the computational efficiency and effectiveness of the proposed solution approach. Specifically, we first examine the effects of algorithmic enhancements on the overall approach to solving PIRP using Benders decomposition and the effectiveness of the developed meta-heuristic for solving large-scale instances of PIRP.
- Examination of the effects—on the solution structure—of using accurate estimation of the fuel cost and incorporating the GHG cost. In this context, we first present a PIRP model that uses the distance traveled as a measure of fuel consumption and compare it to the proposed model. Then we provide an analysis of the delivery, logistics, environmental, and inventory performance indicators.

We randomly generated instances to assess the performance of the developed algorithms for a wide range of situations. Our testbed was composed of instances generated with the following parameters:

- Number of customers, $|\mathcal{V}'|$: 10, 15, 20, 25, 30, 35, 40, 45, 50, 60
- Number of periods in the planning horizon, p: 3, 6
- Number of vehicles, $|\mathcal{K}|$: 1, 2, 3, 4
- Maximum age of the products, $|\mathcal{S}|$: 2, 3
- Demand d_i^t: randomly selected integer from the interval $[30, 300]$
- Positions (x, y) of the supplier and customers: randomly selected from the interval $[0, 150]$
- Inventory capacity of customer i, C_i: $R \max_t d_i^t$, where R is randomly selected from the set $\{2, 3\}$
- Inventory holding cost h_i: randomly generated number in the interval $[0.1, 1.0]$
- Vehicle capacities Q_k: $2 * \sum_{i \in \mathcal{V}, t \in \mathcal{T}} d_i^t / (p * |\mathcal{K}|)$
- For each $g \in \mathcal{S}$, profit from the sale of a unit of product of age g, u^g: a random integer in the interval $[7, 15]$ for each age $g \in \mathcal{S}$
- Fuel cost: \$1.5 per liter
- Vehicle speed: 50 miles per hour

The cost of emitting one ton of GHG was set to \$100, which is consistent with some values found in other studies [99]. All the code was written using MATLAB. The master problem and dual subproblems were solved using Gurobi 7.5.2 on a laptop computer with a 2.8 GHz Intel Core processor and 16 GB of RAM.

2.5.1 Performance of Algorithmic Enhancements

For computational testing of algorithmic enhancements, we generated 3 instances of data with 10 customers, 6 planning periods, and a product with a lifetime of 3 periods. We also varied the number of vehicles from 1 to 3. Table 2.2 reports the computational time in seconds and the calculated gap for each methodology.

Table 2.2 displays the computational results for different algorithms. The first column shows the label of the instance, encoded as $|\mathcal{V}'|$-p-instance#-$|\mathcal{K}|$. The second through fifth sets of columns show the computational time in seconds and the gap percentage for each setting. The gap is defined as $[(\text{UB} - \text{LB})/\text{LB}] * 100$. A gap of 100% indicates that no feasible solution was found at termination. "Standard Benders" refers to the standard Benders decomposition algorithm with no acceleration strategies. Benders+S1 refers to Benders decomposition with S1 acceleration strategies (namely, MP enhanced with a set of valid inequalities, Pareto optimality cuts, knapsack inequalities, and a trust region). Benders+S1+WU refers to Benders decomposition with S1 acceleration strategies and the warm-up start meta-heuristic. GAMS refers to the use of the GAMS modeling language to solve the PIRP directly using the Gurobi solver. As shown in Table 2.2, the standard Benders decomposition technique was unable to find any feasible solution within 30 iterations. When S1 acceleration strategies were utilized, there was significant improvement in solving the PIRP with a single vehicle; however, S1 acceleration strategies were unable to achieve significant improvement for more than one vehicle. For the case of Benders decomposition with S1 acceleration strategies and the warm-up start meta-heuristic, significant

improvement was achieved. In the last set of columns in Table 2.2, we report the computational results as found by GAMS using the Gurobi solver. Note that for the cases where the number of vehicles was more than one, no feasible solution was found within 3 hours and hence the gap result is entered as N.A. Clearly, the results found by GAMS highlight the difficulty of the problem.

Note that since GAMS solver does not enable the user to add the sub-tour cuts dynamically, we used the MTZ formulation to ensure that the GAMS solution does not include sub-tours.

Table 2.2: Summary of the computational results for different algorithms

	Standard Benders		Benders+S1		Benders+S1 +WU		GAMS	
Instance	Time (sec)	Gap (%)	Time (sec)	Gap (%)	Time (sec)	Gap (%)	Time (sec)	Gap (%)
10-6-1-1	6.43	100	8.20	1.17	22.99	1.81	10800	1.97
10-6-1-2	16.14	100	21.21	100	14.62	2.62	10800	N.A.
10-6-1-3	34.93	100	55.28	28.37	22.14	2.75	10800	N.A.
10-6-2-1	6.21	100	6.52	1.33	22.48	1.50	10800	2.37
10-6-2-2	18.64	100	22.70	18.23	13.97	2.48	10800	N.A.
10-6-2-3	33.6	100	43.31	100	17.15	2.95	10800	N.A.
10-6-3-1	8.10	100	6.74	1.12	22.85	1.48	10800	4.38
10-6-3-2	17.42	100	28.61	100	11.61	2.53	10800	N.A.
10-6-3-3	31.04	100	49.32	100	17.13	2.81	10800	N.A.

2.5.2 Computation Time Analyses

In this subsection, we evaluate the solution quality and the performance of the developed algorithm when the parameters and settings are changed for different sizes of instances. There were a total of 120 instances.

We solved the instances with the Benders algorithm combined with the warm-up start meta-heuristic and S1 acceleration strategies. The results are shown in Tables 2.3-2.12. The format of Tables 2.3-2.12 is as follows. Columns 1–4 display the number of nodes in the network (including the supplier) $|\mathcal{V}|$, the length of the planning horizon (p), the number of vehicles $|\mathcal{K}|$, and the maximum age of product $|\mathcal{S}|$. The fifth column displays the computational time (in seconds) spent on solving MP and SP of the Benders decomposition. The sixth column displays the computational time (in seconds) in the meta-heuristic. The seventh and eighth columns display the total time spent by the algorithm (in seconds) and the gap, respectively. The Benders algorithm was terminated after 20 iterations.

Table 2.3: Computational results for the PIRP with 10 customers

$\|\mathcal{V}\|$	p	$\|\mathcal{K}\|$	$\|\mathcal{S}\|$	Benders (sec)	WU (sec)	Total time (sec)	Gap (%)
11	3	2	2	8.62	4.57	13.20	1.33
11	3	2	3	9.57	6.37	15.94	1.87
11	3	3	2	11.02	6.24	17.26	2.81
11	3	3	3	11.00	6.69	17.70	3.08
11	3	4	2	11.02	8.92	19.93	2.82
11	3	4	3	12.79	7.62	20.41	3.70
11	6	2	2	9.42	7.30	16.72	2.12
11	6	2	3	11.96	9.59	21.55	3.31
11	6	3	2	30.37	8.08	38.45	2.75
11	6	3	3	13.64	11.28	24.92	2.89
11	6	4	2	20.48	13.10	33.58	2.53
11	6	4	3	32.33	15.94	48.27	4.14
Avg.						23.99	2.78
Max.						48.27	4.14
Min.						13.20	1.33

Table 2.4: Computational results for the PIRP with 15 customers

$\|\mathcal{V}\|$	p	$\|\mathcal{K}\|$	$\|\mathcal{S}\|$	Benders (sec)	WU (sec)	Total time (sec)	Gap (%)
16	3	2	2	7.64	14.56	22.19	3.61
16	3	2	3	7.31	14.18	21.49	3.94
16	3	3	2	15.30	1.92	17.22	3.02
16	3	3	3	15.89	13.16	29.04	3.28
16	3	4	2	21.94	18.49	40.43	3.29
16	3	4	3	22.42	13.42	35.84	3.28
16	6	2	2	21.38	19.89	41.27	4.61
16	6	2	3	14.50	22.06	36.56	4.69
16	6	3	2	17.91	18.58	36.49	4.09
16	6	3	3	32.46	26.23	58.69	5.78
16	6	4	2	52.27	19.02	71.29	2.93
16	6	4	3	53.85	34.11	87.96	3.15
Avg.						41.35	3.81
Max.						87.96	5.78
Min.						17.22	2.93

Table 2.5: Computational results for the PIRP with 20 customers

$\|\mathcal{V}\|$	p	$\|\mathcal{K}\|$	$\|\mathcal{S}\|$	Benders (sec)	WU (sec)	Total time (sec)	Gap (%)
21	3	2	2	10.17	27.50	37.67	6.16
21	3	2	3	11.61	17.98	29.59	5.84
21	3	3	2	36.26	34.77	71.04	3.79
21	3	3	3	30.09	20.66	50.76	4.48
21	3	4	2	26.54	43.04	69.58	3.58
21	3	4	3	30.40	22.61	53.01	4.73
21	6	2	2	39.33	236.03	275.36	6.23
21	6	2	3	22.73	66.93	89.66	7.22
21	6	3	2	53.03	38.41	91.44	4.57
21	6	3	3	60.46	52.79	113.25	4.44
21	6	4	2	78.55	120.13	198.68	3.56
21	6	4	3	64.43	59.72	124.16	6.01
Avg.						100.35	5.05
Max.						275.36	7.22
Min.						29.59	3.56

Table 2.6: Computational results for the PIRP with 25 customers

$\|\mathcal{V}\|$	p	$\|\mathcal{K}\|$	$\|\mathcal{S}\|$	Benders (sec)	WU (sec)	Total time (sec)	Gap (%)
26	3	2	2	27.08	438.51	465.59	8.47
26	3	2	3	28.70	38.30	67.00	8.63
26	3	3	2	38.33	454.83	493.17	5.62
26	3	3	3	49.29	67.58	116.87	5.19
26	3	4	2	78.89	822.88	901.77	5.38
26	3	4	3	99.74	36.19	135.93	3.18
26	6	2	2	46.20	316.30	362.50	6.87
26	6	2	3	66.58	139.31	205.88	9.07
26	6	3	2	91.39	427.74	519.13	6.24
26	6	3	3	111.30	85.03	196.34	5.85
26	6	4	2	171.67	453.02	624.69	3.73
26	6	4	3	205.80	111.42	317.23	6.00
Avg.						367.17	6.19
Max.						901.77	9.07
Min.						67.00	3.18

Table 2.7: Computational results for the PIRP with 30 customers

$\|\mathcal{V}\|$	p	$\|\mathcal{K}\|$	$\|\mathcal{S}\|$	Benders (sec)	WU (sec)	Total time (sec)	Gap (%)
31	3	2	2	27.54	832.00	859.54	7.70
31	3	2	3	33.38	52.54	85.92	6.20
31	3	3	2	78.11	1570.00	1648.11	5.81
31	3	3	3	77.15	89.71	166.87	4.73
31	3	4	2	146.78	670.08	816.86	5.33
31	3	4	3	110.05	101.47	211.52	3.78
31	6	2	2	34.20	216.30	250.50	10.17
31	6	2	3	69.12	93.18	162.30	9.57
31	6	3	2	199.65	110.58	310.24	9.66
31	6	3	3	223.71	121.97	345.69	7.22
31	6	4	2	292.58	768.48	1061.06	9.42
31	6	4	3	373.36	134.27	507.63	7.13
Avg.						535.52	7.63
Max.						1648.11	10.17
Min.						85.92	3.78

Table 2.8: Computational results for the PIRP with 35 customers

$\|\mathcal{V}\|$	p	$\|\mathcal{K}\|$	$\|\mathcal{S}\|$	Benders (sec)	WU (sec)	Total time (sec)	Gap (%)
36	3	2	2	51.97	2280.00	2331.97	6.84
36	3	2	3	50.14	139.27	189.41	8.56
36	3	3	2	76.34	1620.00	1696.34	4.14
36	3	3	3	89.64	170.00	259.64	7.10
36	3	4	2	160.75	1250.00	1410.75	6.08
36	3	4	3	132.17	86.08	218.25	5.87
36	6	2	2	213.97	1430.00	1643.97	9.78
36	6	2	3	289.20	146.27	435.47	9.51
36	6	3	2	346.97	2150.00	2496.97	6.19
36	6	3	3	451.09	196.06	647.15	8.39
36	6	4	2	521.69	1400.00	1921.69	5.99
36	6	4	3	607.13	332.87	940.00	5.06
Avg.						1182.63	6.96
Max.						2496.97	9.78
Min.						189.41	4.14

Table 2.9: Computational results for the PIRP with 40 customers

$\|\mathcal{V}\|$	p	$\|\mathcal{K}\|$	$\|\mathcal{S}\|$	Benders (sec)	WU (sec)	Total time (sec)	Gap (%)
41	3	2	2	94.15	5200.00	5294.15	12.14
41	3	2	3	65.08	89.15	154.22	11.25
41	3	3	2	129.27	3180.00	3309.27	8.83
41	3	3	3	135.19	257.70	392.89	7.63
41	3	4	2	177.03	2490.00	2667.03	7.04
41	3	4	3	204.72	117.73	322.45	5.98
41	6	2	2	254.53	5160.00	5414.53	7.67
41	6	2	3	168.65	202.18	370.83	6.91
41	6	3	2	636.34	2930.00	3566.34	4.81
41	6	3	3	735.80	307.62	1043.41	4.92
41	6	4	2	622.78	812.27	1435.05	3.01
41	6	4	3	660.16	374.28	1034.44	5.70
Avg.						2083.72	7.16
Max.						5414.53	12.14
Min.						154.22	3.01

Table 2.10: Computational results for the PIRP with 45 customers

$\|\mathcal{V}\|$	p	$\|\mathcal{K}\|$	$\|\mathcal{S}\|$	Benders (sec)	WU (sec)	Total time (sec)	Gap (%)
46	3	2	2	141.28	5260.00	5401.28	14.89
46	3	2	3	77.76	134.11	211.87	13.61
46	3	3	2	214.83	6260.00	6474.83	9.86
46	3	3	3	167.03	223.62	390.65	9.92
46	3	4	2	246.68	7390.00	7636.68	9.52
46	3	4	3	286.57	619.32	905.89	7.31
46	6	2	2	564.51	5590.00	6154.51	10.44
46	6	2	3	254.43	406.97	661.40	9.71
46	6	3	2	1022.65	416.09	1438.74	9.01
46	6	3	3	1103.71	369.65	1473.35	9.41
46	6	4	2	793.78	4180.00	4973.78	12.62
46	6	4	3	1167.78	848.82	2016.59	8.87
Avg.						3144.97	10.43
Max.						7636.36	14.89
Min.						211.87	7.31

Table 2.11: Computational results for the PIRP with 50 customers

$\|\mathcal{V}\|$	p	$\|\mathcal{K}\|$	$\|\mathcal{S}\|$	Benders (sec)	WU (sec)	Total time (sec)	Gap (%)
51	3	2	2	114.71	7290.00	7404.71	14.89
51	3	2	3	135.92	161.28	297.20	13.61
51	3	3	2	266.87	10800.00	11066.87	9.86
51	3	3	3	276.03	214.14	490.17	9.92
51	3	4	2	245.19	10800.00	11045.19	9.52
51	3	4	3	309.68	206.97	516.65	7.31
51	6	2	2	346.86	6890.00	7236.86	10.44
51	6	2	3	443.79	856.57	1300.36	9.71
51	6	3	2	584.45	3450.00	4034.45	9.01
51	6	3	3	744.80	861.22	1606.02	9.41
51	6	4	2	1429.65	4690.00	6119.65	12.62
51	6	4	3	2018.53	785.99	2804.52	8.87
Avg.						4493.55	10.43
Max.						11066.87	14.89
Min.						297.20	7.31

Table 2.12: Computational results for the PIRP with 60 customers

$\|\mathcal{V}\|$	p	$\|\mathcal{K}\|$	$\|\mathcal{S}\|$	Benders (sec)	WU (sec)	Total time (sec)	Gap (%)
61	3	2	2	179.72	10800.00	10979.72	15.03
61	3	2	3	200.41	295.22	495.63	14.07
61	3	3	2	351.10	10800.00	11151.10	13.48
61	3	3	3	458.48	550.54	1009.01	12.23
61	3	4	2	459.94	10800.00	11259.94	10.25
61	3	4	3	616.12	467.74	1083.87	7.76
61	6	2	2	522.44	9290.00	9812.44	15.33
61	6	2	3	542.02	626.99	1169.01	14.27
61	6	3	2	1159.33	10800.00	11959.33	14.06
61	6	3	3	1195.67	736.21	1931.88	11.71
61	6	4	2	1952.81	10800.00	12752.81	10.70
61	6	4	3	2946.21	890.09	3836.30	9.87
Avg.						6453.42	12.40
Max.						12752.81	15.33
Min.						495.63	7.76

As demonstrated by Tables 2.3-2.12, the performance of the developed algorithm is very high when it comes to computational time and quality of the solution obtained, given the complexity of the problem. Also, it is very clear that solving instances where $|\mathcal{S}|= 2$ is more difficult than solving the same size instance with $|\mathcal{S}|= 3$. The intuition behind this is that when $|\mathcal{S}|$ gets close to 1, the problem essentially reduces to solving several instances of VRP, one for each time period within the planning horizon. In the scientific literature, it is well known that algorithms such as branch-price-and-cut perform better than Benders decomposition when solving VRP.

2.5.3 Impact of the Accurate Estimation of the Fuel Cost

To highlight the importance of utilizing a model that accurately calculates fuel consumption levels by incorporating vehicle load and speed in PIRP settings, we compare the solutions obtained by the model presented in this study to those for traditional PIRP models that use just the distance traveled to estimate fuel consumption levels. To this end, similar to what is presented in [39], we employ some key performance indicators (KPIs). These KPIs are classified as one of four types: inventory, delivery, environmental, and logistics. Inventory KPIs include average inventory levels and costs to customers. Delivery KPIs measure the fuel cost and the total distance traveled by the delivery vehicles on all trips. Environmental KPIs measure GHG emissions due to delivery activities. And finally, logistics KPIs measure vehicle fill, average load, and empty running distance. Lastly, note that the generated instances use the same parameters as the instances generated in Tables 2.3–2.12, with a minor difference when it comes to the inventory holding cost. For the sake of consistency, that cost was set to \$0.1 per unit of product per time period across all customers.

The vehicle fill is the ratio of the total load of the vehicle when it departs from the supplier's depot to its capacity. The average load is the ratio of the total load to the number of trips. The empty running KPI is the distance the vehicle travels to get back to the supplier's depot after the last delivery, since all the vehicles return to the depot empty. To provide a more consistent comparison of the two models, we included the cost due to GHG emissions in the traditional model. For the fuel cost, however, we used the accurate estimation procedure utilized in this study to estimate the fuel cost as a function of vehicle

load, speed, and distance traveled.

We ran the comparison experiments on instances with 15 customers, 6 planning periods, a maximum product age of 3 periods, either 1, 2, or 3 vehicles, and three different instances for diversification. We labeled the instances by encoding them as $|\mathcal{V}'|$-p-instance#-$|\mathcal{K}|$. (For instance, 15-6-2-2 means the second instance with 15 customers, six planning periods, and two trucks.) Results of the comparison are displayed in Tables 2.13–2.16. The format of the tables is as follows: the first column displays the instance label, and the next set of columns display the values of the KPIs. Each KPI column is divided into two sub-columns; the first sub-column presents the KPI value found by the model presented in this study (denoted by M1), and the second sub-column presents the KPI value found by the traditional model (denoted by M2). The last set of columns show the deviation between the two models, as $[(\text{M1} - \text{M2})/\text{M1}] * 100$, hence a negative deviation indicates that the M1 value is less than the M2 value.

The inventory and emissions KPIs are presented in Table 2.13. Note that the model presented in this study does not always achieve smaller inventory levels or inventory costs; nonetheless, the levels of GHG emissions are always smaller. This point highlights the importance of utilizing a vendor-managed-inventory system, not only to minimize the overall logistics costs but also to minimize GHG emissions due to transportation. Also, it should be noted that having different inventory levels and costs obtained by the two models immediately implies that different scheduling decisions were implemented, as we show in the analysis of the delivery and logistics KPIs. Furthermore, since it is

not the case that inventory costs are always lower under one of the two models, this illustrates that the cost structure of PIPR is complicated and has several dependencies, and that optimization of all of these components simultaneously is crucial.

Table 2.13: Inventory cost (IC) and emissions KPIs

	IC		Emissions		IC	Emissions
Instance	M1	M2	M1	M2	Dev (%)	Dev (%)
15-6-1-1	455.9	496.0	1430	1492	-8.80	-4.33
15-6-1-2	448.2	411.9	1680	1749	8.10	-4.06
15-6-1-3	583.9	451.3	1811	2015	22.71	-11.27
15-6-2-1	453.1	431.0	1673	1698	4.88	-1.50
15-6-2-2	341.4	345.5	1513	1643	-1.20	-8.64
15-6-2-3	454.0	463.7	2130	2297	-2.14	-7.80
15-6-3-1	467.1	410.7	1803	1979	12.07	-9.76
15-6-3-2	445.4	441.7	2067	2134	0.83	-3.25
15-6-3-3	559.7	576.6	2479	2527	-3.02	-1.96
Max.					22.71	-1.5
Ave.					3.71	-5.84
Min.					-8.8	-11.27

Table 2.14 shows the delivery KPIs. Clearly, solutions found by M1 always indicate a lower fuel cost than those in M2, which implies that traditional models may fail to provide an accurate estimate of the fuel cost unless the vehicle load is incorporated. On the other hand, the total distance traveled (TDT) is not always lower, which implies that minimizing fuel consumption is not always associated with minimizing the total distance traveled during delivery operations, since the fuel consumption is a function of vehicle load as well. Furthermore, this leads to the conclusion that different routing decisions were obtained by the two models, which is consistent with a previous study [13] in the context of VRP.

Table 2.14: Delivery KPIs: fuel cost (FC) and total distance traveled (TDT)

	FC		TDT		FC	TDT
Instance	M1	M2	M1	M2	Dev (%)	Dev (%)
15-6-1-1	3795	3960	3057	2995	-4.33	2.03
15-6-1-2	4461	4643	3634	3708	-4.06	-2.04
15-6-1-3	4807	5349	3622	3817	-11.27	-5.38
15-6-2-1	4442	4509	3567	3594	-1.50	-0.76
15-6-2-2	4015	4363	3266	3417	-8.64	-4.62
15-6-2-3	5656	6098	4662	4967	-7.80	-6.54
15-6-3-1	4787	5254	3801	3672	-9.76	3.39
15-6-3-2	5488	5667	4510	4648	-3.25	-3.06
15-6-3-3	6580	6709	5352	5388	-1.96	-0.67
Max.					-1.5	3.39
Ave.					-5.84	-1.96
Min.					-11.27	-6.54

Tables 2.15 and 2.16 report the logistics KPIs. As shown in Table 2.15, the average vehicle fill (VF) is not always lower in M1 than in M2. The fluctuation in the average vehicle fill is due to the fact in some cases we observe that a vehicle makes a trip for one delivery only and hence the average vehicle fill tends to be lower overall, whereas the average vehicle fill in the traditional model is stable and has less deviation across instances. On the other hand, Tables 2.15 and 2.16 show that the average load (AL) and empty running distance (ER) are always larger in M1, since the vehicle load plays a role in the objective function and hence the model optimizes vehicle load, number of trips, and distance traveled. ER is larger in M1 than in M2, because the vehicle load affects the objective function and a vehicle with a smaller load consumes less fuel.

Table 2.15: Logistics KPIs: vehicle fill (VF) and average load (AL)

	VF		AL		VF	AL
Instance	M1	M2	M1	M2	Dev (%)	Dev (%)
15-6-1-1	0.36	0.60	893	1470	-64.84	-64.6
15-6-1-2	0.76	0.71	925	868	6.23	6.23
15-6-1-3	0.75	0.75	1867	1867	0.00	0.00
15-6-2-1	0.86	0.75	1050	919	12.60	12.5
15-6-2-2	0.50	0.62	595	732	-23.21	-23.07
15-6-2-3	0.91	0.84	715	663	7.36	7.34
15-6-3-1	0.41	0.75	1013	1867	-84.28	-84.29
15-6-3-2	0.90	0.82	707	643	9.01	9.09
15-6-3-3	0.90	0.90	747	747	0.00	0.00
Max.					12.6	12.5
Ave.					-15.23	-15.20
Min.					-84.28	-84.29

Table 2.16: Logistics KPIs (continued): empty running distance (ER)

	ER		ER
Instance	M1	M2	Dev (%)
15-6-1-1	706	679	3.82
15-6-1-2	1080	988	8.52
15-6-1-3	708	369	47.88
15-6-2-1	1122	1007	10.25
15-6-2-2	560	453	19.11
15-6-2-3	1673	1005	39.93
15-6-3-1	783	403	48.53
15-6-3-2	1357	1014	25.28
15-6-3-3	1933	1458	24.57
Max.			48.53
Ave.			25.32
Min.			3.82

2.6 Conclusions

We have addressed the perishable inventory routing problem with accurate estimation of the fuel cost. To solve this problem, we have proposed two differ-

ent algorithms: Benders decomposition and a two-stage meta-heuristic. The Benders decomposition is further improved by several computational enhancements, namely, valid inequalities and a warm-up start heuristic. The computational results show that the Benders decomposition enhanced with several acceleration strategies is efficient in handling small to medium instances, while the two-stage meta-heuristic is capable of handling larger instances with 60 customers and 6 time periods. To demonstrate the practical benefit of our PIRP model with accurate estimation of the fuel cost, we show that savings in fuel and hence GHG can be achieved by utilizing the model.

CHAPTER 3

A SYSTEMS APPROACH TO CARBON POLICY FOR FRUIT SUPPLY CHAINS: CARBON TAX, TECHNOLOGY INNOVATION, OR LAND SPARING?

The material of this chapter is submitted for publication Alkaabneh et al. [6].

3.1 Introduction and Literature Review

The global food system, from fertilizer manufacture, to food storage and packaging, to retailing, is responsible for $19 - 29\%$ of global anthropogenic greenhouse gas (GHG) emissions [126]. Approximately 30% of the total food intake by mass consists of fruits and vegetables, which constitute the largest food group consumed worldwide [121]. Fruit supply chains (FSCs), an important component of this system, play an important role in today's economy, as consumer demand for more healthful diets and fresh products is increasing. The shift toward fresh fruits and vegetables is happening in the context of increased concern over global climate change and the resulting challenges for the food system. Recent debate at the Convention of the Parties of the United Nations Framework on Climate Change (COP21) attests to this concern and to varying viewpoints on how to reduce CO2 emissions. In the context of food systems in particular, COP21 calls for strategies that include agricultural intensification (i.e., sparing of land from agricultural production), food waste reduction in production and distribution, development of CO2-efficient postharvest technologies, and policies to influence behavior of private decision makers (consumers and businesses), among others [52, 61]. Reducing CO2 emissions inform agriculture/food supply chains is challenging because the reductions achievable by

changing farming practices are limited [61, 87] and are hampered by rapidly rising food demand [120, 132]. Hence, interventions to reduce CO2 emissions from these sectors require rigorous approaches that take into account environmental and economic impacts simultaneously.

FSCs possess a set of unique features that require substantial amounts of energy inputs and thus contribute substantially to CO2 emissions. Storage is required to keep fruits fresh, healthful, and consumable during non-harvest seasons. In the meantime, fruit storage is strongly connected to the energy sector, which is the largest contributor to CO2 emissions globally [118, 23, 103]. About 15% of the electricity consumed worldwide is used for refrigeration [36]. The production of field-grown fruit involves consumption of energy by farm machinery and in the manufacture of various agricultural inputs such as fertilizers and pesticides [64]. Cooling during transport and emissions from transport vehicles constitute additional CO2 sources from FSCs. Moreover, a study by Stoessel et al. [121] assessed the life cycle of 34 fruit and vegetable products sold by a large Swiss retailer and showed that shipping of fruits and vegetables is the dominant contributor to the carbon footprint when compared to seedling production, farm machinery use, fuels for the heating of greenhouses, irrigation, and manufacture of fertilizers and pesticides. Hence, reducing CO2 emissions in fruit supply chain systems can play a significant role in stabilizing GHGs globally.

In order to keep food items fresh and to preserve their quality during storage and distribution operations, refrigeration is required at different stages starting from post-harvest activities and ending at retail display. These refrigeration

operations within the FSC are usually referred to as "cold chains" and are an essential part of the modern food system. GHG emissions in cold chains are generated by the energy used to operate equipment and the inherent global warming potential of refrigerant gases; cold chain accounts for approximately 1% of the world's total GHG emissions. For example, about 2.4% of the United Kingdom's GHG emissions are due to food refrigeration; "embedded" refrigeration in imported foods could increase this figure to $3\% - 3.5\%$ of national emissions [51]. Heard and Miller [59] conducted a Life Cycle Analysis to examine social and behavioral factors along with environmental impacts to examine the sustainability implications of expanding the cold chain in developing countries. They pointed out that cold chain expansion in developing countries will provide opportunities to minimize food waste, increase nutrition and improve food safety, but at the expense of higher GHG emissions. Nonetheless, as stated by Garnett [51], there is much room for improving the efficiency of refrigeration in the UK. Garnet [51] argues that energy savings between 20% and 50% are possible through proper specification, use and maintenance of equipment. There is ample information and guidance available from organizations such as the Carbon Trust, the Institute of Refrigeration and the International Institute for Refrigeration to implement energy-saving practices. One particularly promising technology is trigeneration – systems that produce combined heat, power and coolness – and current trials suggest that such technologies are twice as efficient as existing ones. These systems can even use biomass as a fuel source [51].

Several studies addressed the impact of interventions or changes in practices within the food supply chain to reduce GHG emissions. Many of these studies

demonstrated the technical potential of proposed interventions on the environmental dimension using quantitative methodologies. For instance, Westhock et al. [130] used biophysical models to examine the consequences of replacing 25-50% of animal-derived foods with plant-based foods in diets in the European Union and found a 25-40% reduction in GHG emissions in this region. On the production side, Lamb et al. [72] assess the technical potential of land sparing in reducing GHG emissions in the United Kingdom. Lamb et al. [72] found that a land sparing strategy has the potential to reduce 80% of GHG emissions by 2050 (relative to 1990 levels). James & James [68] provided a qualitative estimate of the potential energy savings accruing to different refrigeration processes. These technical studies provide a good foundation for research that integrates economic and environmental impacts of such food supply chain interventions and innovations. Our study offers an integrated framework to simultaneously assess economic and environmental impacts of interventions to reduce GHG emissions in the food supply chains.

This study employs a systems approach to the evaluation of alternative strategies for reducing CO2 emissions in FSCs which considers economic and environmental dimensions simultaneously. Our methodology is based on solving a spatially and temporally disaggregated price equilibrium mathematical model following the work of Takayama and Judge [123] to estimate optimal product flows from supply regions to consumption locations. The model is spatial and considers unique characteristics of different production or consumption locations (e.g., supply functions, carbon sequestration in forests, and consumer preferences). Furthermore, the temporal dimension of the model is critical because fruit production is mostly seasonal. In our model, the decision variables

are production, consumption, export, and import quantities; producer prices for each supply region; retail prices for each consumption location; inter-regional commodity flows; and producers' and consumers' economic surplus (see the Supplemental Material for a detailed description of the mathematical model). The methodology employed here is robust enough to be applied to any FSC in any country.

Figure 3.1 illustrates the U.S. apple supply chain. Generally, apple orchards start the annual production cycle in early spring and apples are harvested in the fall. After harvest, apples enter either sold–for-fresh or the processing markets. Growers typically transport apples from the orchard to packing-shipping facilities, where apples are sorted for fresh or processed markets and, subsequently, stored or shipped to processing facilities. Growers specialized in processed apples typically ship directly from the orchard to processing plants. Apples moved directly into the fresh supply chain are hand-picked and transported from the orchard to packing-shipping facilities. Apples are placed into one of two possible storage types. Apples for sales during harvest season (September to December) are put into regular (cold air) storage, whereas controlled atmosphere (CA) storage is used for fruit distributed during the non-harvest season (January to August). In both periods, fresh market apples are transported in trailer-trucks from packing sheds to retail distribution centers, which are generally located near consumption locations. Fresh apples are also traded in international markets. The United States imported fresh apples by 418.9 million pounds in 2010. Particularly, fresh apple imports peak primarily between April and June. U.S. fresh apples are also exported to other countries. In 2010, the United States exported 1,720 million pounds of fresh apples.

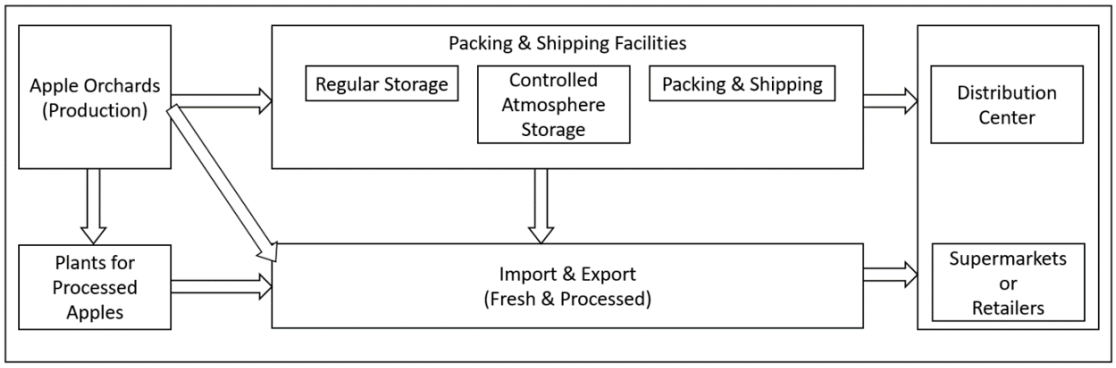

Figure 3.1: Diagram of the fresh apple supply chain

3.2 Methodology and Implementation

We apply our model to the case of the U.S. apple supply chain. The U.S. is the second-largest apple producer worldwide, after China, and apples rank second after bananas in terms of fruit consumed in the country. Furthermore, the apple supply chain is representative of FSCs for most fruits because of its seasonal production and storage requirements. We consider apple production in California, Pennsylvania, Virginia, New York, Michigan, and Washington and forty-nine consumption locations, each corresponding to one of the country's continental states. We take into account five fresh apple varieties (Red Delicious, Golden Delicious, Granny Smith, Gala, and all others) to accommodate regional specialization in specific varieties (e.g., Granny Smith in Washington) and regional differences in consumer preferences. After apples are harvested, they are either shipped directly to consumers, put into short-term storage, or put into long-term storage for shipment during the non-harvest season. The model is inter-temporal and considers two time periods: (1) the harvest season (September through December), during which apples are primarily put into short-term storage prior to distribution; and (2) the non-harvest season (January through August), when apples are put into long-term controlled-atmosphere storage.

Our model takes into account exports and imports of fresh apples, the primary transportation method being heavy-duty diesel trucks, which account for approximately 95 percent of total apple transportation. Apple production in the six states included in the analysis constitutes more than 90% of apple production in the U.S. (see the Supplemental Material for details of the model specification).

3.3 Model Overview

We employ a spatially - and temporally- disaggregated price equilibrium model following Takayama and Judge [123] to estimate optimal product flows from supply regions to consumption locations. The model solves a quadratic programming problem to maximize social surplus measured as the sum of consumers' and producer' surplus minus total costs resulting from all activities within the supply chain. Therefore, CO2 taxes are part of the total costs in the model's objective function. The objective function represents surpluses from both domestic and international sources of fresh apples minus total costs from all practices including storage and transportation. The decision variables are quantities of production, consumption, exports and imports; producer prices of each supply region; retail prices of each consumption location; inter-regional commodity flows; and social welfare levels. Whereas the parameters in the model are supply, demand, import and export function parameters; production yield; capacity parameters (e.g. land capacity for production and the capacity for storage); transportation and storage costs; and CO2 emissions rates due to various activities. On the other hand, model's constraints are related to technical constraints in production and storage (e.g. yield rate in production and loss rate in storage), see the Supplemental Material for details of the mathematical

model.

To parametrize the model, we first identify all activities responsible for emission of CO2, including production, storage and packing, and transportation. Subsequently, we calculate the CO2 emissions from each activity. Then we calculate production yields for each region as well as sequestration rates for apple orchards. Next, we estimate demand and supply functions based on price elasticity estimations for each production region and each demand location (see the Supplemental Material). As for cost and profit components, the model considers the production cost of each apple variety in each state, the cost of electricity for cold air storage, and the shipping cost (see the Supplemental Material).

We formulate three strategies to mitigate CO2 emissions: 1) a carbon tax to penalize emissions; 2) a land-sparing mechanism in which apple production yields increase, allowing some orchard lands to be converted to forests that sequester CO2; and 3) investment in R&D on storage technology, resulting in new storage technologies with lower rates of CO2 emission. To illustrate the impact of different scenarios under each strategy, we use simulation to generate different scenarios. For the carbon-tax strategy, we assume that taxes are in the range of \$50-500 per metric ton of CO2, following the recommendation found in Nordhaus [92]. The tax rate per metric ton is $50 + k * (500 - 50)$, where $k \in [0, 1]$ is the simulation parameter. Effects of CO2 tax is modeled in the following way: First, we identify all activities responsible for emissions of CO2, including production, storage and packing, and transportation activities (please refer to section 3.2 of the Supplementary Material for details). Next, we calculate the levels of CO2

emissions associated with each activity. Subsequently, we quantify CO2 emissions associated with each activity at various apple production levels. In order to calculate the taxes associated with CO2 emissions we multiply CO2 quantities produced by the simulated tax value.

For the land-sparing strategy, we need to specify the improvement in production yield that allows a certain area of land to be spared in order to maintain the same level of production. For this, we assumed that $Production\ level = LB_p + k * (UB_p - LB_p)$, where LB_p and UB_p are lower and upper bounds, respectively, on the future production yield; LB_p was assumed to be the current yield, and UB_p was assumed to be twice the current yield. As production yields increase, the area of orchards required to achieve the same level of production declines, allowing land to be spared; thus $Area\ of\ spared\ land\ =\ k * Orchard\ Area$. The spared land is then used to restore natural habitats; we assume reforestation of spared lands, since forests have higher sequestration rates than apple orchards. Sequestration rates depend on spatial characteristics of the spared land (soil, climate conditions, and other factors). Carbon sequestration rates are available in the Supplemental Material.

For the third strategy we assume that investment in R&D will result in new, innovative storage technologies with lower rates of CO2 emission [126]. In particular, we assume that the CO2 emission rate due to storage activities is $LB_s + (1-k) * (UB_s - LB_s)$, where LB_s and UB_s are lower and upper bounds, respectively, on CO2 emissions; UB_s was assumed to be the current rate, and LB_s was assumed to be 50% thereof. The third step consists of assessment of the eco-

nomic and environmental impacts of each strategy. We employ CO2 emissions as a measure of environmental impact, and apple production quantities—total surplus (producer and consumer)—and producer and retailer prices in each region for measures of economic impact.

Energy savings in cold-storage can be achieved through utilizing new cold storage technologies (such as Phase Change Material, Thermal Energy Storage and Phase Change Thermal Storage Unit) [122, 95, 78], optimized storage practices (such as proper maintenance) [51], and/or clean sources for generating electricity. In our analysis we assessed the impact of several levels of improvements in storage technologies by varying the simulation parameter k. In the three scenarios proposed, namely best case, average case and worst case, where 50%, 25% and 10% reductions in energy use correspond to each case, respectively. The value of the simulation parameter k would be 1, 0.5 and 0.2. From a technical perspective, one particularly promising technology is trigeneration – current trials suggest that such technologies are twice as efficient as existing ones. These systems can even use biomass as a fuel source [51] (see the Supplemental Material for a detailed discussion). As of justifying the figure of assuming increase in production yield by 50%, Lamb et al. [72] assumed increase in production yield of fruits and vegetables by 50% and used that figure in their study to assess the potential of land-sparing strategy in reducing CO2 emissions. Crop technologists argue that there is significant technical scope to further increase crop yields [67, 45]. Nonetheless, the discussion of alternative hypothesis for the increase in production yield is beyond the scope of this study and the interested readers are referred to relevant literature [20, 56, 18, 81, 49].

3.4 Results and Discussion

Figure 3.2 presents the percentage reduction in CO2 emissions (from the current level) as a function of the simulation parameter k for several intervention strategies. Figure 3.2 indicates that investment in R&D which leads to new technologies in the storage sector has the greatest potential to mitigate CO2 emissions. Note that the range of taxes in Figure 3.2 is 50-500$ per ton of CO2.

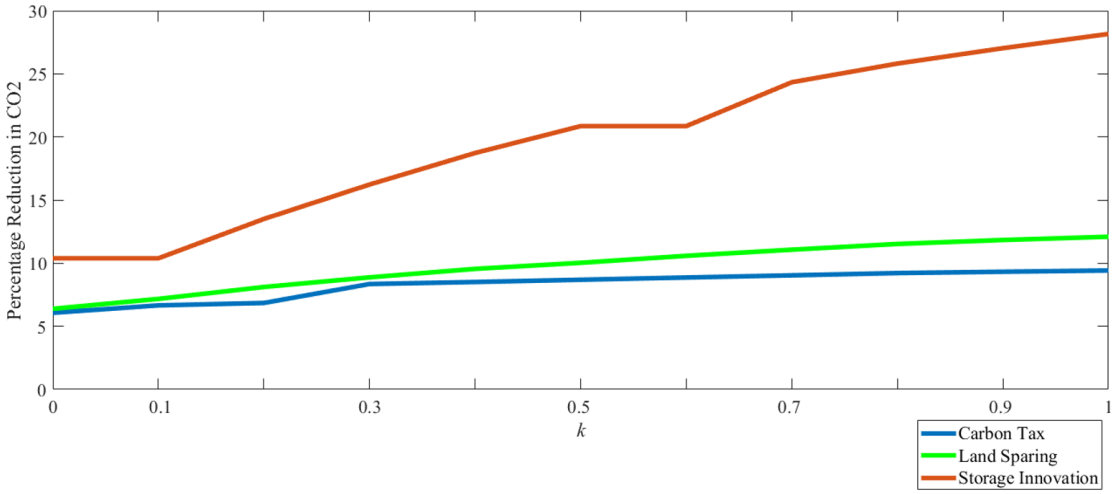

Figure 3.2: Percentage decrease in CO2 emissions (from the current level) due to each strategy

It is challenging to come up with an exact figure for the cost of new storage technologies or new production systems; however, we can evaluate the impact of variable storage or production costs on the performance of the U.S. apple supply chain. If we assume that producers acquire new storage or production technologies and project that this asset fixed cost (as part of the storage or production variable costs) will result in higher variable costs, then our model can easily accommodate for this change by simply changing the current storage or production cost per pound of product (see the Supplemental Material for details

of the mathematical model). To this end, we run several simulation experiments to investigate the impact of such an increase in storage or production costs on the performance of the apple supply chain. We find that if the new storage cost is twice the current value, the consumer price will increase by less than 1%, and that the same is true if the production cost is twice the current value. The main intuition behind this slight increase in the consumer price is that storage or production costs represent a small portion of the total cost of apple production, since labor and ownership costs remain unaffected by the introduction of new technologies (see the Supplemental Material for details on the cost structure of apple production in the U.S.). Higher concentration in production and retailing is likely to increase the impact of higher costs on retail prices [53]. The U.S. food supply chain in general38 and the apple supply chain in particular [54] are highly concentrated and our calibration methods take this feature into account.

As shown in Figure 3.2, innovation in storage technologies has a greater potential to reduce CO2 emissions than land sparing (e.g., 28.2% versus 12.1% for $k = 1$). Indeed, the success of land sparing depends on many factors, including carbon sequestration rates, which in turn depend on several factors, such as forest management [15, 69]. Lamb et al. [72] focused on the case of the UK's agriculture system to show that land sparing has the potential of mitigating CO2 emissions by 80%. However, carbon sequestration rates in U.S. eco-systems are different from those in the UK. We investigated the potential of increasing carbon sequestration rates in selected regions at different increased rates. Our results suggest that if sequestration rates are three times the current rates in these regions, land sparing can offer a 32% reduction in CO2 emissions which is very close to the level of CO2 mitigation resulting from improvements in stor-

age technologies (i.e., approximately 28%). While the potential of land sparing to reduce CO2 emissions depends heavily on spatial characteristics, the degree to which new storage technologies can do so depends on local climate conditions and the particular products under consideration. Given the current trend in global warming, the need for new, innovative storage technologies becomes even more important because of the greater need for storage [68]. Furthermore, different perishable fruits or other food products that need continuous refrigeration require different storage temperatures; hence storage technologies with lower rates of CO2 emission have greater potential to reduce CO2 emissions by larger amounts.

3.5 Additional Strategies

To further explore interventions to reduce CO2 emissions in FSCs, we identify strategies which modify or combine the three strategies discussed earlier. Specifically, we simulate three variations of a carbon-tax strategy: 1) a tax on production activities that emit CO2; 2) a tax on CO2 emissions from storage activities; and 3) a tax on all activities that emit CO2 (strategies 1–3 in Table 3.1). In addition, we consider land-sparing approaches in combination with each of these three tax strategies (strategies 4–6 in Table 3.1), and innovation in storage technology in combination with each of them (strategies 7–9 in Table 3.1). Interventions consisting of a combination of land sparing or innovation in storage technologies with a carbon tax only on transportation activities were not included, since the share of CO2 emissions from transportation is small (9% in our study). In the subsequent discussion, we assume a value of 1 for the simulation parameter k for land sparing and improvement in storage technology

(i.e., that a 100% improvement in production yield will allow for 50% of land to be spared, and that storage technologies will reduce CO2 emissions to 50% of current levels). We note that when considering strategies 1-3, namely carbon tax on different sectors, we assumed that there is no improvement in land sparing nor in storage technologies (i.e., the production yield level is set at its normal levels LB_p) and the CO2 emissions rate due to storage activities are set at their usual levels (UB_s)) and we only change the value of the carbon tax. On the other hand, when considering strategies 4-6, we assumed that the improvement in land sparing is fully realized; nonetheless CO2 emissions rate due to storage technologies is set at usual levels (i.e., the production yield is set at its highest level (UB_p) and the CO2 emissions rate due to storage activities is set at its usual level (UB_s)) and we only change the value of the carbon tax. Lastly, for strategies 7-9, we assumed that there is no improvement in land sparing; while CO2 emissions rate due to storage technologies is set at their lowest levels (i.e., the production yield level is set at its normal level UB_p) and the CO2 emissions rate due to storage activities is set at its lowest level (LB_s)), and we only changed the value of the carbon tax in the simulation.

To analyze how different values of the carbon tax interact with land sparing and improvement of storage technologies if fully realized (i.e., if the production yield level is set at UB_p or the CO2 emissions rate due to storage activities is set at LB_s), we vary the value of the simulation parameter k for a carbon tax. Furthermore, we use new upper bounds on the carbon tax (i.e., $1000 per ton of CO2) and we keep the same lower bound (i.e., $50 per ton of CO2), respectively, per ton of CO2 emissions. While a carbon tax of more than $500 per ton of CO2 emissions are considerably high, our purpose for this exercise was to magnify

Table 3.1: Additional interventions to reduce CO2 emissions

Main Strategy	Variation
Carbon Tax	1. Carbon tax on production
	2. Carbon tax on storage
	3. Carbon tax on transportation
Land Sparing	4. With carbon tax on production, storage, and transportation
	5. With carbon tax on production
	6. With carbon tax on storage
Innovation in Storage Technologies	7. With carbon tax on production, storage, and transportation
	8. With carbon tax on production
	9. With carbon tax on storage

the impact of taxes on land sparing and on innovation in storage technologies.

Figures 3.3-3.10 suggest that strategies that combine a carbon tax with innovation in storage technologies demonstrate greater potential to reduce CO2 emissions in all cases, and that such strategies have the most favorable impact on economic factors (see Figures 3.6-3.10). Figures 3.6-3.8 indicate that the largest reductions in apple production occur through carbon tax strategies alone or strategies that combine a carbon tax and land sparing, except for the cases where tax is imposed on production activities. When carbon tax is imposed on production activities only, all three strategies perform the same when it comes to reduction in apple production or increase in consumer price. In contrast, strategies that combine a carbon tax with innovation in storage technologies have a smaller impact on apple production, because reductions in CO2 emissions that stem from storage innovation alone surpass the net reduction in CO2 emissions due to land sparing. Therefore, improvements in storage technology reduce the cost component that's due to CO2 emissions and hence provide a wider window of feasible operations to growers and packer-shippers. On the other hand,

land-sparing in combination with carbon-tax strategies make apple production economically infeasible when the cost of reducing CO2 emissions reaches a certain threshold.

A critical economic aspect of initiatives to reduce emissions is their impact on prices paid by consumers. Figures 3.9-3.10 show that for a given level of reduction in CO2 emissions, a carbon tax in combination with innovation in storage technologies provides the smallest increase in the consumer price of apples per pound. We also find that, for a given consumer price, a carbon tax in combination with innovation in storage technologies achieves the largest reduction in CO2 emissions.

Our analysis suggests that innovation in storage technologies has a great potential to reduce CO2 emissions in the U.S. apple supply chain. We argue that innovation in storage technologies can contribute to mitigation of CO2 emissions globally. Many food supply chains, as well as supply chains for other perishable products such as pharmaceuticals, are characterized as "cold chains," where continuous refrigeration is used to extend and ensure the shelf life of fresh and processed foods/products [126]. This, together with the fact that consumers expect to have a wide variety of fresh produce available year round, underscores the critical role that innovation in storage technologies will play in initiatives to reduce CO2 emissions in the years to come. Furthermore, James and James [68] point out that use of refrigeration is likely to increase with rises in the average ambient air temperature due to global warming, and this will increase the associated level of GHG emissions. Hence, we argue that realization

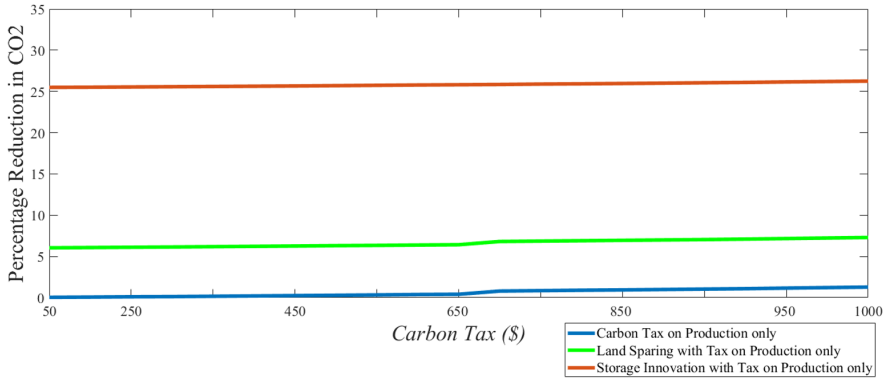

Figure 3.3: Percentage decrease in CO2 emissions with a carbon tax on emissions of CO2 due to production only

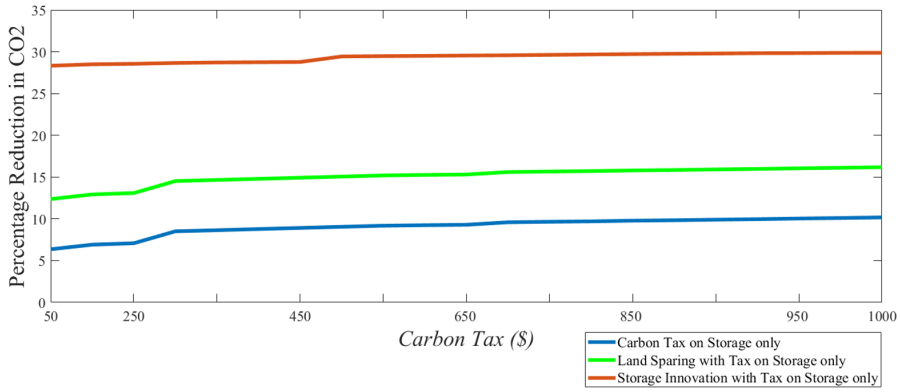

Figure 3.4: Percentage decrease in CO2 emissions with a carbon tax on emissions of CO2 due to storage only

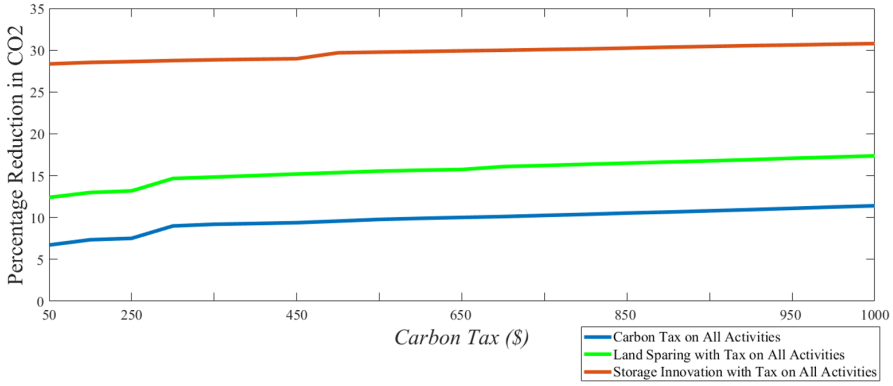

Figure 3.5: Percentage decrease in CO2 emissions with a carbon tax on emissions of CO2 due to all activities in the FSC

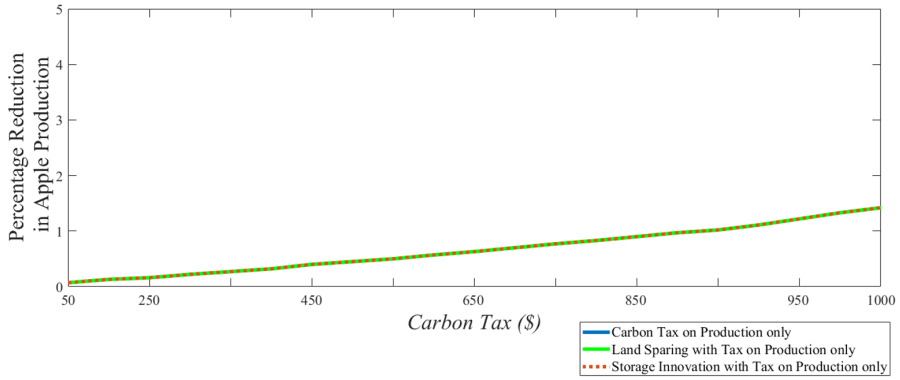

Figure 3.6: Percentage decrease in apple production with a carbon tax on emissions of CO2 due to production only

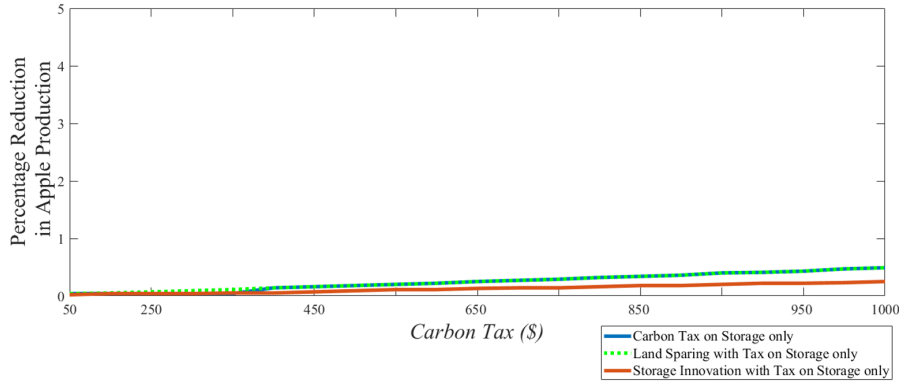

Figure 3.7: Percentage decrease in apple production with a carbon tax on emissions of CO2 due to storage only

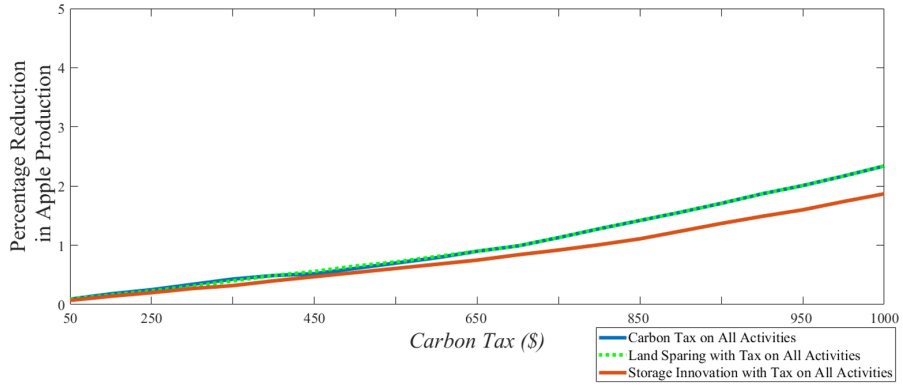

Figure 3.8: Percentage decrease in apple production with a carbon tax on emissions of CO2 due to all activities in the FSC

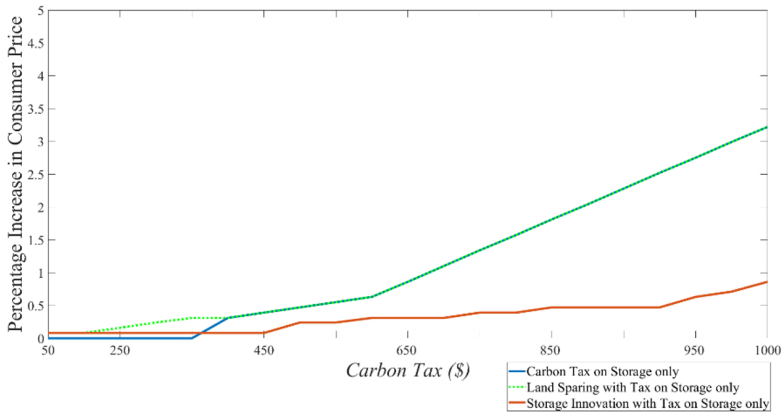

Figure 3.9: Percentage increase in apple prices with a carbon tax on emissions of CO2 due to storage only

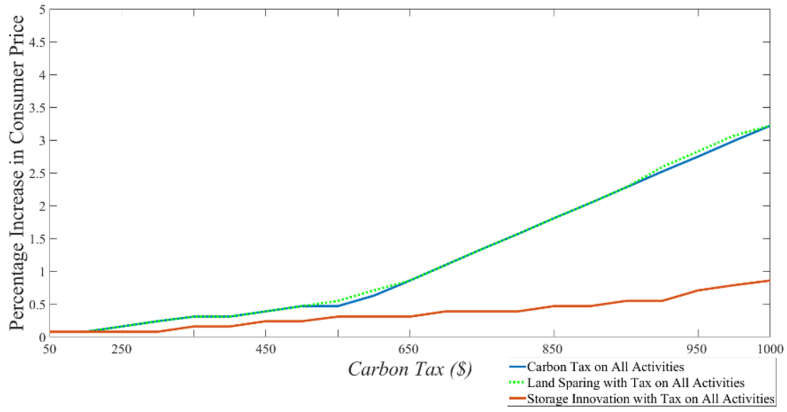

Figure 3.10: Percentage increase in apple prices with a carbon tax on emissions of CO2 due to all activities in the FSC

of CO2 mitigation in storage activities would have far-reaching implications on a global scale. Furthermore, as highlighted in the analysis, the success of land sparing in mitigation of CO2 emissions depends highly on carbon sequestration rates, hence it may not be uniformly effective on a global scale.

In order to cut down CO2 emissions in the apple supply chain case study presented, it might be appealing to propose a carbon tax on all activities within the supply chain to reduce CO2 emissions. Nonetheless, careful examination of Figures 3.6-3.8 clearly shows that such attempts (i.e., proposing carbon tax

on all activities within the FSC) will result in undesired consequences, more specifically decrease in apple production and increase in consumer price and hence compromising the food security dimension. Without taking the systems approach as implemented in our study, measuring such effects will be difficult due to the interactions at the system level among several components in the FSC. Hence, any proposal of carbon tax on different activities within the FSC must be proposed with caution to ensure that the economical and other dimensions are not compromised. While this study shows that carbon tax policy leads to increase in consumer price and decrease in production quantity for the case study presented (i.e., the apple supply chain in the U.S.); projecting these results on the whole food supply chain clearly imply that an increase in prices of food commodities and a decrease in food production is inevitable. Hence, the food security dimension will be compromised.

We evaluate the impact of a carbon tax, land sparing, and innovation in storage technologies on the performance of the apple FSC in the U.S. The idea of exploring the potential for innovation in storage technologies that leads to reduced rates of CO2 emission was inspired by a statement by James and James [68], who argue that new/alternative refrigeration systems/cycles such as magnetic refrigeration have the potential to save energy in the future if applied to food refrigeration. However, none of them appears likely to yield a step-change reduction in refrigeration energy consumption within the food industry in the next decade. Nevertheless, formulation and proposal of sound policies to foster investment in R&D on cold storage technologies could make them a reality in a relatively short time. Our study provides clear evidence that such policies are essential to reducing CO2 emissions, maintaining food security, and strengthen-

ing the economy. In the U.S., one way to achieve these advancements is through reform of agricultural policies and incentives initiated by the U.S. Congress, the United States Department of Agriculture (USDA), and other governmental bodies, while in Europe an obvious mechanism is through reform of the EU's Common Agricultural Policy.

Because our analysis employs a model with spatial and temporal aspects and evaluates the impact of proposed policies on economic and environmental dimensions simultaneously, it contributes to the debate on agricultural production systems by highlighting the importance of implementing a systems approach. As we have shown, optimization on a single dimension of any strategy could result in other dimensions being worsen off. Broadly speaking, our model serves as an excellent tool to assist policy makers in carefully examining the impact of policy options to ensure that domestic objectives are met, since the model takes spatial and temporal characteristics into account. Although it was applied to the U.S. apple production system in this study, it can serve as a model for other agricultural products globally. Our analysis did not incorporate technical aspects of the performance of new storage or production technologies, though we assume that the new technologies will be able to improve twofold, thereby achieving the lower bound on emissions rates posited herein when it comes to storage technologies, and that the production yield can improve twofold as well. However, achieving these benefits in practice calls for reform of agricultural policies by providing incentives to manufacturers to invest in R&D to yield better storage or production technologies. For instance, the European Common Agricultural Policy (CAP) was reformed to dedicate a portion of its funds to rewarding farmers who implement land sharing through agri-environmental

schemes that balance food production against wildlife preservation [62, 98, 84]. Likewise, accomplishing the benefits of R&D and land sparing in practice requires re-shaping of government subsidy schemes and policies to achieve the twin goals of promoting food production and reducing CO2 emissions. Presentation of policy tools and mechanisms to ensure that producers would utilize new production or storage technologies is beyond the scope of this article. We leave it to policy makers to design mechanisms that would achieve this goal; however, implementation of market-based measures and reformulation of subsidy policies seem to be reasonable options.

CHAPTER 4

UNIFIED FRAMEWORK FOR EFFICIENT, EFFECTIVE, AND FAIR RESOURCE ALLOCATION BY FOOD BANKS: APPROXIMATE DYNAMIC PROGRAMMING APPROACH

The material of this chapter is submitted to publication at Omega journal and received a major review request in February of 2020 Alkaabneh et al. [5].

4.1 Introduction.

4.1.1 Motivation

Food insecurity is the state where there is a lack of consistent access to enough food for an active, healthy life[1]. It has been estimated that in 2016, 1 in 8 Americans were food insecure, equating to 42 million Americans, including 13 million children [31]. There are two main programs in the U.S. to combat food insecurity: the Supplemental Nutrition Assistance Program (SNAP) and the Emergency Food Assistance Program (EFAP). SNAP is the federal nutrition program that helps qualified individuals expand their food budget and buy healthy food,[2] while EFAP was established to bridge the food insecurity gap [102, 128, 105, 12]. EFAP food aid services include food banks, community kitchens, soup vans, and subsidized community markets. Note that the term "emergency" usually refers to a short-term solution to a crisis or a problem, and hence it might be thought that services provided by EFAP are temporary so-

[1] As defined by the U.S. Department of Agriculture

[2] https://www.fns.usda.gov/snap/supplemental-nutrition-assistance-program

lutions to food insecurity crises. However, there is increasing evidence in the nutrition and food bank literature showing that EFAP services are becoming more and more critical as the number of individuals who completely rely on them is increasing [12, 38, 70, 86]. This crisis highlights the importance of the emergency food system in the United States, including food banks.

At a high level, the main task of food banks is to collect food that would otherwise be discarded and transfer it to charitable food programs [119]. At the heart of food bank operations is the *resource allocation* operation. Resource allocation basically refers to the distribution of resources to meet some demand. However, because of increased demand combined with limited resources, poor nutritional quality, and unpredictable levels of donated foods [131], the problem of resource allocation for food banks is quite challenging. Furthermore, the evidence linking food insecurity, poor nutrition, and increased risk of chronic health problems underscores the main challenge in resource allocation operations undertaken by food banks [111, 71, 79], namely how to better manage available resources to combat chronic health problems associated with food insecurity rather than simply distributing food without considering its nutritional value. Researchers in the fields of nutrition and nutrition-related diseases suggest that food banks should take a proactive approach in implementing new policies that aim to improve the nutritional quality of products distributed to individuals who are at the risk of hunger or malnutrition [58, 17, 22]. Implementing a new system or policy that is focused more on meeting the nutritional needs of the served population is a challenging task, as it would ideally include having experts in nutrition present at food banks, which would substantially increase the cost of providing services. Thus the availability of a unified frame-

work that increases the efficiency and effectiveness of resource allocation at food banks is paramount.

Given the fact that food banks are non-profit organizations, the measures of success as well as the key performance indices are non-monetary, namely effectiveness, equity, and efficiency. For a food bank, the efficiency performance measure focuses on the total amount (in terms of weight) of food distributed, while effectiveness is a measure of how well the service provided by a food bank meets the nutritional needs of the served population. Lastly, equity (i.e., fairness) refers to the even distribution of resources so that there is no agency at a disadvantage (allocating supply to each recipient in proportion to their demand). Thus our work aims at developing a framework that helps food banks run resource allocation operations more effectively and more efficiently while maintaining equity. Our framework incorporates into the allocation decisions the utility of the agencies served and the nutritional value of the food provided, with a view to combating diseases associated with food insecurity and inequity.

4.1.2 Main Contributions and Results

In this paper, we make the following contributions:

1. We develop a flexible optimization framework and a tractable approximate dynamic programming (ADP) algorithm for resource allocation at food banks where there are multiple resources. The framework considers the effectiveness and efficiency measures and implicitly considers the equity measure. Since our framework is based on dynamic programming,

the proposed framework captures randomness in the system, an important real-life characteristic of the resource allocation problem faced by food banks. To handle the large state space (which arises as a result of considering multiple food resources) in our model, we develop a set of basis functions that estimates the expected utility in the system in order to enhance the performance of the ADP in regard to the amounts of food resources that it indicates should be kept by service providers in their inventory for future use.

2. Using real-world data obtained from a food bank in New York State, we evaluate the quality of solutions produced by our ADP framework. Specifically, we compare the solution proposed by our ADP algorithm to the policy which is currently implemented in practice (namely, the greedy heuristic) and to an offline model (where randomness is revealed up front). The results show that our ADP algorithm outperforms the policy currently implemented in practice by more than 7.73%, while the optimality gap between our ADP and the offline model is less than 9.50%. On the effectiveness side, our framework demonstrates a 3.0% improvement in the nutrition of the served population.

3. We highlight the effectiveness of our framework based on different performance measures that food banks care about. For instance, food banks consider the total amount (in terms of weight) of food distributed as a key performance measure. When considering a utility function that is concave, we show that our model preserves this metric. Our results suggest that the deviation in the total weight of food distributed by our ADP from the total amount distributed under the heuristic currently used in practice is less than 0.30%. This result highlights that keeping some resources to

be used for meeting future needs does not prevent a food bank from distributing essentially the same amount of resources (total) that it currently does.

4.2 Literature Review

Our work is closely related to inventory management for humanitarian logistics, food bank operations, and the approximate dynamic programming literature.

4.2.1 Inventory Management for Humanitarian Logistics

Recent studies in relief inventory management address effective distribution of supplies under supply and demand uncertainty [106, 19, 124, 136, 80]. However, studies that emphasize equitable distribution of donated relief supplies are limited. Equitable and effective distribution is paramount for hunger-relief organizations since supply is almost always below demand. Equitable distribution of resources should ensure a fair sharing of resources among recipients. Only a few studies in the literature explicitly incorporate equity into allocation decisions [10, 93, 94]. Although these studies consider an objective function that is similar to ours, namely effective and equitable distribution Balcik et al. [10] consider designing routes for the multi-vehicle sequential allocation problem faced by food banks when supplies are to be collected from donors such as restaurants and grocery stores and allocated to agencies such as soup kitchens

and homeless shelters. Our study is different in its operational dimension.

4.2.2 Food Banks Operations

Optimizing food bank operations or improving the efficiency of a food bank distribution network has recently been addressed in an extensive body of research. Solak et al. [114] develop a new variant of location–routing that is applicable to nonprofit food distribution networks. Davis et al. [40] study more effective strategies for food collection and delivery operations using a two-phase approach. Specifically, the first phase solves a set-covering model to determine the locations of food delivery points and the assignment of agencies to these points, while the second phase solves the vehicle routing problem for managing food collection and distribution. Lee et al. [74] use a simulation-optimization approach to optimize the staffing operations of a food bank gleaning operation. [44] study the food rescue problem (i.e., collection of food resources from donors and distribution of the collected food to agencies) with the aim of achieving equity and efficiency. In their study, efficiency is defined as collecting and allocating resources to the greatest extent possible. In that context, our work is an important contribution to the literature that focuses on improving bank operations, as we present a unified framework for the resource allocation problem (a problem that food banks have to solve on a daily basis). Schneider et al. [110] examine the problem of determining a partner agency audit schedule for maintaining regulatory compliance by food banks. The audit scheduling problem is basically an extension of the capacitated vehicle routing problem with multiple time windows that includes multiple objectives which stem from having mul-

tiple stakeholders. Lien at al. [77] study the resource allocation problem for a single resource at a food bank where the demand is observed sequentially with an objective function aimed at equitable and effective service. The studies of Orgut et al. [93, 94] consider allocation of a single resource where the capacity of the receiving agencies is uncertain. Our work, on the other hand, considers allocation of multiple resources where supplies are uncertain.

4.2.3 Approximate Dynamic Programming

Currently, there are two general algorithmic strategies for approximating the optimality equation of a stochastic dynamic program, namely approximate value iteration (AVI) and approximate policy iteration (API). In this work, we propose an API algorithmic strategy to obtain a policy that maps the system state (inventory levels of resources) to the action space (how much of each product to allocate to the agencies served). Several studies utilize an API algorithmic strategy to yield high-quality solutions to different kinds of optimization problems. For instance, Maxwell et al. [85], Nasrollahzadeh and Khademi [91], and Perez et al. [97] study ambulance redeployment decisions, Chao et al. [24] and [25] study periodic-review perishable inventory systems with general product lifetimes, Robbins et al. [104] study aeromedical evacuation dispatching, and Silva et al. [112] study surgical scheduling under uncertainty. To the best of our knowledge, however, none of the previous work in the literature considered inventory management and resource allocation in a setting similar to ours.

In that overall context, our work can be viewed as important research that addresses the resource allocation and inventory management problem for food banks. The incorporation of multiple resources to be managed makes our study rather unique and novel. Furthermore, none of the works cited above considers the nutritional quality dimension of resource allocation by food banks, a dimension that is critical to combating diseases associated with food insecurity. We argue that resource allocation by food banks should be an operation that is efficient, effective, and in line with the overall goal of food banks, namely combating food insecurity and diseases associated with it. As a result, our framework considers these important aspects of provision of food aid and key performance measures of resource allocation, as opposed to focusing only on the total weight of food distributed.

4.3 Problem Formulation

This section presents a dynamic programming formulation of the resource allocation problem:

4.3.1 Markov Decision Process Formulation

We have a set of resources that can be used to allocate/distribute a set of products to serve a demand that is known and constant throughout the planning horizon (i.e., deterministic). Each product, when allocated, consumes a certain quantity of resources that is known. At the beginning of a time period, a random

quantity of resources is donated to and collected by the food bank. (The donated quantities are random variables that are time independent; the food bank has no control over the amount of any resource that is donated.) After observing how much of each resource is available (i.e., in inventory), the food bank decides the quantities of individual products to distribute to agencies. Any demand that is not met is lost, and no penalty is paid by the food bank for unmet demand. A food bank can store resources in its storage facilities for later use. Donations of resources occur in discrete quantities. The objective is to maximize the expected utility of agencies over a finite horizon. (The form of the utility function will be defined later.)

Ideally, we would have decision variables that at each time step indicate the quantities of products to allocate as a vector. However, that representation will complicate our problem, as utility is a function of total products distributed. Thus we need a mild assumption to eliminate the curse of dimensionality in the action space. To this end, we assume that products can be put together into bundles, and hence the utility obtained by allocating each bundle is known. From this point on, we refer to an allocation decision to mean selection of a bundle to allocate at a given time step. Parameters and sets of our problem are:

- $\mathcal{T}$ = set of time periods in the planning horizon, $\{1, ..., T\}$, for some finite T;
- $\mathcal{L}$ = set of resources, $\{1, ..., m\}$;
- $\mathcal{J}$ = set of bundles, $\{1, ..., n\}$;

- Q_{it} = random variable representing the donated quantity of resource i received in time period t;
- $\mathbf{Q}_t$ = random variable representing the donated quantity of resources received in time period t, with components $Q_{it},\ i \in \mathcal{L}$;
- d = total daily demand of agencies, which is known and stationary;
- b_j^i = parameter representing the number of units of resource i needed to make bundle j (not necessarily equal to 0 or 1);
- $\mathbf{b}_j$ = vector of the number of units of resource i needed to make bundle j, with components b_j^i;
- r_j = reward associated with allocating bundle j;
- $\mathbf{r}$ = vector of the reward associated with allocating bundle j, with components r_j; and
- size$_j$ = number of servings bundle j provides.

And decision variables of our problem are:

- x_{jt} = binary decision variable equal to 1 if bundle j is distributed in time period t, and 0 otherwise;
- I_{it} = beginning inventory of resource i in time period t; and
- $\mathbf{I}_t$ = vector of beginning inventories of individual resources in time period t, with components $I_{it},\ i \in \mathcal{L}$.

4.3.2 Set of Feasible Actions

Recall that in the introduction we underscored the importance of the resource allocation operation of food banks as a means of combating food insecurity and nutritional insufficiency, as opposed to an operation where the only key performance indicator is based on *"how many products were distributed"*. In order to develop a framework that considers efficiency and effectiveness, we need a notion that considers the nutritional value of the food which is distributed and the overall satisfaction rates of agencies throughout the planning horizon. To this end, we embed the effectiveness in the action space by generating a set of bundles that provide balanced nutritional value to the individuals who ultimately consume the food, and we design bundles of different sizes and with different content to consider different availability states of inventory in the system. Thus it is important to take into account the input of and feedback from nutrition experts in order to come up with a good set of bundles, of different sizes and containing different quantities of food products, in order to provide balanced nutrition to the served population.

We defer the discussion of the efficiency performance measure to §4.3.3.

The constraints in our setting simply state that one and only one bundle is to be allocated at each time step, and that a bundle of a given size and content can be distributed if and only if the resources needed to make up that bundle are available. Let $\mathcal{A}(\mathbf{I}_t)$ denote the set of feasible actions for time period t when

the state of the inventory is $\mathbf{I}_t$. Then

$$\mathcal{A}(\mathbf{I}_t) = \left\{ (\mathbf{x}_t) : \sum_{j \in \mathcal{J}} b_j^i x_{jt} \leq I_{it}\,,\ i \in \mathcal{L}, \right.$$
$$\sum_{j \in \mathcal{J}} x_{jt} = 1,$$
$$\left. x_{jt} \in \{0, 1\} \right\} j \in \mathcal{J}$$

4.3.3 Objective Function and Optimality Equation

In our framework, we embed efficiency in the objective function by using a utility function that is concave and strictly increasing in its argument. Recall that in §4.3.2 we designed different bundles with different sizes and contents. The size of a bundle refers to the number of servings it provides, and hence the number of individuals it can serve. Using the size of a bundle, we can assign a reward value associated with that bundle using any utility function that is concave and strictly increasing. In our study, we define the reward value r_j of bundle j as $\log(\text{size}_j/d)$, where size_j is the number of servings bundle j provides. Using that definition, different bundles of the same size have the same reward value. Thus the efficiency performance measure is explicitly built into the objective function.

In our work, we assume that the decision maker is the food bank manager who is interested in supplying healthful meals to agencies. In practice, at the end of each year food banks report to Feeding America[3] the total quantity of food distributed to agencies. Thus the greater the quantities allocated,

[3]Feeding America is a United States–based nonprofit organization that is a nationwide network of more than 200 food banks that feed more than 46 million people through community-based agencies and other programs. Source: https://www.feedingamerica.org/research/hunger-in-america

the better the performance, provided that the distributed quantity in each operation does not exceed the demand (i.e., oversupply is not permitted). However, having an objective function that is linear and strictly increasing would lead to a situation in which resources are allocated in a greedy way, and no inventory of food would be maintained from one time period to the next; therefore, we utilize an objective function that is strictly increasing and concave. The reasoning behind using a strictly increasing function that is concave as opposed to a strictly increasing function is due to the additive property. Suppose that $g_1(\cdot)$ is a linear function that is strictly increasing and $g_2(\cdot)$ is a concave function that is strictly increasing too, and assume that $g_1(\cdot)$ and $g_2(\cdot)$ are one variable functions. The function $g_1(\cdot)$ satisfies the property of $g_1(a) = g_1(0.6a) + g_1(0.4a) = g_1(0.5a) + g_1(0.5a)$ (where a is a strictly positive scalar); on the other hand $g_2(a) < g_2(0.6a) + g_2(0.4a) < g_2(0.5a) + g_2(0.5a)$. In the context of food banks operations, maintaining stable (i.e., equal) filling ratio throughout the year is preferred over having unstable (unequal) filling ratio. Lastly, our proposed objective function takes into account the utility of the agencies in our framework through the concept of filling ratio. Filling ratio in the context of food banks simply refers to the number of meals allocated over the demand size.

In the context of dynamic programming, a policy refers to the function that maps the state space to the action space (i.e., a prescription of the action to be taken at each possible state of the system). Throughout the paper, we use $\mu(\mathbf{I}) \in \mathcal{A}(\mathbf{I})$ to denote the action to be taken under policy $\mu \in \mathcal{P}$ when the state of the system is $\mathbf{I} \in \mathcal{I}$, where $\mathcal{P}$ is the set of all stationary nonanticipative policies (i.e., policies that cannot see the future) and $\mathcal{I}$ is the state space. If we follow policy

μ, then the state trajectory of the system, $\{\mathbf{I}_t^\mu : t = 1, 2, ..., T\}$, evolves according to $\mathbf{I}_{t+1}^\mu = f(\mathbf{I}_t^\mu, \mu(\mathbf{I}_t^\mu), \mathbf{Q}_{t+1})$, where the transformation function f is simply the state update of the inventory, namely $f(\mathbf{I}_{t+1}^\mu, \mu(\mathbf{I}_t^\mu), \mathbf{Q}_{t+1}) = \mathbf{I}_t^\mu - \mathbf{b}_j \cdot \mu(\mathbf{I}_t^\mu) + \mathbf{Q}_{t+1}$. Note that the random variables are state and action independent. From this point on, we call the function f the state transformation function. Under policy μ, the discounted total expected utility achieved by starting from initial state $\mathbf{I}$ is given by

$$V^\mu(\mathbf{I}) = \mathbb{E}\left[\sum_{t=1}^{T} \gamma^t * \mathbf{r} \cdot \mu(f(\mathbf{I}_t^\mu, \mu(\mathbf{I}_t^\mu), \mathbf{Q}))|\mathbf{I}_1^\mu = \mathbf{I}\right],$$

where $\gamma \in [0, 1)$ is a fixed discount factor. The expectation in the expression above involves the random variable $\mathbf{Q}$. The policy μ^* that maximizes the discounted expected utility can be found by computing the value function via the following optimality equation:

$$V(\mathbf{I}) = \max_{x_j \in \mathcal{A}(\mathbf{I})} \{\sum_{j \in \mathcal{J}} (r_j x_j) + \gamma \mathbb{E}[V(f(\mathbf{I}_t, x_j, \mathbf{Q}))]\} \tag{4.1}$$

The optimization problem (4.1) is intractable, as the state variable is a high-dimensional vector with an exponentially large number of states. To overcome this challenge, the value function at each state is approximated. In our work, we construct high-quality allocation policies based on value function approximations. Our approximation strategy involves the design of an appropriate set of basis functions for use within a linear architecture, as detailed in §4.4.1.

4.4 Approximate Dynamic Programming

4.4.1 Lower Bound

The ADP approach that we use to construct approximations to our value function is closely related to the traditional policy iteration algorithm used in the Markov decision process literature. Instead of finding the optimal policy based on the optimal value function, the policy iteration algorithm searches the policy space by manipulating an existing policy to find a better one. Therefore, a policy iteration algorithm consists of two main steps: policy improvement and policy evaluation. However, policy iteration needs to implement these two steps for each state, which is clearly impractical when the state space is a high-dimensional vector. As a remedy for that shortcoming, the value function at each state can be approximated using the following form:

$$\overline{V}(\omega, \mathbf{I}) = \sum_{p=1}^{P} \omega_p \phi_p(\mathbf{I}) \tag{4.2}$$

In equation (4.2), the components of the vector $\omega = \{\omega_p : p = 1, ..., P\}$ are tunable parameters and $\{\phi_p : p = 1, ..., P\}$ is the set of P basis functions. The basis functions should capture the essential information about the solution of the optimality equation, so that the value function approximation $\overline{V}(\omega, \cdot)$ is a good approximation to the optimality equation (equation (4.1)). Once a good set of basis functions is available, we can use the approximate version of the policy iteration algorithm to tune the parameters $\omega = \{\omega_p : p = 1, ..., P\}$. Thus the greedy policy is the policy that is induced by solving the following optimization

problem:

$$\arg\max_{x_j \in \mathcal{A}(\mathbf{I})} \{ (\sum_{j \in \mathcal{J}} (r_j x_j) + \gamma \mathbb{E}[\overline{V}(\omega, f(\mathbf{I}))]) \} \tag{4.3}$$

Note that solving the optimization problem (4.3) involves computing an expectation that is difficult to evaluate. To overcome this difficulty, we use Monte Carlo simulation to generate a set of samples. Specifically, for each state we generate a set of samples to represent the future state of the system. Algorithm **??** displays the main steps of our ADP framework. Note that A in this algorithm is the number of iterations before termination.

Algorithm 1: Approximate Policy Iteration

1 Initialize the iteration counter $iter$ to 1, and initialize the tunable parameter vector $\omega^{iter} = \{\omega_p^{iter} : p = 1, ..., P\}$ arbitrarily.

2 Solve (4.3) for the function $\overline{V}(\omega^{iter}, \cdot)$ to obtain the greedy policy μ^{iter}.

3 Generate a set of random realizations for the vector $\mathbf{Q}$ over the planning horizon $[0, T]$ for W replications, and follow policy μ^{iter} (note that we can generate the data up front and then follow the policy since the randomness in our system is state and action independent). Let $\{\mathbf{I}_k^{iter}(w) : k = 1, ..., T\}$ be the state trajectory of policy μ^{iter} in replication w. Calculate the discounted reward achieved by starting from state $\mathbf{I}_k^{iter}(w)$ as $Reward_k^{iter}(w) = \sum_{t=k}^{T} \gamma^{t-k} \mathbf{r} \cdot \mu^{iter}(\mathbf{I}_t^{iter}(w))$ and let $Reward_k^{iter}(w)$ be the discounted reward achieved by starting from state $\mathbf{I}_k^{iter}(w)$ and following policy μ^{iter} in replication w.

4 Update the tunable parameters at the next iteration as

$$\omega^{iter+1} \leftarrow \arg\min_{\omega \in \mathbb{R}^P} \{ \sum_{w=1}^{W} \sum_{k=1}^{T} [Reward_k^{iter}(w) - \overline{V}(\omega, \mathbf{I}_k^{iter}(w))]^2 \}.$$

5 If $iter > A$, stop; otherwise, $iter \leftarrow iter + 1$ and go to Step 2.

4.4.2 Basis Functions

In this subsection, we describe the set of basis functions used to obtain the value function approximations used in equation (4.2). In our work we use the following five sets of basis functions:

Baseline

Similar to the work of Maxwell et al. [85], who use a baseline function as a basis function, we use $\phi_1(\mathbf{I}) = 1$ as the first basis function. When ϕ_1 is multiplied by ω_1, the basis function shifts to any desired level.

Inventory Levels

The basis functions for the inventory levels capture information about the inventory levels of certain resources that are critical in the system. Specifically, we define a set of resources that are shared by different bundles, and hence it is more likely that the food bank will run out of such resources quickly. That definition is based on the quantity of supplies of these resources as well as on the importance of such resources in making up different bundles. Denoting $\mathcal{C}$ as the set of critical resources, the second basis function takes the form

$$\phi_2(\mathbf{I}) = \sum_{i \in \mathcal{C}} I_i$$

Similar to $\phi_2(\mathbf{I})$, we can define a basis function that calculates the average inventory level of all resources, hence the third basis function takes the form

$$\phi_3(\mathbf{I}) = \frac{\sum_{i \in \mathcal{L}} I_i}{|\mathcal{L}|}$$

Utility

The fourth basis function computes the utility achieved by the current policy, given the state of the system. Specifically, we use the greedy policy to find the best feasible action for a given state based on the reward function. Thus the algorithm first finds the best action for a given state, $x_j^*(\mathbf{I}) = \arg\max_{x_j \in \mathcal{A}(\mathbf{I})} \sum_{j \in \mathcal{J}} r_j x_j$. Then $\phi_4(\cdot)$ can be calculated as follows:

$$\phi_4(\mathbf{I}) = \sum_{j \in \mathcal{J}} r_j x_j^*(\mathbf{I})$$

Future Utility

Assuming that the random variables for the next time period take their expectation values, a future state can be obtained based on any given state and policy. Specifically, given a state of the system ($\mathbf{I}$), we first obtain the state at the next time period using the transformation function $f(\mathbf{I})$ where the random component in the transformation function is replaced by its expectation value. Once the next state is obtained, we find the utility achieved by the current policy in that state in the same fashion in which we find the utility value for the basis function $\phi_4(\cdot)$. If we denote a future state by $\bar{\mathbf{I}}$, the algorithm first finds the best action for a given state $x_j^*(\bar{\mathbf{I}}) = \arg\max_{x_j \in \mathcal{A}(\bar{\mathbf{I}})} \sum_{j \in \mathcal{J}} r_j x_j$. Then $\phi_5(\cdot)$ can be calculated as follows:

$$\phi_5(\bar{\mathbf{I}}) = \sum_{j \in \mathcal{J}} r_j x_j^*(\bar{\mathbf{I}})$$

Worst-Case Future Utility

Another way to estimate a future state is to assume that the random variables take one of their lowest values, for instance a value in their lowest 5th percentile. Similar to the future utility function where randomness is realized as its expectation value, the worst-case future utility assumes that the values of the random variables lie in their 5th percentile value.

4.4.3 Upper Bound

This section provides an upper bound on the total utility for the resource allocation problem we study in our work. The bound is based on solving the offline model of the resource allocation, where the values of the random variables are revealed up front, at the beginning of the planning horizon (i.e., all unknown parameters are set to their deterministic values). This is achieved by solving a mixed integer programming model that decides which bundle to allocate at each time step throughout the planning horizon. Therefore, the value of the random variable Q_{it} is no longer unknown, and we denote the value of the supply of resource i received at time t by q_{it}—a value that is known and deterministic. To this end, the offline model of resource allocation can be formulated as follows:

$$\max_{x,I} U = \sum_{t\in\mathcal{T}} \sum_{j\in\mathcal{J}} r_j x_{jt} \tag{4.4}$$

$$s.t. \quad \sum_{j\in\mathcal{J}} x_{jt} = 1, \quad t \in \mathcal{T} \tag{4.5}$$

$$I_{i,1} = \text{Inv}_i + q_{i,1} - \sum_{j\in\mathcal{J}} b_j^i x_{j,1}, \quad i \in \mathcal{L} \tag{4.6}$$

$$I_{it} = I_{i,t-1} + q_{it} - \sum_{j\in\mathcal{J}} b_j^i x_{jt}, \quad i \in \mathcal{L},\, t \in \mathcal{T} - \{1\} \tag{4.7}$$

$$\sum_{j\in\mathcal{J}} b_j^i x_{jt} \leq I_{it}, \quad i \in \mathcal{L},\, t \in \mathcal{T} \tag{4.8}$$

$$x_{jt} \in \{0,1\},\; I_{it} \geq 0, \quad i \in \mathcal{L},\, j \in \mathcal{J},\, t \in \mathcal{T} \tag{4.9}$$

The objective function (4.4) maximizes the total utility of allocating bundles throughout the planning horizon. Constraints (4.5) ensure that one and only one bundle is allocated at each time step. Constraints (4.6) and (4.7) define inventory conservation for resources, where Inv_i is the initial inventory level of resource i at the beginning of the planning horizon for time period 1. Constraints (4.8) constitute the restriction that a bundle can be allocated only if the resources needed for that bundle are available. Constraints (4.9) enforce binary and non-negativity conditions on the variables.

The value of U upon solving the offline model (4.4)–(4.9) is clearly an upper bound on the total utility that can be achieved throughout the planning horizon. We compare the value of U against the value of total utility achieved by our ADP described in the previous section. Further details are provided in §4.5.3.

4.5 Computational Results and Case Study

We now present the results of our framework using real-world data provided by the Food Bank of the Southern Tier (FBST), which is located in Elmira, New York. The FBST service area includes Broome, Chemung, Schuyler, Steuben, Tioga, and Tompkins counties, covering nearly 4,000 square miles. FBST serves 18,555 people per week, and it distributed 11,553,304 pounds of food and groceries in 2018. Lastly, it is worth mentioning that FBST is located in a food desert.[4]

4.5.1 Experimental Setup

Feeding America (FA) groups items received by food banks into 31 groups. These groups fall into three broad categories: Foods to Encourage (e.g., cereal, pasta, meat, fish, poultry), Other Food (e.g., grains, baby food), and Non Food (e.g., cleaning, health and beauty, pet) [7]. In our work we consider only the first two groups (Foods to Encourage and Other Food). We exclude the Non Food items since they no nutritional value contributing to the health and well-being of the served population. We further classify the items to reflect the USDA 2015–2020 Dietary Guidelines for Americans [125]. To this end, items are divided into 11 groups: milk, yogurt, cheese, meat, poultry, beans, vegetables, fruits, bread, cereal, and pasta. That grouping identifies the set of resources in our study, hence the state of the system is described by the inventory level of these re-

[4]USDA defines food deserts as parts of the country vapid of fresh fruit, vegetables, and other healthful whole foods, usually found in impoverished areas. This is largely due to a lack of grocery stores, farmers markets, and healthy food providers.

sources. The action space in our work is based on which bundle of products to allocate/distribute. (Recall) that bundles differ in size and content, as described in §4.3.2.) However, each bundle is designed in a way to ensure that its nutritional content is consistent with the Dietary Guidelines for Americans in terms of necessary nutrients and calories.

FBST serves agencies that in turn serve the population which is at risk of hunger. Specifically, each agency receives supplies from FBST once or twice a week on a fixed schedule. The time horizon in our study is divided into weeks, where our algorithm decides which bundle to offer during that week. Fianu and Davis [48] examined different allocation rules that food banks can follow when deciding how much to allocate to each recipient, given the available supplies to be allocated. They found that the proportional allocation rule maximizes equity (allocating supply to each recipient in proportion to their total demand). Thus once a bundle of products to be allocated in a given week is decided, calculating the share of each agency becomes immediate, based on the size of the population served by that agency, using the proportional allocation rule.

FBST relies on four sources to obtain its supplies of food: donations, USDA commodity trading, transfer from other food banks, and purchase from FA. FBST provided us with data on its supplies during the period January 2016 through July 2018. We note that donations constitute more than 86% of total supplies received by FBST. While it is clear that donations and transfer from other food banks are stochastic processes, we claim that purchase of supplies from FA is a stochastic process as well. Note that FBST participates in the Choice system

[65], which is an online auction that allows food banks to order food based on their shares [21]. Feeding America posts available products twice a day, and then food banks bid for products using shares they hold. The food bank with the highest bid wins the bid and pays the price of the second-highest bid. Thus a food bank has no control over acquisition of the supplies that it bids on, since the process of acquiring supplies is a function of other bids, which is clearly out of the food bank's control. Furthermore, supplies acquired from FA arrive in bulk, usually a truckload of supplies. Thus in our analysis we separate the process of donations from the process of purchase of supplies from FA.

Table **??** summarizes the type of supply distribution of food in each category used in our analysis, based on the data provided by FBST. The first column in Table **??** displays the food category, the second column displays the type of supply distribution for supplies obtained via donation and transfer from other food banks, and the third column displays the type of supply distribution for supplies obtained via purchase from FA (through the auction process) and USDA commodity trading. Note that in Table **??**, Gamma(k, θ) denotes a gamma distribution with a shape parameter k and a scale parameter θ (in pounds), Uniform[a, b] denotes a uniform distribution with a minimum value of a pounds and a maximum value of b pounds, and Binomial(p, n) denotes a binomial distribution with parameters p and n (in pounds). On the other hand, Figure 4.1 shows the total amount of food (in pounds) collected in each food category by FBST in 2018.

Table 4.1: Probability distribution of supplies in numerical study

Food Category	Distribution of Supplies from Donation and Transfer	Distribution of Supplies from FA and USDA
Beans	Gamma (1.99, 8500)	-
Bread	Gamma (3.78, 2300)	Binomial(0.10, 20000)
Cereal	Uniform [10000, 20000]	Binomial (0.25, 50000)
Cheese	Gamma (1.33, 5400)	Binomial (0.05, 30000)
Fruits	Uniform [15000, 25,000]	-
Meat	Gamma (1.67, 50)	Binomial (0.15, 40000)
Milk	Uniform [7000, 12000]	-
Pasta	Uniform [6000, 9000]	Binomial (0.13, 40000)
Poultry	Uniform [5000, 10000]	Binomial (0.10, 20000)
Vegetables	Uniform [60000, 80000]	-
Yogurt	Gamma (2.26, 165)	Binomial (0.25, 15000)

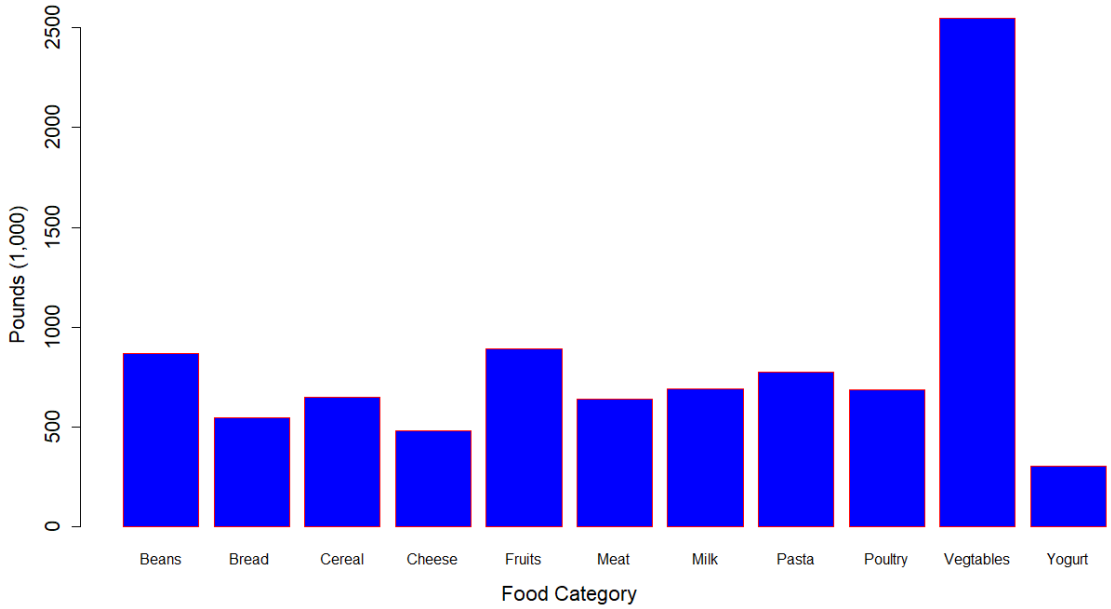

Figure 4.1: Total weight of food collected by FBST in each food category

The simulation horizon is 52 weeks (i.e., one year). The discount factor (γ)

used in our numerical experiments was set to 0.8. The initial value of the tunable parameter vector $\mathbf{r}$ was set to $\mathbf{0}$, and we used $W = 30$ replications in Step 3 of our algorithm.

4.5.2 Performance of Static Policies

In this subsection, we investigate the performance of different static policies. A static policy searches the feasible action space and takes an action based on a pre-specified rule. In our study, we examine three static policies: greedy policy (for any given state, search the feasible action space and take the action that maximizes the utility), allocate 90% of available inventory as long as it does not exceed the demand, and allocate 80% of available inventory as long as it does not exceed the demand.

Once all policies are examined, the policy that performs best in terms of the optimality gap compared to the offline model (where randomness is revealed up front) will be adopted as a benchmark against which to compare performance of the ADP algorithm that we present in the next subsection.

Table 4.2: Performance of static benchmarks

	Performance (95% confidence interval)		
Static benchmark	Average gap (%)	Standard deviation	Confidence interval
Greedy	18.9	2.44	0.24
Allocate 90%	21.3	1.92	0.19
Allocate 80%	28.9	2.20	0.22

Table 4.2 shows the performance of the three static policies. Note that the greedy policy (the one used by FBST personnel) performs the best. We note also that the policy that allocates 90% performs slightly worse than the greedy policy. Thus we adopt the greedy policy as the one against which to compare it against the performance of the ADP.

4.5.3 Baseline Performance

The goal of this subsection is to analyze the performance of the ADP against two benchmark policies: an offline model where all randomness is revealed at the beginning of the horizon (see §4.4.3) and the best static policy as identified in §4.5.2. Figure 4.2 displays the gap between the static policy and the offline policy, and the gap between the ADP algorithm and the offline model for 30 iterations. The horizontal axis shows the iteration number, and the vertical axis shows the gap with respect to the offline model. From Figure 4.2, we observe that the best policy is obtained at the twelvth iteration, and this policy yields a gap of 5.56% against the offline model. To further analyze the performance of this policy (namely, the performance of the ADP when the values of the tunable parameters in ω are set as found in the fifth iteration) carefully, we simulated its performance for an independent set of 400 replications. From these 400 replications, the gap between the ADP algorithm and the offline model is $9.45\% \pm 0.32$, where ± 0.32 is a 95% confidence interval.

The best policy obtained by our ADP approach improves on the best static policy by $7.45\% \pm 0.28$. These improvements are obtained without acquisition of

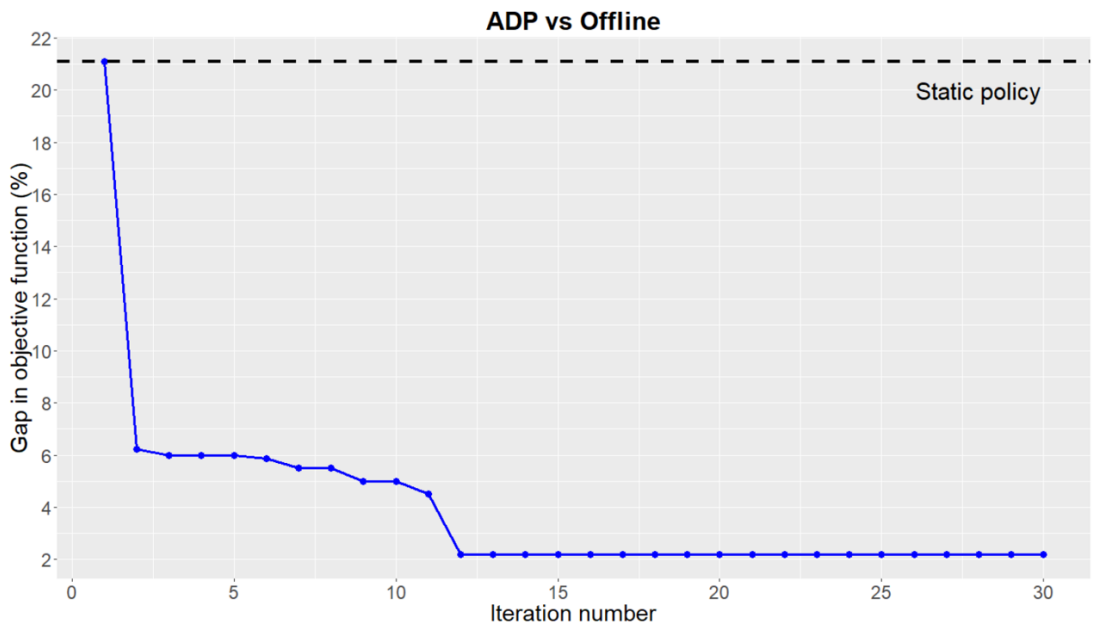

Figure 4.2: Peformance of our ADP approach and the static policy against the offline policy

any extra supplies of food. The food bank personnel could realize these kinds of improvements by simply using their existing resources more efficiently.

The CPU time for each iteration of our approximate policy iteration algorithm is 34.6 seconds. Such runtimes are acceptable, given that we run the approximate policy iteration algorithm in an offline fashion to search for a good value function approximation. Once we have a good value function approximation, it takes about 80 milliseconds to make one allocation decision by solving an optimization problem of the form (4.3). This CPU time includes enumerating over all feasible decisions and estimating the expectations through Monte Carlo samples; it is far faster than necessary for real-time operation.

4.5.4 Contributions of Different Basis Functions

The performance of the ADP algorithm depends heavily on the number and design of the basis functions. Specifically, the smaller the number of basis functions, the smaller the computation time. On the other hand, having a small number of basis functions may affect the quality of solutions obtained by the ADP algorithm. In this subsection, we investigate the importance of different subsets of the set of basis functions on the computation time and performance of the ADP.

In the first set of experiments, we included all the basis functions except the third one (the one for the utility), hence the basis functions for the baseline, the inventory levels, and the future utility and worst-case future utility functions were included. In this setting, the gap between the ADP algorithm and the offline model is 15.83%, with an average time of 27.7 seconds per iteration.

In the second set of experiments, we included all the basis functions except those for the inventory levels, hence the basis function for the baseline and the basis functions for the utility, future utility, and worst-case future utility functions were included. In this case, the gap between the ADP algorithm and the offline model is 13.57%, with an average time of 26.52 seconds per iteration.

In the last set of experiments, we included all the basis functions except the ones for the future utility and the worst-case future utility. In this case, the performance of the ADP is very similar to that of the static policy that allocates

90% of available resources (see §4.5.2), with an average gap of 21.54% and a computation time of 24.80 seconds. This observation highlights the importance of including basis functions that extract information about future states of the system.

4.5.5 Testing for Nutrition

In order to demonstrate the benefits realized by our model in regard to the nutritional content of the food supplied, we need to compare it to the current allocation policies implemented by food banks. Martin et al. [83] state that currently there is no way to rank foods nutritionally for food banks and food pantries. Current systems rank food items based on either a binary system (i.e., foods are either healthful or not) or a three-tier ranking system (choose frequently, choose occasionally, or choose rarely). However, such ranking systems are not informative when it comes to allocation decisions, since food bank staff cannot use them to make decisions on bundle content. Thus the benchmark we use in this section to compare the results on the nutrition dimension are based on the greedy static policy developed in §4.5.2.

We find that the nutritional content of meals allocated by our model exceeds that of meals allocated by the greedy policy by $3.41\% \pm 0.15$. This result is somewhat counterintuitive, as one might expect to see higher nutritional content in meals distributed by the greedy policy, since the total weight of food distributed by the greedy policy is slightly more than the weight of food allocated by the ADP algorithm. However, we note that in many cases the greedy policy would

allocate food items from a certain category that prevents provision of food for a full healthful meal in the next time period. That note is consistent with the line of reasoning that recommends keeping some amount of scare resources on hand for future use, since a healthful meal is by definition a meal with certain nutritional content rather than a meal of a certain weight.

Based on that observation, another interesting point to discuss is that food banks can improve the nutritional quality of food items they distribute, by deciding what foods and how much of them to allocate in each time period, rather than simply allocating all the food that is available. Food bank staff may believe that they have limited capacity to change what is stocked on the shelves. Therefore, they should make their decisions based on a model that sets reasonable standards for the types of foods that are available, so that staff members do not feel as if everything they stock is in the "unhealthful" category.

4.5.6 Managerial Insights

One of the metrics that food banks use as a measure of efficiency of their resource allocation operations is the total weight of food distributed over the course of an entire year. Recall that the objective function used in our study is a concave function that is strictly increasing, as opposed to an affine function that is more in line with the objectives of food banks. The intuition behind using a concave function to assess the utility dimension in our study is to have a more balanced filling ratio throughout the year. In this subsection, we provide

some insights highlighting the efficiency, effectiveness, and equity performance measures achieved by our framework.

Savas [108] identifies efficiency, effectiveness, and equity as key performance measures in nonprofit settings. In this subsection, we analyze the performance of our framework in regard to these three metrics and provide some managerial insights.

As defined by savas [108], *efficiency* "measures the ratio of service outputs to service inputs." In the context of food bank operations, food bank personnel focus on the total number of pounds distributed as a measure of efficiency. Comparison of our ADP approach to the static policy shows that the deviation in the total weight of food distributed by our ADP from that of the static policy is less than 0.30%. That is an important insight which shows that our framework does not compromise the performance measure of the total weight of food distributed.

Effectiveness measures how well the need for the service is satisfied and the extent to which unintended adverse effects are avoided. In the context of food banks, one of the most important measures of effectiveness is how well the service provided by a food bank meets the nutritional needs of the served population. Comparison of our ADP approach to the offline model shows that the percentage increase in distributed healthful meals is $2.83\% \pm 0.14$, where ± 0.14 refers to the 95% confidence interval. Also, the difference between the static policy and our ADP framework is $3.15\% \pm 0.20$, where ± 0.20 refers to the 95%

confidence interval.

Equity refers to fairness, impartiality, or equality of service. In the context of food bank operations, equity refers to the even distribution of resources so that none of the agencies served is at a disadvantage. While our framework does not consider resource allocation at the micro level, namely deciding the portion that each agency receives at each time step we argue that incorporating equity into our framework is a trivial task. Our framework decides the total quantity of each resource to be allocated each week (or at each time step). Once this quantity is decided, the food bank can decide how much to allocate to each agency simply by following the proportional allocation rule, where the quantity allocated to an agency is proportional to the size of the population it serves.

Managerial insights: While traditionally the mission of food banks has been to distribute resources to individuals who are at risk of hunger, the rise in obesity, chronic diseases, and diet-related diseases among food-insecure individuals has pushed food bank personnel to actively seek better ways to distribute resources so as not only to bridge the gap in food insecurity but also to combat diet-related diseases. Handforth et al. [58] conducted a survey to assess nutrition-related policies and practices among a sample of 20 food banks from the national Feeding America network. They found that most food bank personnel reported efforts to promote the health of the served population. For instance, some food banks described the use of nutrition-profiling systems to evaluate the quality of the products they distribute. The goal was to ensure that the total distribution of each targeted nutrient equated to the amount necessary to supply the reference

daily intake for the total population receiving products over a selected period of time. However, a major obstacle in implementing a nutrition-profiling system across food banks is the shortage of nutrition-trained personnel to run the system. In fact, some of the respondents of the aforementioned survey voiced concern that to be sustainable, these systems require extensive nutrition expertise. Furthermore, one participant suggested that Feeding America should develop a system for all food banks to use, so that even those with no personnel trained in nutrition could evaluate their inventories. The design of the action space in our framework, which is in line with the Dietary Guidelines for Americans, makes our framework consistent with the requirement of a nutrition-profiling system that assists food banks in providing services that not only fight food insecurity but combat diseases related to food insecurity as well. Therefore, we claim that our framework has the added benefit of assisting food banks to better manage their resources in an effective manner.

In many systems that are designed to provide real-world relief inventory management for humanitarian logistics, accurate estimation of randomness is a very challenging task. In the case of food banks, it is almost impossible to accurately predict the donations they will receive in the future. Our framework improves the ability of food bank personnel to effectively manage the available resources, by developing a dynamic programming model to optimize distribution decisions in the presence of randomness. One important finding from our case study is the importance of designing basis functions within the ADP model that capture information about future states.

4.6 Conclusions

Combating food insecurity and diseases associated with it in developed countries requires substantial commitment from food banks, donors, and public health organizations. The number of individuals who are food insecure in the U.S. is more than 40 million, with an attendant health care cost of more than $\$160$ billion in 2014 [33]. Several food banks in the U.S. within the Feeding America network are seeking new practices and policies to provide more nutritious food items to individuals who are at risk of hunger. Our framework presented in this study serves as a unified system to help food banks more efficiently manage their food resources in order to serve their population and combat food insecurity in an effective manner. One important feature of our framework is that food banks can run an efficient and effective system without the cost of having nutrition experts on staff.

We tested our framework against different allocation strategies in order to analyze the contribution of each strategy on different performance measures. Our results using real-world data obtained from one of the food banks in New York State demonstrate significant improvement in the allocation process over static policies. We also show that our framework leads to improvement in the nutrition dimension of the served population over the static policies by 3.0%. This improvement is due to the fact that our developed framework explicitly considers the nutrition dimension of the served population as well as future utility.

Future research could utilize our system as a baseline model and extend our framework to consider non-stationary distribution of supplies, stochastic demand, other utility functions, and more resource allocation operations at food banks, such as the school BackPack program (a program at food banks which is dedicated to children who receive free or reduced-price meals at school—for many of these children, school meals may be the only meals they eat) and the Mobile Food Pantry program (a program at food banks which is dedicated to providing food for senior citizens and for people in communities in remote areas who have limited or no means of traveling to their local food bank). Incorporating these complexities may require constructing additional basis functions.

CHAPTER 5

ANALYZING DEMAND AT MOBILE FOOD PANTRY PROGRAMS USING DATA ANALYTICS

The Mobile Food Pantry (MFP) is a program operated by food banks to directly serve clients and underserved population to help them bridge the food insecuiruty gap. The MFP is dedicated to populations with limited mobility, such as senior, populations in areas where there is no access to hunger-relief agencies, or rural communities with little transportation. Clients of MFP receive food items in a pre-packed boxes or they can pick the food products and groceries they need in a shopping fashion. The Mobile Pantry Program plays a critical role in expanding the capacity of food banks to increase the accessibility of underserved communities to food products and groceries. Furthermore, MFP allows food banks to provide food and grocery products – including fresh produce, rice, meat, and hot meals – to people more efficiently.

Food banks offering the Mobile Food Pantry program to their local communities start by identifying the locations and addresses of the temporarily distribution centers where the service takes place at a certain time via a predefined schedule. These distribution centers are carefully selected to cover areas of underserved population to increase their accessibility. After carefully selecting these distribution centers – usually a church, fire station, or ambulance base – food bank personnel decide on the visiting schedule of each distribution center, namely the visit date and time. The product of this decision making process is called 'Master Plan' where distribution centers are located and schedule of visits to these distribution centers is decided and then this information is shared

with the local communities. It is worth mentioning that any individual has the freedom to visit multiple distribution centers within the same month or even within the same week, this is at least true in the case of the Food Bank of the Southern Tier.

The main challenge food bank personnel face is to predict how many people will show up at each distribution centers at each visit throughout the year. Accurate prediction of the number of people is critical to the program as over estimating the number of people leads to food waste and hence lost in food products; on the other hand, under estimation leads to under serving the recipients and thus denying the goal of the MFP program.

We partnered with the Food Bank of the Southern Tier to help them predict the number of recipients showing up at their distribution centers throughout the year. The goal is basically to inform food bank personnel about the guidelines they need to follow when estimating the number of people showing up by utilizing data analytics enabled tools and operational policy recommendation.

5.1 Data Description and Methodology

In this section, we describe the data, our demand representation and the data-analytics methodology we applied for our study to building guidelines for the food bank personnel to use in predicting demand.

5.1.1 Study Population

We gather data from the Food Bank of the Southern Tier located in Elmira-NY, the data we gather is from January 2019 to December 2019. We excluded MFP programs that have 4 or less visits in the year of 2019. The final data set consists of 727 unique observations (72 unique programs), whose relevant variables are summarized in Table 5.1. The dataset contains demographics data of each town/city, weather, spatial, and temporal information. Figure 5.1 displays the total head count each day aggregated across different programs taking place on the same day, note that the FBST runs multiple MFP programs within a given day serving multiple distribution centers. Figure 5.2 shows the locations of the distribution centers and the color of the circles reflect the average demand at each site. The average demand is calculated as the total demand throughout the year at that distribution center divided by the number of visits to the distribution center. Note that some locations received 12 visits during the year of 2019, namely a visit each month, while other locations received less than 6 visits; however, as mentioned earlier, distribution centers that received less than 4 visits were excluded from the analysis.

Table 5.1: Summary statistics for the study data set (Jan 2019 - Dec 2019)

	Mean (standard deviation)
Demographics	
Population	8,697 (14,000)
Income per capita	17,660 (3,483)
Poverty	14.19 (7.93)
Weather	
Total snow (cm)	0.29 (1.23)
Temperature ($^{\circ}C$)	7.12 (11.71)
Wind speed (km per hour)	11.2 (7.37)
Spatial	
Address	-
Site	Factor: church, fire station, ambulance base,...
Accessibility	Factor: Seniors only, Students only, Public
Temporal	
Date	-
Day of the week	Factor (Sunday, Monday,...)
Time during the day	Time
Primary outcome	
Head count	Factor: Normal, Too high, Too low

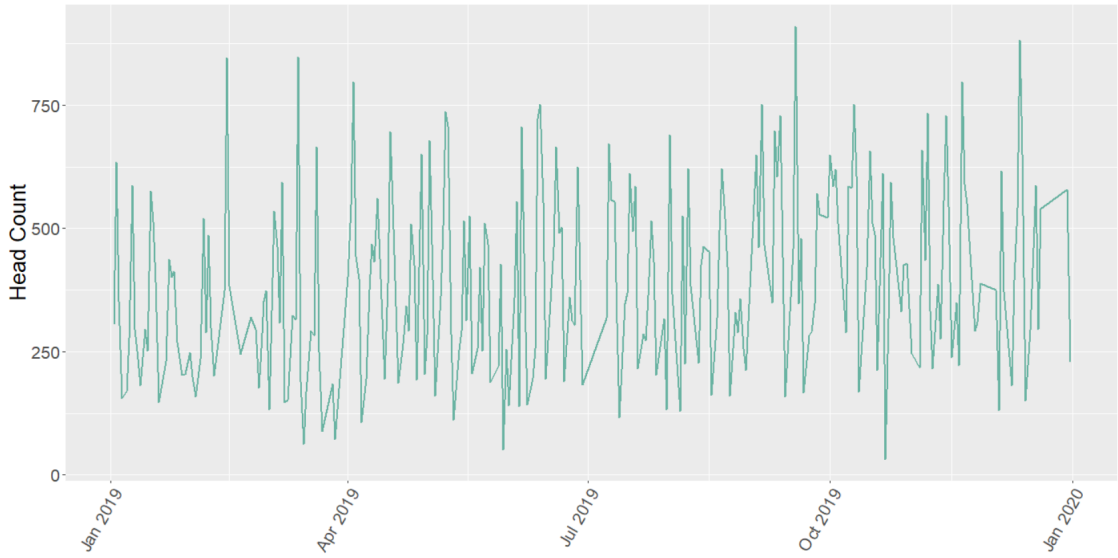

Figure 5.1: Headcount of recipients at different MFP during the year of 2019

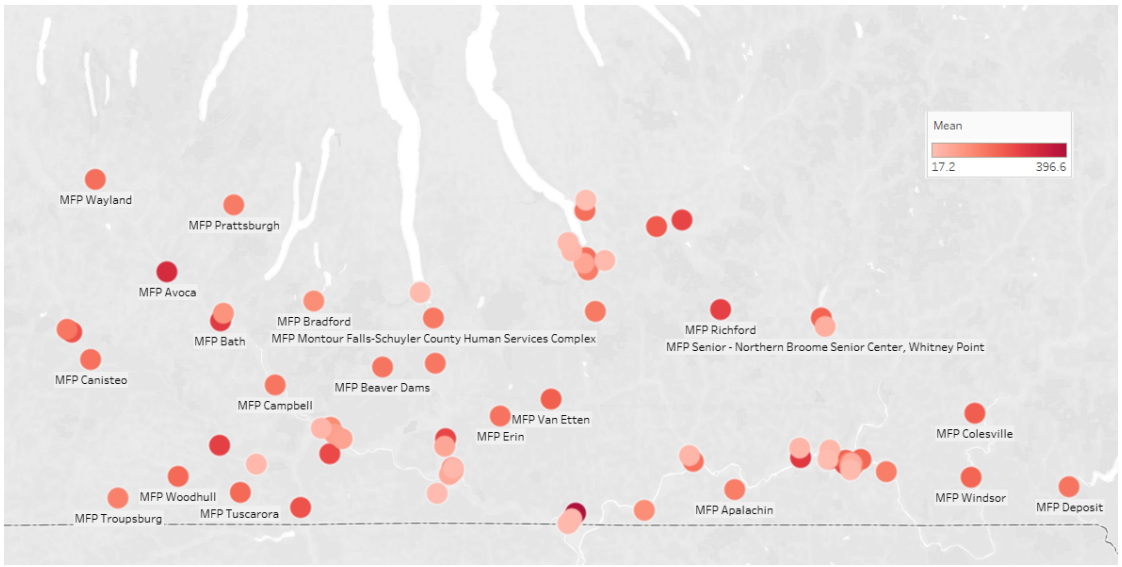

Figure 5.2: Distribution of MFP across the six counties in the Southern of NYS

5.1.2 Current Guidelines

Currently, food bank personnel use only weather data to predict the demand at the distribution centers throughout the year. Food bank personnel claim that if the weather is nice, more people will show up. On the other hand, if the weather is cold, less people will show up. However, we argue that this guideline is not enough. Later on in this chapter we will reveal interesting aspects about the behavior of people to better predict the number of people showing up. Furthermore, we will provide some policy recommendation to food bank personnel on how to increase the efficiency of their MFP network and improve the accessibility for people living in certain locations by changing the schedule of pickups of close by locations.

5.2 Results and Discussion

5.2.1 Is Weather the Most Important Factor to Predict the Number of Recipients at MFP Distribution Centers?

Food banks personnel believe that the weather is the most critical factor in predicting the number of people showing up at each location. Nonetheless, the data suggest otherwise. Figures 5.3 and 5.4 are double y-axis plots showing the headcounts at two MFP programs during the year of 2019 as well as the temperature in Celsius. The stories we see from the First Assemble of God Church and the American Legion programs tell us clearly that the temperature is not the most important factor since there are days with cold weather and high demand! In the next subsection we will run a set of hypothesis to analyze the importance of different factors and develop guidelines for the food bank personnel to better predict the demand.

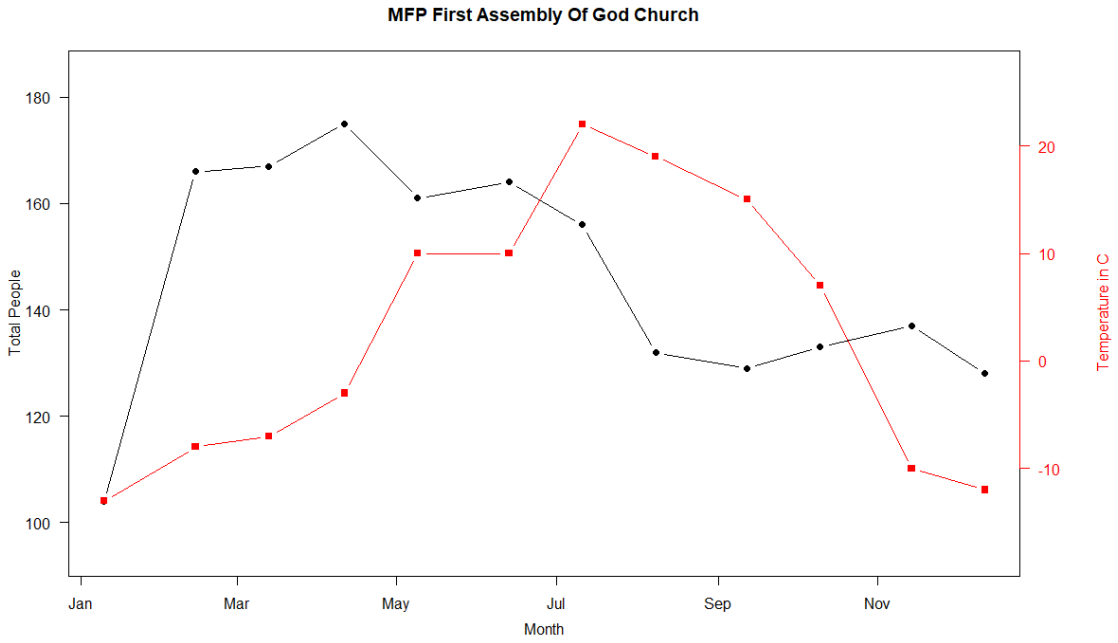

Figure 5.3: Headcount at First Assembly Of God Church distribution center

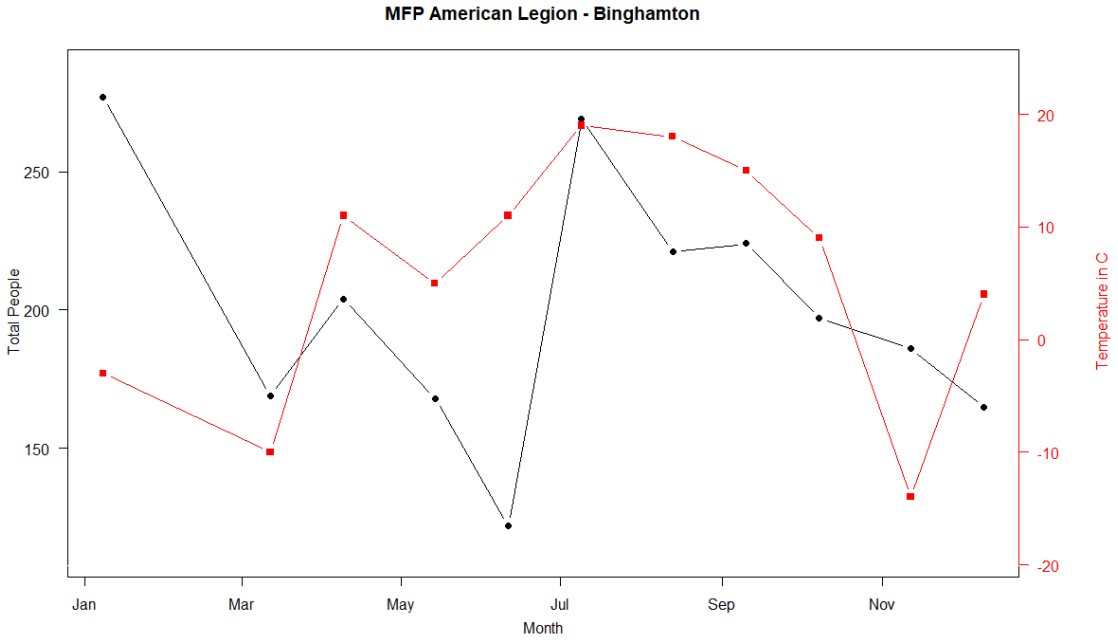

Figure 5.4: Headcount at American Legion distribution center

5.2.2 Demand Clusters and the Migration Effect

Figure 5.5 shows the demand profile of four MFP programs with distribution centers in Birnie transportation services center, Lamphear court, Bradford, and Campbell. Birnie transportation services center and Lamphear court distribution centers are located in the city of Elmira with a schedule of fourth Saturday and first Friday, respectively. We note that there was a significant drop in demand at the distribution center of Lamphear court in the month of February, specifically February first since the temperature was $-24°C$ whereas the demand at Birnie transportation services distribution center witnessed a spike in demand in the month of February, specifically on February twenty third and the temperature was $-5°C$. Clearly, we can see that the people who did not attend the food pickup at Lamphear court distribution center decided to go later on to Birnie transportation services distribution center. Likewise, the lost demand at Campbell distribution center was compensated by spike in demand at Bradford distribution center.

We also notice that there is a second cluster of demand at Campbell distribution center due to the discontinuity of service at Birnie transportation services distribution center. As shown in Figure 5.6, Campbell center is only six miles away from Birnie.

Hence, the story of Birnie and Lamphear distribution centers tells us that in extreme weathers, people will move from one distribution center to the other for convenience. It is also worth mentioning that we notice the same behavior in other distribution centers too; thus we provide food personnel new guidelines basically saying that demand at each site is fairly stable throughout the

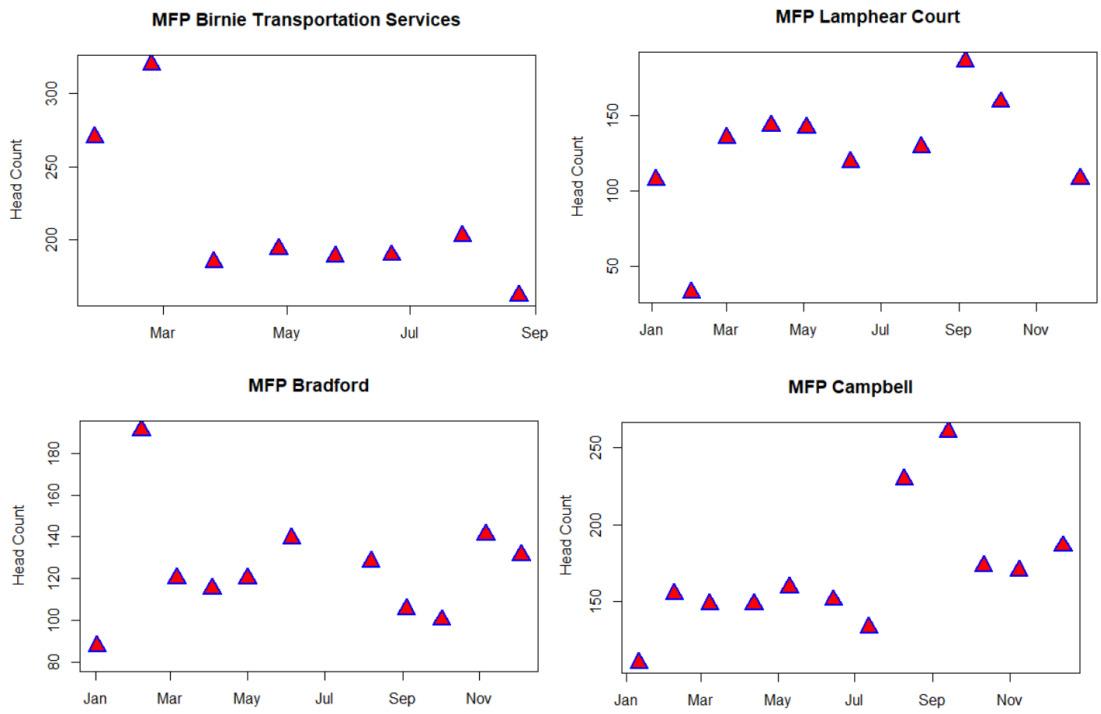

Figure 5.5: MFP headcount of Birnie, Lamphear, Bradford, and Campbell distribution center

year unless the weather is extremely cold. In the case of extremely weather, the demand will migrate to a close by location if the weather was better later on. Another interesting point that we find in the analysis that we conducted and the observations we collect is that the demand always follows a backlog order fashion meaning that people don't go to a new distribution center instead of the old convenient center they go to in anticipation of extreme weather events.

5.2.3 Effect of Scheduling

In section 5.2.2 we demonstrated how demand variability can be explained through migration of demand to different distribution centers based on distance and schedule. However, we find that in case where there was little demand at

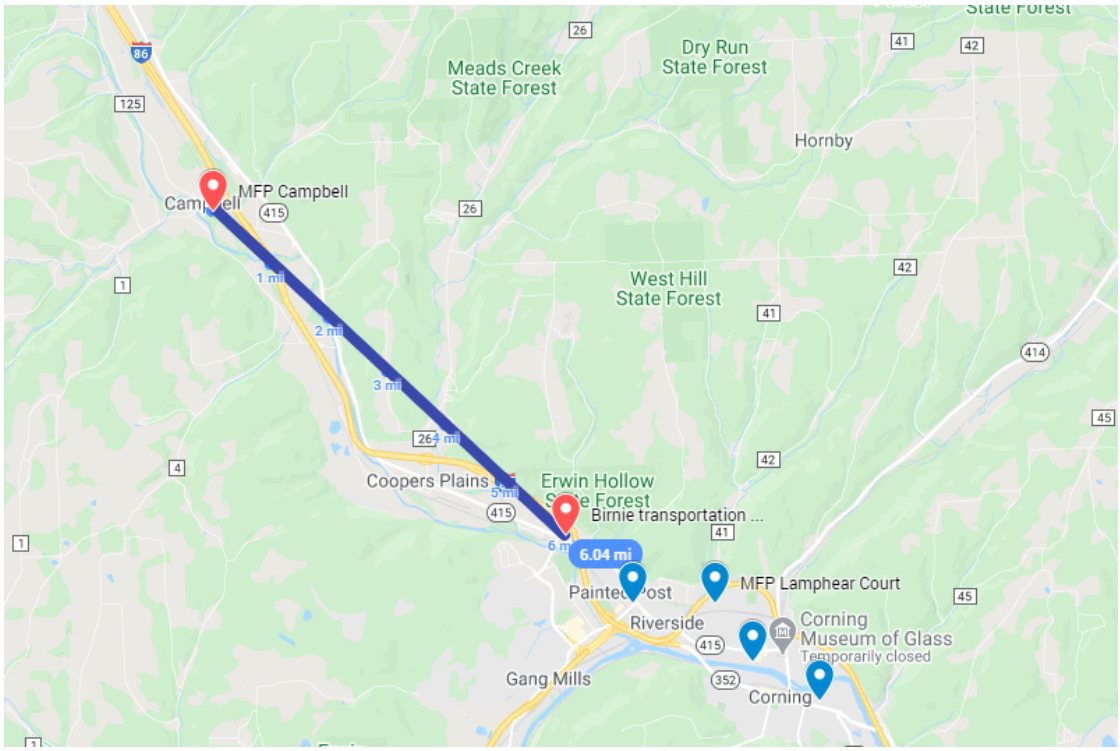

Figure 5.6: Birnie transportation center and Campbell distribution centers location on the map

some distribution centers, this lost demand cannot migrate to a near by distribution centers if the schedule was not set to allow so. We see this impact of bad schedule in the cases of Whitney Point and Wayland distribution centers.

Figure 5.7 shows the headcount of people at Whitney Point MFP program throughout the year of 2019, we note that there is a significant drop in demand in the month of February, specifically on the day of February first, as the temperature on that day was $-23°C$. Figures 5.8 and 5.9 show the location of Whitney Point distribution center on the map and the location of Whitney Point distribution center with respect to close by MFP programs, respectively. According to the hypothesis we made in section 5.2.2, we would expect that the demand lost at Whitney Point distribution center migrated to Richford MFP since it is a close

by distribution center. Nonetheless, we don't observe any spike in demand at Richford MFP due to the bad schedule of delivery at Richford. Specifically, the delivery schedule of Whitney Point is on the first Friday of each month; on the other hand, the delivery schedule of Richford is on the first Thursday of each month. Clearly, if a recipient in Whitney Point missed the pickup due to any reason, they cannot go to Richford MFP since the schedule of Richford MFP is already ahead of the schedule of Whitney Point. Also note that there are MFP programs' distribution centers to the west and north west of Richford. Hence, if someone missed the delivery at Richford, they can easily get their food product by going to a near by MFP. This point highlights the importance of scheduling the close by locations in a manner that allows people to get food products and groceries from near by locations.

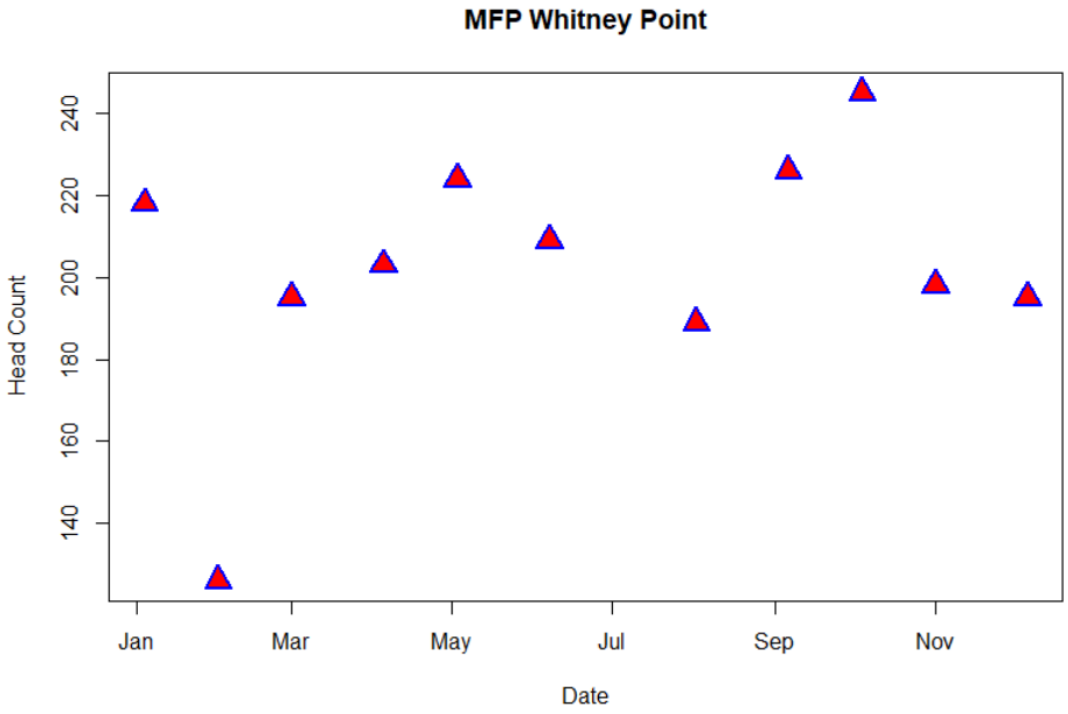

Figure 5.7: Headcount of recipients at Whitney Point distribution center

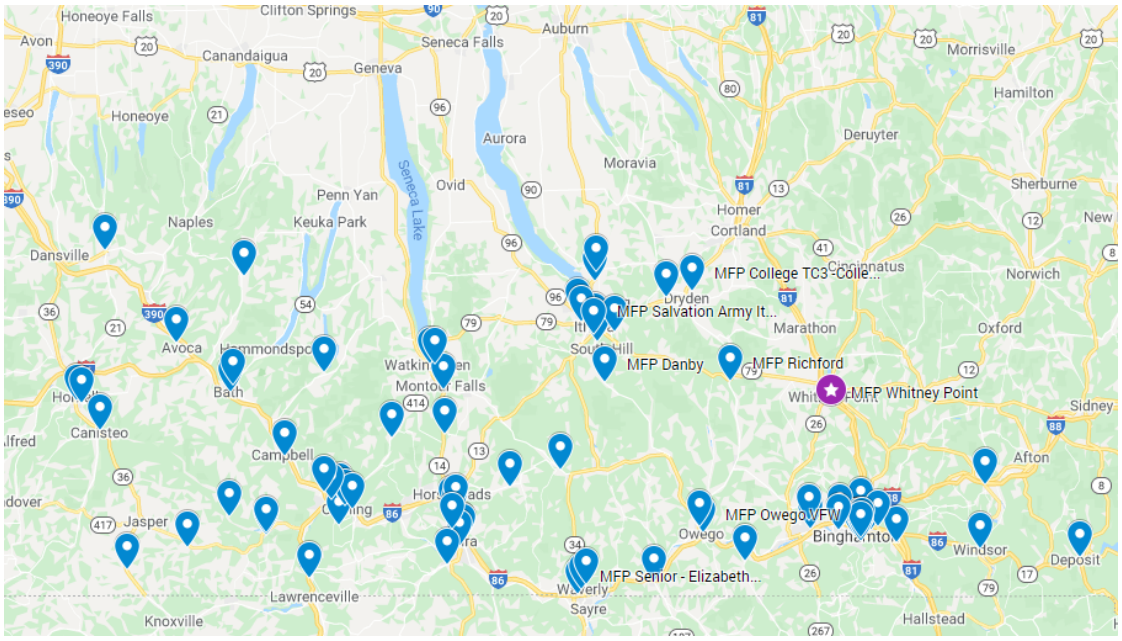

Figure 5.8: Whitney Point distribution center location on the map

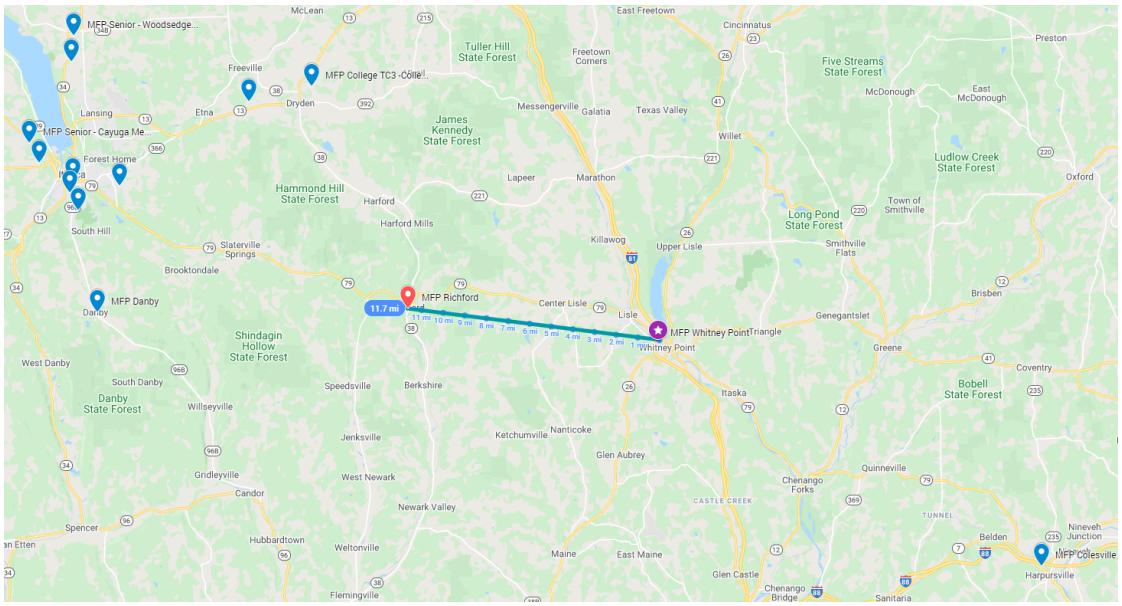

Figure 5.9: Whitney Point distribution center and distribution centers close by

Figure 5.10 shows the headcount of people at Wayland MFP program throughout the year of 2019, we note that there is a significant drop in demand in the months of February, March, and December, as the temperature on these

days were $-6°C$, $-6°C$, and $-17°C$, respectively. Figures 5.11 and 5.12 show the location of Wayland distribution center on the map and the location of Wayland distribution center with respect to close by MFP programs, respectively. According to the hypothesis we made in section 5.2.2, we would expect that the demand lost at Wayland distribution center migrated to Avoca, Prattsburgh, or Rehoboth MFP since they are the closest distribution centers to Walmand MFP. Nonetheless, we don't observe any spike in demand at any of these MFPs due to the incompatible schedule of delivery at them. Specifically, the delivery schedule of Wayland is on the second Tuesday 12-1 PM; on the other hand, the delivery schedule of Avoca, Rehoboth, and Prattsburgh are 2nd Tuesday 12-1 PM, 2nd Friday, and 1st Friday. Once again, if a recipient in Wayland missed the pickup due to any reason, they cannot go to Avoca, Rehoboth, or Prattsburgh MFP since the schedule of these distribution centers is either on the same day of the schedule of Wayland or very immediate so in case of severe weather, it is likely that these places will experience the same severe weather in the next day or two. Also note that there are MFP programs' distribution centers to the east and south east of Avoca, Rehoboth, and Prattsburgh. Hence, if someone missed the delivery at these MFPs, they can easily get their food product by going to a near by MFP.

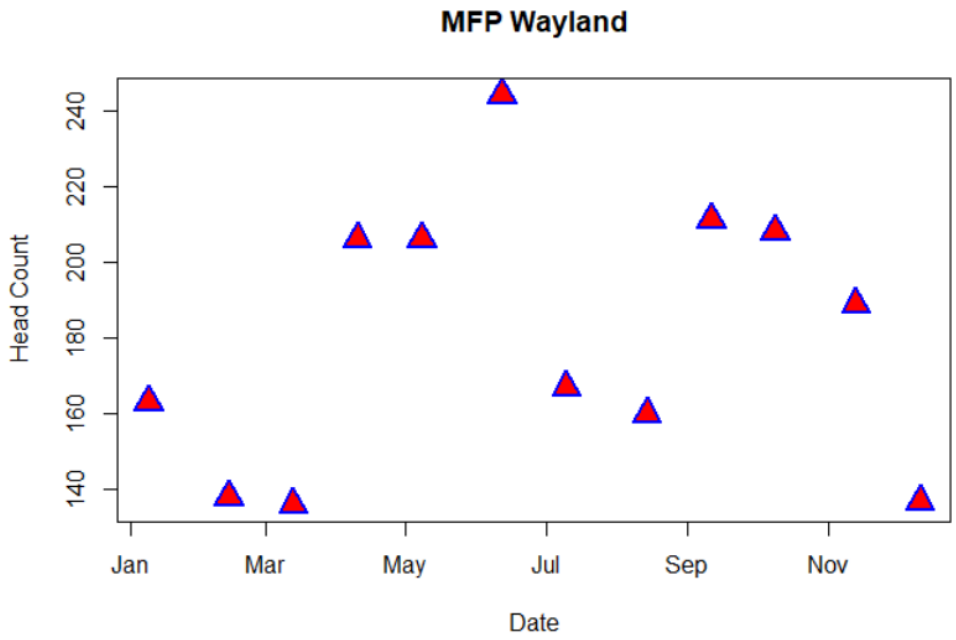

Figure 5.10: Headcount of recipients at Wayland distribution center

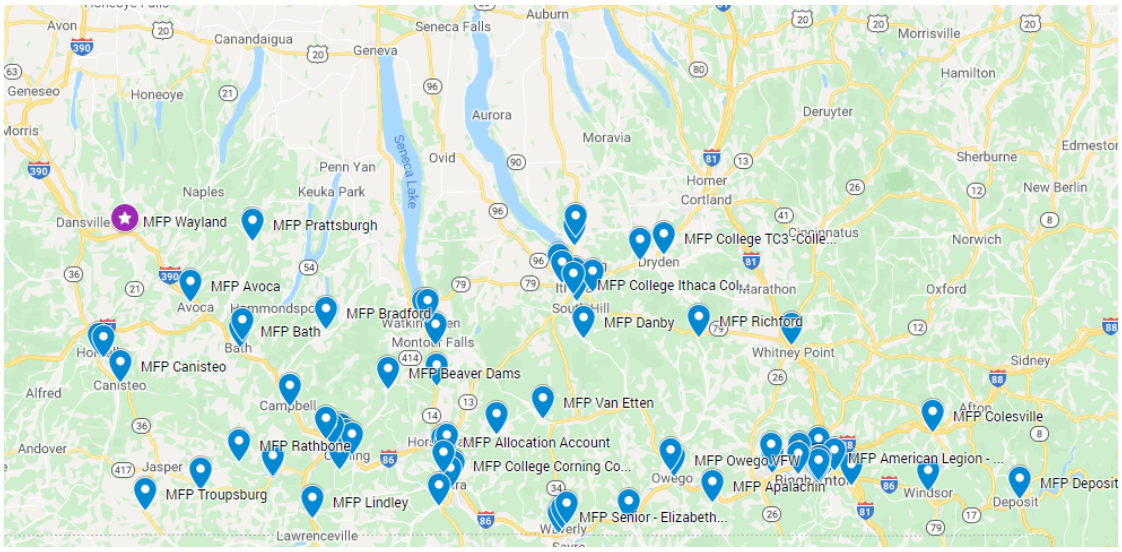

Figure 5.11: Wayland distribution center location on the map

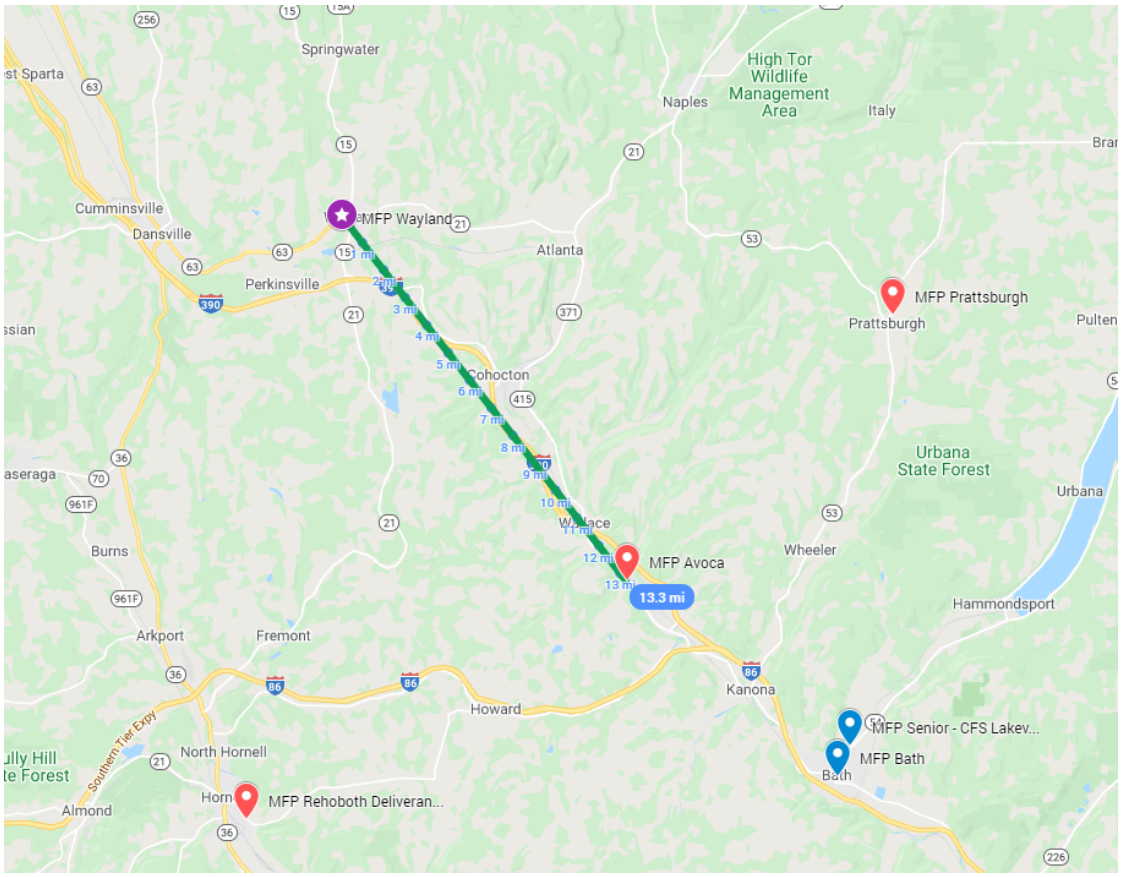

Figure 5.12: Wayland distribution center and distribution centers close by

Lastly, before we make our policy recommendation we will demonstrate a successful story of how compatible scheduling of near by MFPs can improve the accessibility of recipients to food products and groceries. This story essentially comes from the MPF at Deposit.

Figures 5.13 and 5.14 show the headcount of people at Deposit MFP program and Colesville throughout the year of 2019, respectively. We note that there is a significant drop in demand in the month of November, as the temperature on that day was $-2°C$ and cloud coverage was 100. Figures 5.15 and 5.16 show the location of Wayland distribution center on the map and the location of Way-

land distribution center with respect to close by MFP programs, respectively. We observe a spike in demand at Colesville MFP in November too implying that the lost demand at Deposit in November migrated to Colesville due to the convenient scheduling. Specifically, the delivery schedule of Deposit is on the third Tuesday and the delivery schedule of Colesville is third Thursday. Hence, if a recipient in Deposit missed the pickup due to any reason (such as extreme weather), they can go to Colesville MFP since the schedule of this distribution center is either within the same week with days of a difference.

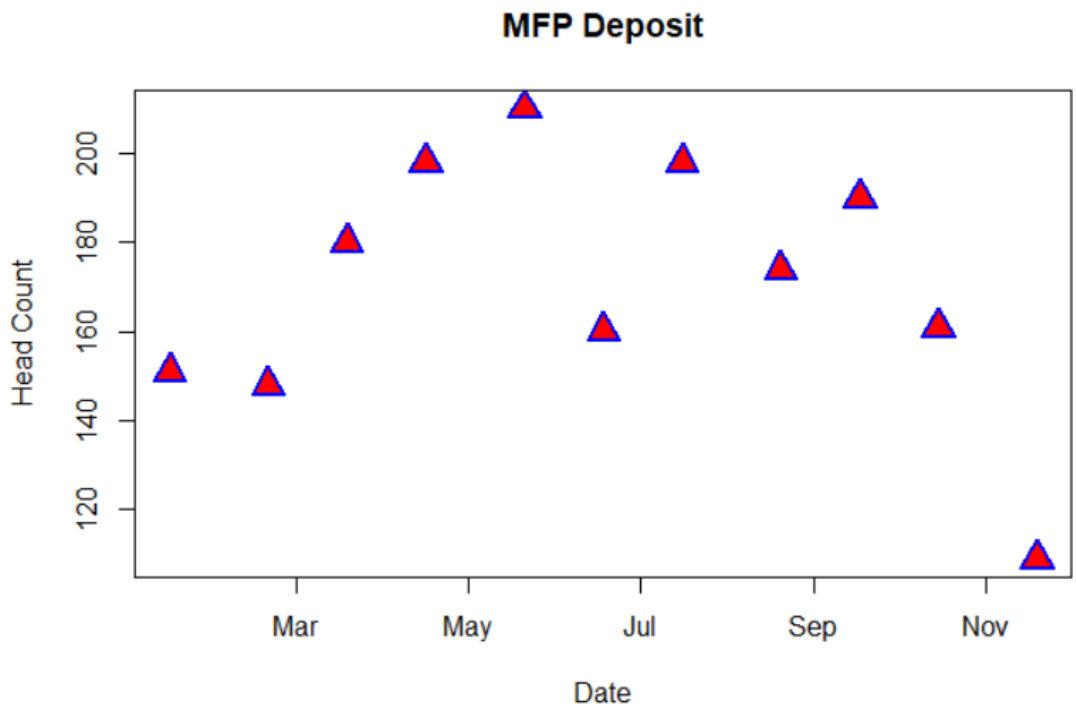

Figure 5.13: Headcount of recipients at Deposit distribution center

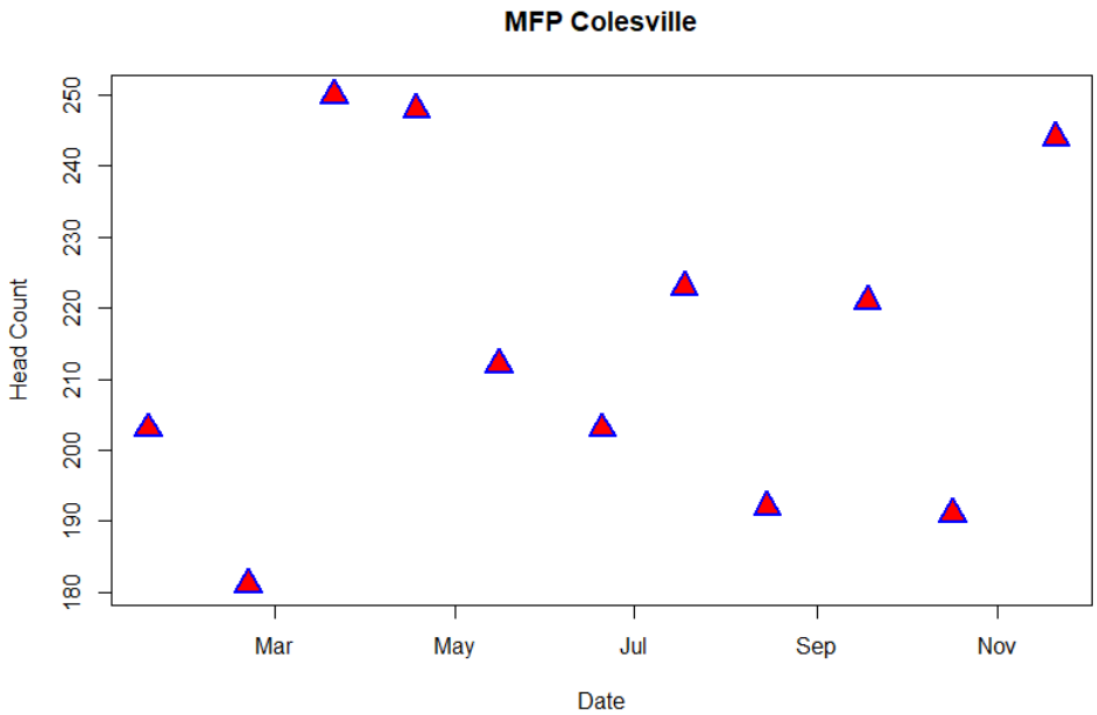

Figure 5.14: Headcount of recipients at Colesville distribution center

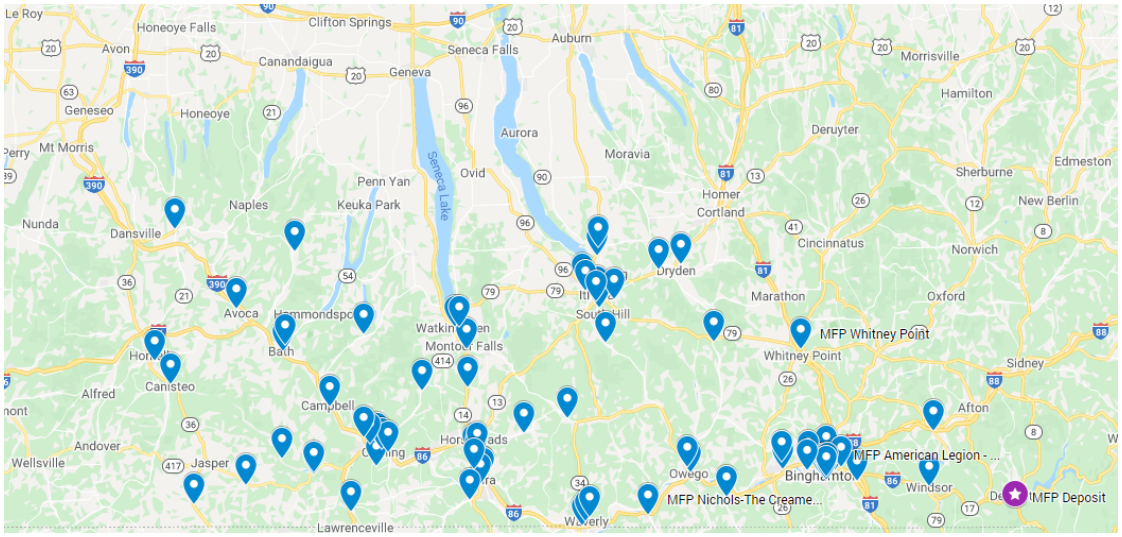

Figure 5.15: Deposit distribution center location on the map

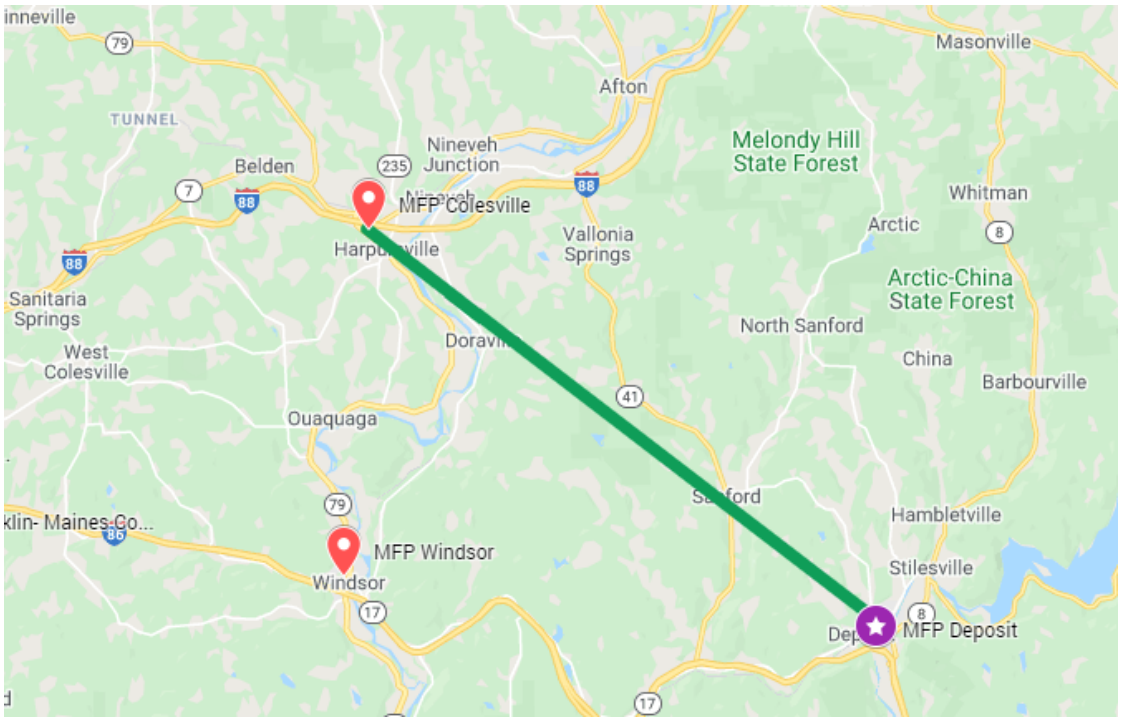

Figure 5.16: Deposit distribution center and distribution centers close by

To conclude this section, we recommend food banks to take into account the possibility that people may not be able to go to their closest MFP distribution center due to extreme weather; hence, near by distribution centers need to have a scheduling that is close to each other allowing the possibility of migration. Furthermore, these days need to be enough separated to take into account the possibility of having extreme weather that last for few days. We call this good scheduling that enable people to migrate to different distribution centers that are close by *'compatible scheduling'*.

5.3 Conclusion

In this study, we demonstrate how data analytics modeling can be used in combination with operational policy techniques to explain the variation of the head count at MFP distribution centers and to provide a guideline to food bank personnel to help them better predict the headcount of people showing up at the MFP distribution centers. We find that the effect of migration between distribution centers is very significant during winter times when the weather is extremely cold. The ability of identifying such clusters is critical to help food bank personnel better predict the demand of near by distribution centers. Furthermore, an interesting point we find is how delivery scheduling at distribution centers greatly affect the ability of people to access food products and groceries. As a result we introduced the concept of schedule compatibility to increase the effectiveness and efficiency of MFP program.

APPENDIX A

CHAPTER 1 OF APPENDIX

Supplementary Material

A systems approach to carbon policy for fruit supply chains: carbon tax, technology innovation, or land sparing?

1. The U.S. apple supply chain

Figure 1.1 illustrates the U.S. apple supply chain. Generally, apple orchards start the annual production cycle in early spring and apples are harvested in the fall. After harvest, apples enter either the fresh or the processed supply chain. Growers typically transport apples from the orchard to packing-shipping facilities, where apples are sorted for fresh or processed utilization and, subsequently, stored or shipped to processing facilities. Alternatively, some growers specialized in processed apples ship directly from the orchard to processing plants. Apples moved directly into the fresh supply chain are hand-picked and transported from the orchard to packing-shipping facilities. Apples are placed into one of two possible storage types. Apples for sales during harvest season (September to December) are put into regular (cold air) storage, whereas controlled atmosphere (CA) storage is used for fruit distributed during the non-harvest season (January to August). In both periods, fresh market apples are transported in trailer-trucks from packing sheds to retail distribution centers, which are generally located near consumption locations. Fresh apples are also traded in international markets. The United States imported 418.9 million pounds of fresh apples in 2010.

Particularly, fresh apples import peak primarily between April and June. U.S. fresh apples are also exported to other countries. In 2010, the United States exported 1,720.3 million pounds of fresh apples.

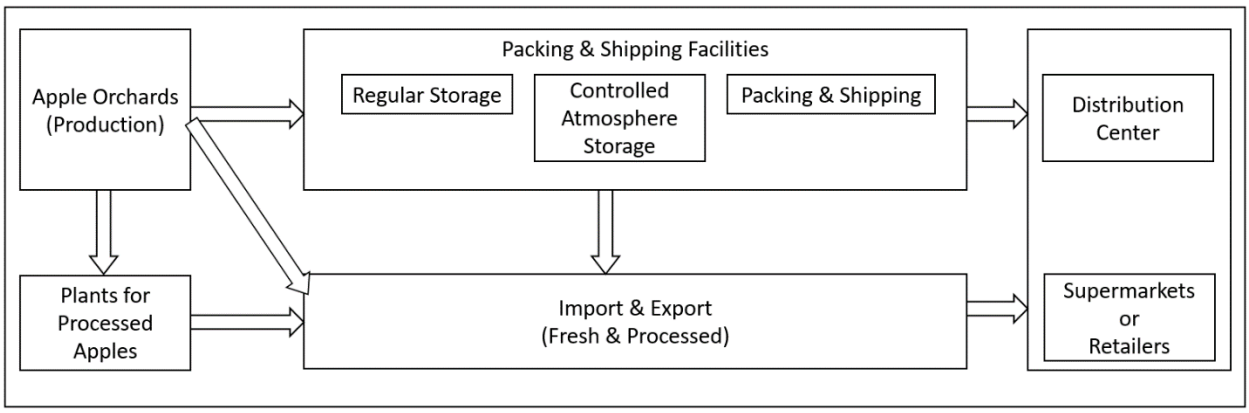

Figure 1.1 Diagram of the fresh apple supply chain

Our model focuses solely on the supply chain of fresh apples. The model considers six apple producer states (Washington, New York, Michigan, California, Pennsylvania and Virginia) and forty-nine consumption locations, each corresponding to the country's continental states. We take into account five fresh apple varieties (Red Delicious, Golden Delicious, Granny Smith, Gala and All others) to accommodate regional specialization on specific varieties (e.g. Granny Smith in Washington) and regional differences in consumer preference. The model is inter-temporal and, considers two time periods: (1) the harvest season (September to December), during which apples are primarily put into short-term storage prior to distribution; and (2) the non-harvest season (January to August), when apples are put into long-term CA storage. Our model takes into account exports and imports of fresh apples. The primary transportation method employed in our model is heavy-duty diesel trucks which account for approximately 95 percent of total apple transportation (USDA AMS 2011).

2. The mathematical model: Spatial price equilibrium model

We employ a spatially- and temporally-disaggregated price equilibrium model following Takayama and Judge (1964) to estimate optimal product flows from supply regions to consumption locations. The model solves a quadratic programming problem to maximize social surplus measured as the sum of consumers and producers' surplus less total costs resulting from all activities within the supply chain. The objective function of the model can be expressed as:

$$
\begin{aligned}
Max \quad & \sum_t \sum_k \sum_j (\delta^{t-1} * \alpha^t_{k,j} * qd^t_{k,j}) - 0.5 * \sum_t \sum_k \sum_j \left(\delta^{t-1} * \left[\sum_l (\beta^t_{kl,j} * qd^t_{l,j}) \right] * qd^t_{k,j} \right) \\
& - \sum_i \sum_k (a^i_k * qs_{k,i}) + 0.5 * \sum_i \sum_k (b^i_k * qs_{k,i} * qs_{k,i}) \\
& + \sum_t \delta^{t-1} \left(exc_t * qex_t - 0.5 * exs_t * qex_t * qex_t \right) \\
& - \sum_t \delta^{t-1} \left(imc_t * qim_t - 0.5 * ims_t * qim_t * qim_t \right) - \sum_t \sum_s \sum_i \delta^{t-1} \left[sc^t_{s,i} \cdot \left\{ \sum_k sa^t_{k,s,i} \right\} \right] \\
& - \sum_t \sum_i \sum_j \delta^{t-1} \left[tc^t_{i,j} \cdot \left\{ \sum_k \sum_s tfa^t_{k,s,i,j} \right\} \right] - \sum_t \sum_m \sum_j \delta^{t-1} \left[tc^t_{m,j} \cdot \left\{ \sum_k tfam^t_{k,m,j} \right\} \right]
\end{aligned}
\qquad , (2.1)
$$

where the objective function represents surpluses from both domestic and international sources of fresh apples minus total costs from all practices including storage and transportation. The model yields optimal quantities for production, consumption, exports and imports; producer prices for each supply region; retail prices for each consumption location; inter-regional commodity flows; and social welfare levels. The objective function in equation (2.1) is constrained to ensure balance between supply and demand, capacity restrictions (e.g. land capacity for production and the capacity for storage), and technical constraints in production and storage (e.g. yield rate in production and loss rate in storage). These constraints are stated as follows:

$$qs_{k,i} \le \mu_i \cdot PCAP_{k,i} \quad \forall k, i \text{, where } PCAP_{k,i} = aveyield_{k,i} \times \theta_{k,i} \cdot acre_i \quad \forall k \qquad (2.2)$$

$$\sum_t \sum_s \frac{1}{\lambda_{s,i}^t} sa_{k,s,i}^t \le qs_{k,i} \quad \forall k,i \text{, where } sa_{k,s=rs,i}^{t=spring} = 0 \ \ \forall k,i \tag{2.3}$$

$$\sum_t \sum_k sa_{k,s,i}^t \le SCAP_{s,i} \quad \forall s,i \tag{2.4}$$

$$\sum_j tfa_{k,s,i,j}^t + qex_{k,s,i}^t \le \frac{1}{\lambda_{s,i}^t} sa_{k,i,s}^t \quad \forall t,k,s,i \tag{2.5}$$

$$qd_{k,j}^t \le \sum_s \sum_i tfa_{k,s,i,j}^t + \sum_j tfam_{k,m,j}^t \quad \forall t,k,j \tag{2.6}$$

$$\sum_j tfam_{k,m,j}^t \le qim_{k,m}^t \quad \forall t,k,j \tag{2.7}$$

Equation (2.2) ensures that the total quantity of apple variety *k* produced in supply area *i*, $qs_{k,i}$, does not exceed the maximum production capacities, $\mu_i \cdot PCAP_{k,i}$, of each region, where μ_i is the percent rate of fresh utilization in supply region *i*. The maximum production capacities are determined by average yield, $aveyield_{k,i}$, production percentage of variety *k*, $\theta_{k,i}$ and total acreages in production region *i*, $acre_i$. Equations (2.3) and (2.4) specify the balance of apples moved from orchards to storage facilities and the maximum storage capacity in each production region *i*, respectively. In equation (2.3), the total amount of stored apples in each region *i*, $sa_{k,s,i}^t$, after considering storage loss rates, $\lambda_{s,i}^t$, must be less than or equal to total fresh apple supply in region *i*, $qs_{k,i}$. Following standard management practices, apples for sale during the harvest season are put into regular storage, whereas those for sale during the non-harvest season are put into CA storage. In the model, apples for sale in the harvest season can be distributed from either regular or CA storage. In contrast, apples for sales during the non-harvest season can be distributed only from CA storage. Therefore, the amounts stored in regular storage during the non-harvest season are set to equal to zero in our model. Equation (2.4) ensures that the total amount of stored apples at storage facility *s* in each supply region *i*, $sa_{k,s,i}^t$, must be less than or equal to the maximum storage capacity, $SCAP_{s,i}$.

Equation (2.5) ensures that the total amount of apples in storage facility *s*, taking into account storage losses must be greater than or equal to the sum of shipments to both consumption locations, $tfa^{t}_{k,s,i,j}$, and export point of shipment, $qex^{t}_{k,s,i}$. Equation (2.6) ensures that fresh apple demand for variety *k* in location *j* at time *t*, $qd^{t}_{k,j}$, is less than or equal to the total shipments from all supply regions *i*, $tfa^{t}_{k,s,i,j}$, plus imports from all import points *m*, $tfam^{t}_{k,m,j}$. Equation (2.7) specifies that total shipment from import point *m* to consumption location *j*, $tfam^{t}_{k,m,j}$, must not exceed total imports at point *m* at *t*, $qim^{t}_{k,m}$. Finally, all decision variables in the model are required to be non-negative. Table 2.1 presents the indices and variables used in the model. The discount factor δ is calculated as $\delta = \frac{1}{1+r}$ where *r* is the interest rate and in our experiments we set *r* to be 0.025.

It is worth mentioning that the presented model does not provide the option for producers to select a storage and/or production technologies, as such decisions are beyond the scope of our study and analysis. If the decision maker is interested in analyzing the response of producers regarding the selection of production and/or storage technologies, such study can be carried out using agent based modeling to incorporate the behavior of the producers in the system. The authors do acknowledge that incorporating such variables is one of the limitations of the presented study. Nonetheless, the developed framework can be adjusted to add decision variables for each producer reflecting their behavior; however, the resulting model will be a large-scale mixed integer non-linear programming model that might be very challenging to solve when there are large number of producers and the existence of binary variables reflecting the selection of storage/production technology.

Table 2.1 Index, variables and definitions

Index (variable)	Definition
t	time period
k	apple variety
i	supply region
j	consumption location
r	demand region
s	storage facility
m	import and export port
$pd_{k,j}^{t}$	retail price of fresh apple variety *k* at time *t* in consumption location *j* ($/pound)
$qd_{k,j}^{t}$	fresh apple quantities consumed of variety *k* at time *t* in consumption location *j* (million pounds)
$ps_{k,i}$	price received by farmer for apple variety *k* in supply region *i* ($/pound)
$qs_{k,i}$	fresh apple quantities produced of apple variety *k* in supply region *i* (million pounds)
$ppim^{t}$	price differential between import price and retail price at time *t* ($/pound)
qim^{t}	quantities of imported apple at time *t* (million pounds)
$ppex^{t}$	price differential between export price and producers price at time *t* ($/pound)
qex^{t}	quantities of exported apple at time *t* (million pounds)
$sa_{k,s,i}^{t}$	fresh apples of variety *k* put into storage facility s at time *t* in region *i* (million pounds)
$sc_{k,s,i}^{t}$	storage cost to operate storage facility *s* at time *t* in region *i* ($/pound)
$tc_{i,j}^{t}$	transportation cost at time *t* from supply region *i* to consumption site *j* ($/pound)
$tc_{m,j}^{t}$	transportation cost at time *t* from supply region *i* to port *m* ($/pound)
$tfa_{k,s,i,j}^{t}$	shipment of apple variety *k* at time *t* from storage facility *s* in supply region *i* to consumption location *j* (million pounds)
$tfam_{k,m,j}^{t}$	shipment of apple variety *k* at time *t* from port *m* to consumption site *j* (million pounds)
$PCAP_{k,i}$	production capacity for variety *k* in supply region *i* (million pounds)
$aveyield_{k,i}$	average yield per acre in supply region *i* (pounds)
$\theta_{k,i}$	production percentage of variety *k* in supply region *i* (%)
$acre_{i}$	bearing acreage for apple in supply region *i* (acres)
$\lambda_{s,i}^{t}$	apple loss rate at storage *s* in supply region *i* at time *t* (%)
$SCAP_{s,i}$	capacity of storage facility *s* in supply region *i* (million pounds)
μ_{i}	percentage rate of fresh utilization in supply region *i* (%)
exc_{t}	constant of export function at time *t*

exs_t	slope of export function at time *t*
imc_t	constant of import function at time *t*
ims_t	slope of import function at time *t*
δ	discount factor
$\alpha_{k,j}^t$	constant of the inverse demand function for variety *k*, at location *j* and time *t*
$\beta_{kl,j}^t$	slope of the inverse demand function between varieties *k* and *l*, at location *j* and time *t*
a_k^i	constant of supply function at for variety *k* at location *i*
b_k^i	slope of supply function at for variety *k* at location *i*

3. Estimation of demand function parameters

The objective function (2.1) of the spatial equilibrium model employs an inverse-demand function of the form:

$$p_{k,j}^{t} = \alpha_{k,j}^{t} - \sum_{l} \beta_{kl,j}^{t} \cdot q_{l,j}^{t} \quad \forall k, j, t \quad (3.1)$$

Note that the inverse demand function parameters ($\alpha_{k,j}^{t}, \beta_{kl,j}^{t}$) needed in equations (2.1) and (3.1) are for each variety k (Red Delicious, Golden Delicious, Granny Smith, Gala and All others), for each consumption location j (forty-nine consumption locations, corresponding to the U.S. continental states), and for each season t (harvest and non-harvest seasons). Note that the index l refers to apple variety too. The coefficient $\beta_{kl,j}^{t}$ can be calculated as:

$$\beta_{kl,j}^{t} = \frac{1}{\varepsilon_{kl,j}^{t}} \cdot \frac{p_{k,j}^{t}}{q_{l,j}^{t}} \quad (3.2)$$

where $\varepsilon_{kl,j}^{t}$ is the cross price elasticity of demand of variety k with respect to variety l, in consumption location j, in season t. If $k = l$, then $\varepsilon_{kk,j}^{t}$ becomes the own price elasticity of demand for variety *k*. In turn, the coefficient $\alpha_{k,j}^{t}$ can be calculated as $\alpha_{k,j}^{t} = p_{k,j}^{t} + \sum_{l} \beta_{kl,j}^{t} \cdot q_{l,j}^{t}$, given observed prices $p_{k,j}^{t}$ and quantities $q_{l,j}^{t}$.

Therefore, we first need to estimate the cross and own price elasticities of demand $\varepsilon_{kl,j}^{t}$ to calculate the coefficients $\alpha_{k,j}^{t}$ and $\beta_{kl,j}^{t}$. After calculating the cross and own price elasticities of demand for each consumption location, for each season and for each variety, we can then calculate the price coefficient $\beta_{kl,j}^{t}$ following equation (3.2).

To calculate the cross and own price elasticities of demand, we employ a Linear Approximated Almost Ideal Demand System (LA-AIDS) following Deaton and Muellbauer (1980). The LA-AIDS is useful for capturing consumer demand patterns in household-level micro data by controlling for different socio-economic variables (e.g. race, education level and gender) and income levels (Blundell, Pashardes and Weber 1993). We use Nielsen's Homescan panel database for the period of January/2005 – December/2006 to estimate these price elasticities of demand, namely $\varepsilon^{t}_{kl,j}$ (Nielsen Homescan). That said, a LA-AIDS model has to be developed for each consumption location and each season to estimate the price elasticities of demand. In our work, we assume that the price elasticities of demand of demand location (i.e., states) located in the same Census Division are the same. There are four Census Divisions, namely Northeast, South, Midwest and West. As a result, we introduce a new index R to denote the set of regions $R = \{r = 1,...,4\}$ each corresponding to a Census Division. Therefore, a LA-AIDS model for each region and for each season can be specified as follows:

$$w^{t}_{k,r,h} = \sigma^{t}_{k,r} + \sum_{n} \varsigma^{t}_{k,r} \eta^{t}_{n,r,h} + \sum_{l} \gamma^{t}_{kl,r} \ln p^{t}_{l,r,h} + \pi^{t}_{k,r} \ln(X^{t}_{r,h} P^{t}_{r,h}) + \rho YEAR + \theta^{t}_{k,r} \quad (3.3)$$

Note that equation (3.3) represents eight demand systems (4 regions X 2 seasons); and each of the eight systems consists of five equations (i.e., five apple varieties). In equation (3.3), $w^{t}_{k,r,h}$ is the budget share of household h that is in region r for variety k at season t; $\sigma^{t}_{k,r}$ is the budget share mean of variety k for region r at season t; $\varsigma^{t}_{k,r}$ are the coefficients of household characteristics in region r for variety k at season *t*; $\eta^{t}_{n,r,h}$ are the socio-economic variables describing household characteristics (e.g. race, education level and gender) (*n=1*,⋯, *N*) in region r for variety k at season *t*; $\gamma^{t}_{kl,r}$ are the coefficients of Stone price index; $\pi^{t}_{k,r}$ is the expenditure level on apple variety k for region r at season t; $X^{t}_{r,h} = \sum_{k=1}^{5} p^{t}_{k,r,h} q^{t}_{k,r,h}$

is the total expenditure of household h for five apple varieties at season t in region r in season *t*; $\ln P_{r,h}^{t} = \sum_{k=1}^{5} w_{k,h}^{t} \ln p_{k,r,h}^{t}$ is the Stone Price Index in region r for variety k at season t; ρ is the coefficient of year dummy variable; $YEAR$ is a year dummy variable; and $\theta_{k,r}^{t}$ is the error term. The error is assumed to be normally distributed with a mean of 0 and a variance Ω. Upon solving the systems of equations in (3.3) for each region and for each season, the parameters $w_{k,r}^{t}, \sigma_{k,r}^{t}, \varsigma_{k,r}^{t}, \gamma_{kl,r}^{t}, \pi_{k,r}^{t}$ and $\theta_{k,r}^{t}$ are obtained.

To be consistent with economic theory (see Barten (1964), Barnett (1979), Theil (1965), and Barnett and Seck 2008), the parameter restrictions for estimation of equations (3.3) include the following: for homogeneity, $\sum_{k=1}^{5} \sigma_{k,r} = 1$, $\sum_{k=1}^{5} \pi_{k,r} = 0$, $\sum_{k=1}^{5} \gamma_{kl,r}^{t} = 0$, $\sum_{l=1}^{5} \gamma_{kl,r}^{t} = 0$; and for symmetry, $\gamma_{kl,r}^{t} = \gamma_{lk,r}^{t}$. Finally, the own price elasticities of demand are calculated as $\varepsilon_{kk,r}^{t} = \dfrac{\gamma_{kk,r}^{t} + \pi_{k,r}^{t} \sigma_{k,r}^{t}}{\sigma_{k,r}^{t}} - 1$, and the cross price elasticities as $\varepsilon_{kl,r}^{t} = \dfrac{\gamma_{kl,r} + \pi_{k,r} \sigma_{k,r}}{\sigma_{l,r}}$ when $k \neq l$.

While the use of household-level data is preferable in the complete demand system, one has to solve the zero expenditure problem presented in the data. That is, households do not always purchase all apple varieties in each season specified in the model. Parameters estimates are likely to be biased if the zero expenditure problem is not addressed (Park et al. 1996). To address this issue, we follow the censored method suggested by Heckman (1978) to deal with the zero consumption problem. That is, we specify a LA-AIDS model for each region r and for each season t incorporating the Inverse Mills Ratio. In order to calculate the parameter of Mills Ratio, we estimate a probit model to determine the probability that a given household would purchase a specific variety *k* as follows:

$$\omega_{k,r,h}^{t} = f(p_{1,r,h}^{t},\cdots,p_{k,r,h}^{t},X_{r,h}^{t},\eta_{1,r,h}^{t},\cdots,\eta_{N,r,h}^{t}) \qquad (3.4)$$

where $\omega_{k,r,h}^{t}$ is a binary variable equal to 1 if variety k is purchased by household h in region r for variety k at season t, zero otherwise; $p_{k,r,h}^{t}$ is the price of variety k at season t in region r; $\eta_{n,r,h}^{t}$ are the socio-economic variables describing household characteristics ($n=1,\cdots,N$); and $X_{r,h}^{t}$ is the expenditure level of household h at season t in region r. Second, using the fitted value, $\widehat{\omega}_{k,r,h}^{t}$, from the probit estimation in equation (3.4), we compute the inverse Mills ratio, $MR_{k,r,h}^{t} = \phi(p_{k,r,h}^{t},\eta_{n,r,h}^{t},X_{r,h}^{t})/\Phi(p_{k,r,h}^{t},\eta_{n,r,h}^{t},X_{r,h}^{t})$ for households consuming apple variety k. $\phi(\cdot)$ and $\Phi(\cdot)$ refer to the density and cumulative probability functions, respectively (Heien and Wessells 1990). Similarly, $MR_{k,r,h}^{t} = \phi(p_{k,r,h}^{t},\eta_{n,r,h}^{t},X_{r,h}^{t})/\{1-\Phi(p_{k,r,h}^{t},\eta_{n,r,h}^{t},X_{r,h}^{t})\}$ is computed for households that do not purchase the variety k. Finally, we estimate the missing prices stemming from zero purchase of variety k at season t in region r, employing seasonal and regional dummy variables for the complete data set. The LA-AIDS model incorporating the inverse Mills ratio is given by:

$$w_{k,r,h}^{t} = \sigma_{k,r}^{t} + \sum_{n}\varsigma_{k,r}^{t}\eta_{n,r,h}^{t} + \sum_{l}\gamma_{kl,r}^{t}\ln p_{l,r,h}^{t} + \pi_{k,r}^{t}\ln(X_{r,h}^{t}P_{r,h}^{t}) + \delta_{k,r}^{t}MR_{k,r,h}^{t} + \rho YEAR + \theta_{k,r}^{t} \quad (3.5)$$

Table 3.1 reports the estimated own price elasticities of demand for the four multistate Census Divisions, varieties and seasons, Tables 10.1-10.8 report the estimated cross price elasticities of demand for each Census Division and season, and Tables 7.1-7.8 report the estimated parameters of LA-AIDS model. From Tables 7.1-7.8, we note that only 14.8% of cross price elasticity parameters are statistically significant at the 1 percent level. Specifically, only 19 out of 128 of the estimates cross price elasticity parameters are

statistically significant. Furthermore, the magnitude of the cross price elasticities is much smaller than the own price elasticities. For instance, the cross price elasticity of demand of variety Gala Smith with respect to variety Red Delicious, in the Midwest during the non-harvest season is 0.29, whereas the own price elasticity of Golden Delicious is -4.70. Table 10.9 reports the ratio between own and cross price elasticities (for cross elasticities that are statistically significant) to compare the magnitude difference between the cross (for those that are statistically significant) and own price elasticities. Table 10.9 shows that the reported ratio is greater than two for all parameters except for three cases.

Based on the comparison of own and cross price elasticities in the previous paragraph, we argue that the demand systems in equation (3.3) are primarily driven by the own price elasticities. The majority of the cross price elasticities are statistically insignificant; and for those that are significant, the magnitude is quite modest in comparison to the own price elasticities. As a result, in the optimization problem (2.1) we assume that cross price elasticities are zero, which implies that the matrix B is a diagonal.

In Table 3.1, the results show differences in the own price elasticities of demand across regions, varieties and seasons. Red Delicious apples tend to have the same own price elasticity, regardless of the region, but the own price elasticity is higher in the non-harvest season. The other varieties (Golden Delicious, Granny Smith and Gala) exhibit own elasticities that appear to be more sensitive to changes in prices compared to Red Delicious, the most consumed variety. Our price elasticity of demand estimates is comparable to previous studies analyzing the demand for fruits in general (Durham and Eales 2010) and apple demand in particular (Richards et al. 2012).

Now that the price elasticities are estimated for each census/region, (i.e., northeast, south, Midwest and west) and for each season (i.e., harvest and non-harvest) the next step is to calculate the demand parameters ($\alpha_{k,j}^{t}$ and $\beta_{kl,j}^{t}$) for each consumption location (i.e., each state). This leaves us with eight systems of equations to estimate (four regions X 2 seasons), each system consisting of five questions (one of each

apple variety).To calculate the parameters $\beta_{kl,j}^{t}$ we use equation (3.2) in which the elasticities are from the LA-AIDS model, and the prices and quantities ($p_{k,j}^{t}$ and $q_{l,j}^{t}$) are the average prices and the consumption for variety *k* in state *j* in season *t*. Average prices are from the Nielsen Homescan panel sample employed in the analysis, and demand is calculated as the population of state *j* multiplied by the per capita consumption reported by USDA (Nielsen Homescan, USDA Apple Statistics and Phillips 2003).

In their seminal work, Takayama and Judge (Takayama and Judge 1964a and 1964b) present two models for spatial price equilibrium similar to the one used here. In their earlier work, the inverse demand function is a linear function of the form $p_{k,j}^{t} = \alpha_{k,j}^{t} - \beta_{kk,j}^{t} \cdot q_{k,j}^{t}$ (pp. 69). On the other hand, in their recent work the inverse demand function takes the form of $p_{k,j}^{t} = \alpha_{k,j}^{t} - \sum_{l} \beta_{kl,j}^{t} \cdot q_{l,j}^{t}$ to account for substitution effects, with the conditions that $\alpha_{k,j}^{t} > 0;$ $\beta_{kk,j}^{t} > 0;$ and matrix β_{j}^{t} is a positive definite (pp. 353). As discussed earlier, we follow Takayama and Judge (1964a) because we assume that substitution effects are negligible. Thus we assume that the inverse demand function takes the form of $p_{k,j}^{t} = \alpha_{k,j}^{t} - \beta_{kk,j}^{t} \cdot q_{k,j}^{t}$.

Table 3.1 Price elasticities of demand by season, region and variety

Time period	Region			
Harvest season (September-December)	Northeast	Midwest	South	West
Golden Delicious	-1.545	-1.193	-0.992	-0.615
Granny Smith	-3.377	-1.527	-2.034	-2.103
Red Delicious	-1.020	-1.049	-1.038	-0.965
Gala	-1.548	-0.741	-0.830	-1.166
Others	-0.951	-0.936	-0.939	-0.976
Non-harvest season (January-August)	Northeast	Midwest	South	West
Golden Delicious	-1.997	-2.727	-1.716	-3.222
Granny Smith	-2.562	-4.701	-1.974	-2.716
Red Delicious	-1.002	-1.116	-1.004	-0.907
Gala	-0.717	-1.280	-0.735	-0.972
Others	-1.041	-1.031	-1.039	-1.022

4. Estimation of supply function parameters

We also need to estimate price elasticities of supply in the six production regions. For this purpose, we employ Nerlove's (1956) model on yearly data showing fresh apple production and farm gate prices for the period 1973 to 2008 (for east coast: Cornell Cooperative Extension, for Washington: Washington State University-School of Economic Sciences and for California University of California Davis-Agricultural & resource Economics). Since these are national data, price elasticities of supply are assumed to be identical

across all varieties in each supply region. Following Nerlove (1956), the general supply function of partial adjustment is specified as follows:

$$\ln Q_t^{i*} = \alpha_0 + \alpha_1 \ln p_{t-1}^i + \alpha_2 z^i + \alpha_3 T + u_t^i, \tag{4.1}$$

where Q_t^{i*} implies desired (equilibrium) output in production region *i* at time *t*, $\ln p_{t-1}^i$ is output price in region *i* at time *t-1*, T is a time trend and z^i represents weather conditions (e.g. precipitation). The supply dynamics for the actual adjustment to the equilibrium relationship is given by:

$$\ln Q_t^i - \ln Q_{t-1}^i = \varphi^i (\ln Q_t^{i*} - \ln Q_{t-1}^i), \tag{4.2}$$

where Q_t^i is the actual output in region *i* and φ^i is the partial adjustment coefficient. By substituting equation (4.2) into equation (4.1), rearranging terms and employing regional dummy variables, the Nerlovian model for estimating price elasticities of supply for each supply region is given as:

$$\ln Q_t^i = \beta_0 + \beta_1 \ln p_{t-1}^i + \sum_j \beta_1^j \cdot d^j \cdot \ln p_{t-1}^i + \beta_2 \ln Q_{t-1}^i + \beta_3 z^i + \beta_4 T + e_t^i, \tag{4.3}$$

where $d^j = 1$ if $i = j$ and zero otherwise. $\beta_1 = \varphi\alpha_1$ is the short-run price elasticity of apple supply in each region. Table 4.1 presents the estimation results of equation (4.3). Based on the estimates, the price elasticities of supply are obtained for each supply region. The estimated elasticities for each supply region suggest that supply in California tends to be the most sensitive with respect to farm gate prices among all six production regions. In contrast, supply in Washington seems to be the most inelastic to farm gate prices.

Table 4.1 Estimate results of Nerlovian model and estimated price elasticities of supply

	Coefficient	Standard Errors
Constant	2.818**[a]	(1.199)
lnp_{t-1}	0.359**	(0.105)
$d_{CA} \cdot lnp_{t-1}$	0.206**	(0.069)
$d_{MI} \cdot lnp_{t-1}$	0.012	(0.040)
$d_{PA} \cdot lnp_{t-1}$	0.143**	(0.059)
$d_{VA} \cdot lnp_{t-1}$	0.186**	(0.068)
$d_{WA} \cdot lnp_{t-1}$	-0.242**	(0.068)
lnq_{t-1}	0.746**	(0.045)
Precipitation	-0.020	(0.029)
Temperature	-0.006	(0.017)
Time	-0.009**	(0.003)
R^2	0.95	
# of Observations	210	
Price Elasticities of Supply		
California	0.565	
Michigan	0.359	
New York	0.359	
Pennsylvania	0.501	
Virginia	0.545	
Washington	0.117	

a. ** indicates 5% significance level.

Finally, we estimate price elasticities of apple imports and exports for the harvest and non-harvest seasons. The quantities of exports and imports are assumed to be dependent on the differential between domestic and international import (export) prices and domestic production quantities.[1]

[1] Due to data limitations, we assume that fresh apples are exported only from Washington and New York. Furthermore, fresh apples are assumed to be imported through four major ports (e.g. LA, Miami, Newark and Seattle) and distributed to forty-nine consumption locations in the same proportion. Linear import functions for the non-harvest season and the harvest season are estimated to be $p_{nh}=1.151+0.003im_{nh}$, $p_h=1.151+0.022im_h$, respectively. Linear export functions for non-harvest and harvest season are estimated to be $p_{nh}=6.423-0.005ex_{nh}$,

5. Costs in storage and transportation

To build the optimization model in equation (2.1), a specification of cost structure in the fresh apple supply chain is required. To this end, we compiled per unit costs for storage and transportation activities. Storage costs depend on the amount of time that apples are stored and the costs of energy. Storage costs were obtained from a direct survey of apple packer-shippers,[2] and other states' data are generated by adjusting the industry's electricity price data for each state (BLS 2011). Transportation costs were compiled from the "Agricultural Refrigerated Truck Quarterly"(USDA AMS 2011) and missing data were generated taking into account the relationship between costs and distances.[3]

5.1 CO2 emissions in production, storage and transportation

Bringing apples from the orchard to consumers requires various activities including farm-level production, storage and transportation, which generate CO2 emissions released into the atmosphere. Therefore, accounting for CO2 emissions along the fresh apple supply chain is critical to assess the economic impacts of CO2 emissions reduction policies.

First, farm-level activities in orchards contribute to CO2 emissions in two ways: direct and indirect energy use. CO2 emissions from direct energy use are primarily associated with water irrigation which is a critical input in apple production in some parts of the United States. Because of regional differences in rainfall patterns, irrigation requirements are different across the supply locations. Table 5.1 shows CO2

$p_h=6.423-0.008ex_h$, respectively. The data for estimating import and export parameters is from USDA Economics Research Service, Fruits and Tree Nuts Yearbook Table (https://www.ers.usda.gov/data-products/fruit-and-tree-nut-data/fruit-and-tree-nut-yearbook-tables/). Note that the subscript *nh* refers to the non-harvest season whereas the subscript *h* refers to the harvest season.

[2] We collected storage costs data from H.H. Dobbins, Inc in Lyndonville, NY. In western New York, the storage costs operating regular (cold air) storage are $23.50 per bin. In contrast, CA storage costs $33.50 per bin for apple storage. See Section 4.0 for data table for storage costs.

[3] See the Section 4.0 for data table for transportation costs.

emissions resulting from irrigation activities in each supply region (NYSERDA 2008). These data show that the Western states, California and Washington, are arid and require relatively more irrigation due to lower precipitation. In contrast, the Eastern states need less energy for irrigation in apple production. However, given differences in yields across supply regions, CO2 emissions per million pounds of apples are lowest in Washington and highest in California.

Table 5.1 CO2 emissions per unit apple production and storage

	CA	MI	NY	PA	VA	WA
	Metric Ton of CO2 per million pounds					
Production						
Direct use[a]						
Rainfall (*inch*)	0.5	3.0	3.0	3.5	3.5	1.0
Energy use (*kBTU/acre*)	20,347	3,393	3,391	3,393	3,393	23,739
CO2 emissions	312.98	208.65	163.29	185.97	185.97	154.22
Indirect use[b]						
CO2 emissions from fertilizer use	3.145	2.367	1.892	1.197	2.783	2.328
CO2 emissions from ag-chemical use	17.246	10.770	8.198	8.629	15.699	11.943
	Metric Ton of CO2 Ton per Acre					
CO2 sequestration rate[c] during apple production	0.105	0.145	0.129	0.129	0.129	0.105
Storage[d]	*Metric Ton of CO2 per million pounds*					
Regular Storage	80.45					
CA Storage	314.45					
Transportation[e]	*Kg Ton of CO2 per mile per truck*					
Heavy-diesel truck (class 8)	1.64					

a. Source: NYSERDA (2008).

b. Source: Saunders, Barber and Taylor (2006).

c. Source: Kroodsma and Field (2006).

d. Source: Canals et al. (2004).

e. Source: Mobile 6.2, US EPA (2011)

Another CO2 emission source in farm-level apple production comes indirectly due to the application of fertilizer and agricultural chemicals.[4] Data on fertilizer and agricultural chemicals usage in each supply location are from the U.S. Department of Agriculture (USDA NASS 2008). Subsequently, the data were converted into CO2 emissions following Saunders, Barber and Taylor (2006). Table 5.1 reports CO2 emissions resulting from the use of fertilizers and agricultural chemicals. Our accounting process suggests that, on a per unit basis, CO2 emissions are highest in California. In contrast, Pennsylvania shows the lowest emissions in terms of fertilizer and agricultural chemical use.

Although food supply chain activities release CO2 to the atmosphere, agricultural practices can capture a considerable amount of CO2 in soils and biomass (Lewandrowski et al. 2004). The extent to which carbon is sequestered varies between crop types. Particularly, orchards extract relatively more CO2 from the atmosphere than the average of all crops. For instance, non-silage annual crop capture an average of 14 g of CO2 per m^2 annually, whereas orchards sequester 26 g of CO2 per m^2 annually (Kroodsma and Field 2006). We take into account CO2 capturing, naturally occurring in orchard farms. Table 5.1 reports annual carbon sequestration rates during apple production by each region. Given differences in soil characteristics and climatic conditions across supply regions, carbon sequestration rates are relatively low in the Western states (California and Washington) and is relatively high in the Eastern states (New York, Pennsylvania and Virginia). Net CO2 emissions in apple production are obtained by deducting the sequestered CO2.

Storage activities also discharge a substantial amount of CO2 into the atmosphere. As described in section 1.0, apples for fresh utilization are put into either regular or CA storage depending on the time of year that

[4] Components of fertilizer such as nitrogen, phosphate, potash and sulfur are converted to CO2 when they are applied to soil. Furthermore, the use of agricultural chemicals including herbicide, insecticide and fungicide also generates CO2 emissions.

the apples are sold. Each storage facility is operated using electricity to maintain the proper temperature for apple freshness (Canals et al. 2007). Table 5.1 shows CO2 emissions generated by storage operation. Transport activities also emit CO2 during apple distribution. Fresh apples are mostly moved by heavy-duty trucks (class 8) which haul about 40,000 pounds with fuel economy of 6.1 mpg (King et al. 2010)[5]. We compiled CO2 emission data in fresh apple transportation using the MOBILE 6.2 model developed by the U.S. Environmental Protection Agency (US EPA 2011). We used the average CO2 emission rate of 1.64 kg/mile with fuel economy of 6.1 mpg.

6. Model validation and baseline solutions

Before validating the mathematical model (2.1)-(2.7), we construct the linear supply and demand functions as in equation (3.1) using the estimated price elasticities of supply and demand, quantities for supply and demand, and producer prices and retail prices, respectively. We solve the mathematical model (2.1)-(2.7) using the General Algebraic Modeling System (GAMS). The estimated solutions were compared with actual data in 2006 for model validation. Table 6.1 presents the baseline solutions of the model, the actual 2006 data and the ratio of our estimated to the actual value for all supply locations and for selected consumption locations.

[5] There are three transportation options depending on distribution networks: 1) a semi-trailer hauling 40,000 pounds of apples; 2) a mid-size truck hauling 10,000 pounds of apples; and 3) a pick-up truck hauling 1,000 pounds of apples (King et al. 2010).

Table 6.1 Baseline solutions and comparison with actual data in 2006

	Estimated[a]	Actual	Estimated/Actual (%)
Total Supply (*million pounds*)	**5,567**	**5,656**	98.4
Quantity (*million pounds*)			
California	152	155	98.1
Michigan	287	295	97.3
New York	681	690	98.7
Pennsylvania	130	132	98.5
Virginia	32	34	94.1
Washington	4,285	4350	98.5
Producer Price ($/pound)			
California	0.397	0.412	96.4
Michigan	0.225	0.245	91.8
New York	0.292	0.302	96.7
Pennsylvania	0.250	0.257	97.3
Virginia	0.213	0.238	89.5
Washington	0.295	0.313	94.2
Export (*million pounds*)	1,565	1,508	103.8
Import (*million pounds*)	294	345	85.2
Total demand (*million pounds*)	**4,454**	**4,493**	99.1
Retail Price (Non-harvest) ($/pound)			
Atlanta	1.239	1.25	99.1
Los Angeles	1.177	1.16	101.5
New York	1.248	1.24	100.6
Philadelphia	1.247	1.26	99.0
Retail Price (Harvest) ($/pound)			
Atlanta	1.243	1.40	88.8
Los Angeles	1.191	1.27	93.8
New York	1.249	1.33	93.9

Philadelphia	1.249	1.34	93.2

a. Source: Authors' calibration

The estimated total production accounts for 98.4 percent of actual apples produced in all six states. Due to the slightly low quantities estimated by the model, prices in each supply region are also modestly underestimated in comparison to actual producer prices in 2006. These differences may be because we do not take into account direct distribution systems (e.g. orchard to retailers and orchard to consumers). The estimated retail prices for the harvest season are practically the same as the actual retail prices in selected consumption locations (Table 6.1). However, the estimates for the non-harvest season are higher in comparison to actual data.

Table 6.2 presents CO2 emissions derived from the baseline model. The results show that the largest emissions along the fresh apple supply chain are attributable to farm-level apple production activities, accounting for about 46.6 percent of total supply chain CO2 emissions. Storage activities rank second in CO2 emissions, generating 43.6 percent of total CO2 emissions. Emissions from transportation activities are relatively low compared to production and storage activities, discharging 9.8 percent of total CO2 emissions in supply chain. Note that the values presented in Table 6.2 are based on the values obtained after solving the mathematical model (2.1) -(2.7) for the baseline model. Hence, CO2 emissions values in controlled atmosphere are not proportional to the levels of productions. This is due to the fact that the model optimizes the quantities of apple of each region to be stored in the controlled atmosphere versus the quantities that has to be stored in the regular storage.

Table 6.2 CO2 emissions along the fresh apple supply chain (Metric tons of CO2)

	CA	MI	NY	PA	VA	WA	Total	%
Production[a]	49,586	61,836	114,941	24,642	6,335	709,544	966,884	40.58
Regular storage[a]	11,688	21,107	3,680	574	43	152,673	189,765	7.96
CA storage[a]	1,974	7,744	199,765	38,678	9,923	750,777	1,008,859	42.34
Transportation[a]							217,225	9.12
Total Emission							2,382,735	100

a. Source: Authors' calibration

7. Estimation results of the LA-ADIS model and cost data tables

Table 7.1 Estimation results of LA-AIDS model for the non-harvest season in the Northeast

Budget Share	Variables	Parameter	Std. Err.	t-value	Probability
GD	*Constant*	1.199	0.011	107.01	<.0001
	η	-0.126	0.002	-78.45	<.0001
	lnp_{gd}	-0.038	0.019	-2.01	0.045
	lnp_{gs}	0.054	0.016	3.32	***0.0009***
	lnp_{rd}	-0.011	0.009	-1.18	0.2383
	lnp_{gl}	-0.005	0.011	-0.46	0.6448
	lnp_{ot}	-0.001	0.006	-0.11	0.9131
	X/P	0.003	0.002	2.04	0.0414
	MR_{gd}	-0.165	0.001	-114.92	<.0001
	T	0.000	0.003	-0.04	0.9669
GS	*Constant*	1.283	0.034	37.34	<.0001
	η	-0.287	0.009	-33.67	<.0001
	lnp_{gd}	0.054	0.016	3.32	0.0009
	lnp_{gs}	-0.096	0.029	-3.29	0.001
	lnp_{rd}	0.012	0.015	0.8	0.4248
	lnp_{gl}	-0.006	0.015	-0.41	0.6842
	lnp_{ot}	0.036	0.016	2.26	0.0241
	X/P	0.000	0.005	0	0.999
	MR_{gd}	-0.344	0.009	-37.36	<.0001
	T	-0.009	0.009	-1.02	0.3083
RD	*Constant*	1.203	0.007	161.51	<.0001
	η	0.024	0.001	16.41	<.0001
	lnp_{gd}	-0.011	0.009	-1.18	0.2383
	lnp_{gs}	0.012	0.015	0.8	0.4248
	lnp_{rd}	-0.002	0.008	-0.2	0.8436
	lnp_{gl}	-0.002	0.008	-0.2	0.8436
	lnp_{ot}	0.002	0.007	0.28	0.7813
	X/P	-0.007	0.002	-3.39	0.0007
	MR_{gd}	0.332	0.002	193.52	<.0001
	T	0.004	0.004	0.98	0.3264
GL	*Constant*	1.067	0.007	145.44	<.0001
	η	0.013	0.001	10.07	<.0001
	lnp_{gd}	-0.005	0.011	-0.46	0.6448
	lnp_{gs}	-0.006	0.015	-0.41	0.6842
	lnp_{rd}	-0.014	0.011	-1.25	0.2122
	lnp_{gl}	0.032	0.013	2.37	0.0179
	lnp_{ot}	-0.007	0.006	-1.11	0.2651
	X/P	-0.005	0.002	-2.72	0.0066
	MR_{gd}	0.357	0.002	169.99	<.0001
	T	0.004	0.004	1.27	0.2044
# of Observations	1465		R^2	0.93	

Table 7.2 Estimation results of LA-AIDS model for the harvest season in the Northeast

Budget Share	Variables	Parameter	Std. Err.	t-value	Probability
GD	*Constant*	1.080	0.011	94.94	<.0001
	η	-0.110	0.002	-61.64	<.0001
	lnp_{gd}	-0.028	0.016	-1.75	0.0796
	lnp_{gs}	0.040	0.015	2.74	**0.0063**
	lnp_{rd}	-0.008	0.010	-0.78	0.4347
	lnp_{gl}	0.000	0.011	0.02	0.9806
	lnp_{ot}	-0.005	0.006	-0.82	0.4132
	X/P	-0.004	0.002	-2.19	0.0289
	MR_{gd}	-0.148	0.001	-103.62	<.0001
	T	-0.007	0.004	-1.99	0.0462
GS	*Constant*	1.154	0.030	38.03	<.0001
	η	-0.245	0.008	-32.21	<.0001
	lnp_{gd}	0.040	0.015	2.74	**0.0063**
	lnp_{gs}	-0.167	0.029	-5.76	<.0001
	lnp_{rd}	0.025	0.018	1.41	0.1595
	lnp_{gl}	0.070	0.018	3.95	**<.0001**
	lnp_{ot}	0.031	0.014	2.23	0.0261
	X/P	-0.014	0.004	-3.25	0.0012
	MR_{gs}	-0.302	0.008	-37.34	<.0001
	T	-0.007	0.009	-0.82	0.4149
RD	*Constant*	1.072	0.011	95.31	<.0001
	η	0.019	0.002	8.31	<.0001
	lnp_{gd}	-0.008	0.010	-0.78	0.4347
	lnp_{gs}	0.025	0.018	1.41	0.1595
	lnp_{rd}	0.000	0.010	-0.03	0.9723
	lnp_{gl}	0.000	0.010	-0.03	0.9723
	lnp_{ot}	-0.016	0.010	-1.66	0.0969
	X/P	-0.018	0.003	-5.97	<.0001
	MR_{rd}	0.289	0.003	112.44	<.0001
	T	-0.009	0.006	-1.59	0.1131
GL	*Constant*	0.926	0.011	84.93	<.0001
	η	0.012	0.002	5.9	<.0001
	lnp_{gd}	0.000	0.011	0.02	0.9806
	lnp_{gs}	0.070	0.018	3.95	**<.0001**
	lnp_{rd}	0.007	0.016	0.42	0.6729
	lnp_{gl}	-0.068	0.019	-3.7	0.0002
	lnp_{ot}	-0.009	0.009	-0.98	0.329
	X/P	-0.016	0.003	-5.74	<.0001
	MR_{gl}	0.306	0.003	103.44	<.0001
	T	-0.001	0.006	-0.19	0.8525
# of Observations	1707		R^2	0.83	

Table 7.3 Estimation results of LA-AIDS model for the non-harvest season in the Midwest

Budget Share	Variables	Parameter	Std. Err.	t-value	Probability
GD	*Constant*	1.212	0.014	85.73	<.0001
	η	-0.124	0.002	-59.47	<.0001
	lnp_{gd}	-0.074	0.017	-4.28	<.0001
	lnp_{gs}	0.070	0.019	3.76	**0.0002**
	lnp_{rd}	-0.007	0.010	-0.65	0.5177
	lnp_{gl}	0.005	0.012	0.4	0.6879
	lnp_{ot}	0.006	0.007	0.9	0.3683
	X/P	-0.003	0.002	-1.23	0.2176
	MR_{gd}	-0.167	0.002	-94.32	<.0001
	T	-0.003	0.004	-0.65	0.5137
GS	*Constant*	1.386	0.037	37.46	<.0001
	η	-0.311	0.009	-34.19	<.0001
	lnp_{gd}	0.070	0.019	3.76	**0.0002**
	lnp_{gs}	-0.212	0.035	-5.98	<.0001
	lnp_{rd}	0.053	0.018	2.89	**0.0039**
	lnp_{gl}	0.045	0.019	2.4	0.0164
	lnp_{ot}	0.044	0.015	2.85	**0.0044**
	X/P	-0.010	0.005	-1.98	0.0481
	MR_{gs}	-0.361	0.010	-37.56	<.0001
	T	-0.010	0.009	-1.07	0.285
RD	*Constant*	1.168	0.009	122.91	<.0001
	η	0.025	0.002	12.66	<.0001
	lnp_{gd}	-0.007	0.010	-0.65	0.5177
	lnp_{gs}	0.053	0.018	2.89	**0.0039**
	lnp_{rd}	-0.020	0.010	-2.09	0.0367
	lnp_{gl}	-0.020	0.010	-2.09	0.0367
	lnp_{ot}	-0.007	0.008	-0.81	0.4175
	X/P	-0.005	0.003	-2.04	0.0417
	MR_{rd}	0.326	0.002	146.36	<.0001
	T	0.010	0.005	1.9	0.0573
GL	*Constant*	1.035	0.010	103.32	<.0001
	η	0.014	0.002	7.95	<.0001
	lnp_{gd}	0.005	0.012	0.4	0.6879
	lnp_{gs}	0.045	0.019	2.4	0.0164
	lnp_{rd}	-0.016	0.013	-1.18	0.2377
	lnp_{gl}	-0.025	0.016	-1.5	0.1344
	lnp_{ot}	-0.009	0.008	-1.17	0.2404
	X/P	-0.005	0.002	-2.25	0.0244
	MR_{gl}	0.346	0.003	119.17	<.0001
	T	0.000	0.005	-0.01	0.992
# of Observations	1113		R^2	0.92	

Table 7.4 Estimation results of LA-AIDS model for the harvest season in the Midwest

Budget Share	Variables	Parameter	Std. Err.	t-value	Probability
GD	*Constant*	1.144	0.013	85.02	<.0001
	η	-0.113	0.002	-50.79	<.0001
	lnp_{gd}	-0.012	0.017	-0.69	0.4881
	lnp_{gs}	0.012	0.018	0.68	0.4987
	lnp_{rd}	0.004	0.011	0.36	0.7226
	lnp_{gl}	-0.005	0.011	-0.44	0.6583
	lnp_{ot}	0.001	0.007	0.13	0.8938
	X/P	-0.012	0.002	-4.92	<.0001
	MR_{gd}	-0.156	0.002	-94.54	<.0001
	T	0.002	0.005	0.36	0.7209
GS	*Constant*	1.062	0.039	27.14	<.0001
	η	-0.226	0.010	-23.5	<.0001
	lnp_{gd}	0.012	0.018	0.68	0.4987
	lnp_{gs}	-0.033	0.033	-0.99	0.3205
	lnp_{rd}	0.001	0.019	0.07	0.944
	lnp_{gl}	0.008	0.019	0.4	0.6865
	lnp_{ot}	0.012	0.016	0.78	0.4342
	X/P	-0.018	0.005	-3.37	0.0008
	MR_{gs}	-0.282	0.010	-27.81	<.0001
	T	0.003	0.010	0.33	0.7436
RD	*Constant*	1.105	0.012	93.16	<.0001
	η	0.023	0.002	9.49	<.0001
	lnp_{gd}	0.004	0.011	0.36	0.7226
	lnp_{gs}	0.001	0.019	0.07	0.944
	lnp_{rd}	-0.005	0.010	-0.56	0.5785
	lnp_{gl}	-0.005	0.010	-0.56	0.5785
	lnp_{ot}	0.006	0.009	0.6	0.5469
	X/P	-0.016	0.003	-5.07	<.0001
	MR_{rd}	0.301	0.003	110.18	<.0001
	T	-0.007	0.006	-1.11	0.2654
GL	*Constant*	0.981	0.012	78.74	<.0001
	η	0.010	0.002	3.99	<.0001
	lnp_{gd}	-0.005	0.011	-0.44	0.6583
	lnp_{gs}	0.008	0.019	0.4	0.6865
	lnp_{rd}	-0.024	0.017	-1.41	0.1575
	lnp_{gl}	0.036	0.017	2.09	0.0372
	lnp_{ot}	-0.014	0.010	-1.51	0.1303
	X/P	-0.025	0.003	-7.56	<.0001
	MR_{gl}	0.317	0.003	91.66	<.0001
	T	-0.005	0.006	-0.74	0.4587
# of Observations	1282		R^2	0.86	

Table 7.5 Estimation results of LA-AIDS model for the non-harvest season in the South

Budget Share	Variables	Parameter	Std. Err.	t-value	Probability
GD	*Constant*	1.232	0.007	169.82	<.0001
	η	-0.130	0.001	-118.42	<.0001
	lnp_{gd}	-0.030	0.009	-3.41	0.0007
	lnp_{gs}	0.026	0.009	2.83	**0.0046**
	lnp_{rd}	-0.004	0.005	-0.73	0.4641
	lnp_{gl}	0.003	0.007	0.39	0.6967
	lnp_{ot}	0.005	0.005	1.06	0.2878
	X/P	-0.003	0.001	-2.67	0.0077
	MR_{gd}	-0.168	0.001	-180.15	<.0001
	T	0.002	0.002	1.15	0.2513
GS	*Constant*	1.425	0.025	56.79	<.0001
	η	-0.323	0.006	-50.82	<.0001
	lnp_{gd}	0.026	0.009	2.83	**0.0046**
	lnp_{gs}	-0.066	0.022	-3	0.0027
	lnp_{rd}	0.001	0.010	0.14	0.8851
	lnp_{gl}	-0.006	0.012	-0.46	0.6475
	lnp_{ot}	0.044	0.014	3.12	**0.0019**
	X/P	-0.010	0.003	-2.89	0.0039
	MR_{gs}	-0.377	0.007	-56.3	<.0001
	T	0.000	0.007	-0.07	0.9455
RD	*Constant*	1.203	0.006	210.97	<.0001
	η	0.024	0.001	20.34	<.0001
	lnp_{gd}	-0.004	0.005	-0.73	0.4641
	lnp_{gs}	0.001	0.010	0.14	0.8851
	lnp_{rd}	0.001	0.005	0.12	0.902
	lnp_{gl}	0.001	0.005	0.12	0.902
	lnp_{ot}	0.001	0.006	0.13	0.8929
	X/P	-0.008	0.002	-5.16	<.0001
	MR_{rd}	0.332	0.001	252.43	<.0001
	T	0.002	0.003	0.81	0.4188
GL	*Constant*	1.062	0.007	158.7	<.0001
	η	0.013	0.001	10.18	<.0001
	lnp_{gd}	0.003	0.007	0.39	0.6967
	lnp_{gs}	-0.006	0.012	-0.46	0.6475
	lnp_{rd}	-0.020	0.009	-2.35	0.019
	lnp_{gl}	0.033	0.012	2.74	0.0062
	lnp_{ot}	-0.010	0.007	-1.38	0.1673
	X/P	-0.009	0.002	-5.58	<.0001
	MR_{gl}	0.353	0.002	182.4	<.0001
	T	-0.004	0.003	-1.26	0.209
# of Observations	2487		R^2	0.93	

Table 7.6 Estimation results of LA-AIDS model for the harvest season in the South

Budget Share	Variables	Parameter	Std. Err.	t-value	Probability
GD	*Constant*	1.064	0.009	115.59	<.0001
	η	-0.107	0.002	-68.94	<.0001
	lnp_{gd}	0.001	0.012	0.09	0.9291
	lnp_{gs}	0.016	0.011	1.47	0.1423
	lnp_{rd}	0.001	0.008	0.08	0.9389
	lnp_{gl}	-0.019	0.009	-2.17	0.0303
	lnp_{ot}	0.001	0.006	0.09	0.9301
	X/P	-0.012	0.002	-7.27	<.0001
	MR_{gd}	-0.145	0.001	-126.47	<.0001
	T	0.003	0.003	0.86	0.3877
GS	*Constant*	1.289	0.022	58.02	<.0001
	η	-0.282	0.006	-50.15	<.0001
	lnp_{gd}	0.016	0.011	1.47	0.1423
	lnp_{gs}	-0.081	0.021	-3.93	<.0001
	lnp_{rd}	0.011	0.012	0.94	0.3477
	lnp_{gl}	0.027	0.013	2.14	0.0322
	lnp_{ot}	0.027	0.013	2.06	0.0391
	X/P	-0.017	0.003	-5.11	<.0001
	MR_{gs}	-0.339	0.006	-57.66	<.0001
	T	-0.007	0.007	-0.98	0.329
RD	*Constant*	1.105	0.009	129.45	<.0001
	η	0.021	0.002	11.16	<.0001
	lnp_{gd}	0.001	0.008	0.08	0.9389
	lnp_{gs}	0.011	0.012	0.94	0.3477
	lnp_{rd}	-0.004	0.007	-0.54	0.591
	lnp_{gl}	-0.004	0.007	-0.54	0.591
	lnp_{ot}	-0.004	0.009	-0.46	0.6424
	X/P	-0.020	0.002	-8.47	<.0001
	MR_{rd}	0.301	0.002	156.17	<.0001
	T	0.008	0.005	1.64	0.1018
GL	*Constant*	0.970	0.009	109.97	<.0001
	η	0.010	0.002	5.44	<.0001
	lnp_{gd}	-0.019	0.009	-2.17	0.0303
	lnp_{gs}	0.027	0.013	2.14	0.0322
	lnp_{rd}	-0.021	0.012	-1.79	0.073
	lnp_{gl}	0.031	0.014	2.29	0.0218
	lnp_{ot}	-0.018	0.009	-1.97	0.049
	X/P	-0.021	0.002	-8.99	<.0001
	MR_{gl}	0.318	0.002	136.15	<.0001
	T	0.006	0.005	1.19	0.233
# of Observations	2747		R^2	0.85	

Table 7.7 Estimation results of LA-AIDS model for the non-harvest season in the West

Budget Share	Variables	Parameter	Std. Err.	t-value	Probability
GD	*Constant*	1.267	0.007	188	<.0001
	η	-0.136	0.001	-146.98	<.0001
	lnp_{gd}	-0.052	0.009	-5.9	<.0001
	lnp_{gs}	0.053	0.007	7.16	**<.0001**
	lnp_{rd}	0.000	0.005	-0.1	0.9224
	lnp_{gl}	-0.004	0.005	-0.75	0.4559
	lnp_{ot}	0.003	0.002	1.55	0.1216
	X/P	0.000	0.001	0.18	0.8557
	MR_{gd}	-0.172	0.001	-194.21	<.0001
	T	-0.001	0.002	-0.4	0.689
GS	*Constant*	1.471	0.030	49.06	<.0001
	η	-0.343	0.008	-45.52	<.0001
	lnp_{gd}	0.053	0.007	7.16	**<.0001**
	lnp_{gs}	-0.075	0.018	-4.18	<.0001
	lnp_{rd}	-0.020	0.010	-2.08	0.0381
	lnp_{gl}	0.014	0.012	1.11	0.2692
	lnp_{ot}	0.028	0.008	3.5	**0.0005**
	X/P	-0.011	0.003	-3.72	0.0002
	MR_{gs}	-0.383	0.008	-49.02	<.0001
	T	-0.007	0.006	-1.19	0.2338
RD	*Constant*	1.185	0.007	175.08	<.0001
	η	0.024	0.001	20.94	<.0001
	lnp_{gd}	0.000	0.005	-0.1	0.9224
	lnp_{gs}	-0.020	0.010	-2.08	0.0381
	lnp_{rd}	0.010	0.005	1.89	0.0591
	lnp_{gl}	0.010	0.005	1.89	0.0591
	lnp_{ot}	0.001	0.004	0.25	0.8065
	X/P	-0.003	0.001	-2.17	0.0302
	MR_{rd}	0.327	0.002	204.82	<.0001
	T	0.001	0.003	0.35	0.7258
GL	*Constant*	1.029	0.009	118.15	<.0001
	η	0.009	0.002	5.78	<.0001
	lnp_{gd}	-0.004	0.005	-0.75	0.4559
	lnp_{gs}	0.014	0.012	1.11	0.2692
	lnp_{rd}	-0.012	0.011	-1.04	0.2984
	lnp_{gl}	0.003	0.013	0.24	0.8115
	lnp_{ot}	-0.001	0.005	-0.18	0.8538
	X/P	-0.006	0.002	-3.36	0.0008
	MR_{gl}	0.340	0.002	138.27	<.0001
	T	0.001	0.004	0.33	0.7445
# of Observations	1842		R^2	0.93	

Table 7.8 Estimation results of LA-AIDS model for the harvest season in the West

Budget Share	Variables	Parameter	Std. Err.	t-value	Probability
GD	*Constant*	1.055	0.010	104.6	<.0001
	η	-0.112	0.001	-75.5	<.0001
	lnp_{gd}	0.011	0.012	0.91	0.3625
	lnp_{gs}	0.014	0.010	1.31	0.1888
	lnp_{rd}	-0.016	0.007	-2.23	0.0259
	lnp_{gl}	-0.009	0.006	-1.53	0.1266
	lnp_{ot}	0.000	0.004	-0.06	0.9501
	X/P	-0.004	0.001	-2.74	0.0062
	MR_{gd}	-0.143	0.001	-110.57	<.0001
	T	-0.003	0.003	-1.07	0.2848
GS	*Constant*	1.298	0.027	47.43	<.0001
	η	-0.290	0.007	-41.45	<.0001
	lnp_{gd}	0.014	0.010	1.31	0.1888
	lnp_{gs}	-0.081	0.020	-4.01	<.0001
	lnp_{rd}	0.000	0.012	0.01	0.9927
	lnp_{gl}	0.040	0.012	3.3	**0.001**
	lnp_{ot}	0.027	0.010	2.71	**0.0069**
	X/P	-0.012	0.004	-3.18	0.0015
	MR_{gs}	-0.342	0.007	-47.61	<.0001
	T	0.012	0.008	1.51	0.1303
RD	*Constant*	1.032	0.011	96.24	<.0001
	η	0.020	0.002	9.96	<.0001
	lnp_{gd}	-0.016	0.007	-2.23	0.0259
	lnp_{gs}	0.000	0.012	0.01	0.9927
	lnp_{rd}	0.006	0.007	0.93	0.3547
	lnp_{gl}	0.006	0.007	0.93	0.3547
	lnp_{ot}	0.003	0.007	0.44	0.6568
	X/P	-0.016	0.003	-6.37	<.0001
	MR_{rd}	0.280	0.002	113.45	<.0001
	T	-0.003	0.005	-0.63	0.5302
GL	*Constant*	0.963	0.011	88.41	<.0001
	η	0.011	0.002	4.83	<.0001
	lnp_{gd}	-0.009	0.006	-1.53	0.1266
	lnp_{gs}	0.040	0.012	3.3	**0.001**
	lnp_{rd}	0.001	0.013	0.1	0.9232
	lnp_{gl}	-0.021	0.012	-1.79	0.0742
	lnp_{ot}	-0.010	0.007	-1.44	0.1501
	X/P	-0.023	0.003	-8.68	<.0001
	MR_{gl}	0.312	0.003	112.47	<.0001
	T	-0.006	0.005	-1.18	0.2398
# of Observations	1973		R^2	0.84	

Table 7.9 Average production costs by varieties[a] (Washington)

	Golden Delicious	Granny Smith	Red Delicious	Gala	Fuji (Others)
Variable Costs					
Labor	1,760	1,760	1,570	2,010	1,815
Chemicals	380	380	380	380	380
Operator Labor	285	333	285	333	285
Other	275	275	275	275	275
Total	2,700	2,748	2,510	2,998	2,755
Ownership Costs					
Depreciation	490	490	490	777	775
Interest	770	770	770	1,055	1,055
Taxes & Ins.	150	150	150	210	210
Total	1,410	1,410	1,410	2,042	2,040
Total Cost per Acre	4,110	4,158	3,920	5,040	4,795
Yield (bin)	50	50	40	40	35
$/pound	**0.1025**	**0.1040**	**0.1225**	**0.1575**	**0.1713**

a. Source: Schotzko and Granatstein (2005).

Table 7.10 Unit storage cost by storage facility in each region

	Regular Storage ($/pound)	Controlled Atmosphere Storage ($/pound)
California	0.031	0.044
Michigan	0.019	0.027
New York	0.029	0.042
Pennsylvania	0.020	0.029
Virginia	0.015	0.021
Washington	0.015	0.022

Table 7.11 Transportation costs from supply regions to consumption locations

	ALB	ATL	BAL	BIL	BMH	BOS	BPT	BSE	BUR	CIN
	$/ pound									
California	0.056	0.112	0.125	0.057	0.106	0.135	0.130	0.036	0.133	0.106
Michigan	0.072	0.045	0.039	0.063	0.041	0.049	0.044	0.087	0.041	0.027
New York	0.087	0.048	0.023	0.086	0.051	0.027	0.024	0.104	0.024	0.033
Pennsylvania	0.084	0.039	0.014	0.086	0.042	0.029	0.022	0.105	0.030	0.030
Virginia	0.084	0.036	0.016	0.087	0.039	0.033	0.025	0.105	0.033	0.030
Washington	0.064	0.114	0.121	0.041	0.109	0.131	0.125	0.026	0.128	0.102
	CHA	CHE	CHI	CHT	COL	DAL	DEN	DET	FAG	IND
California	0.122	0.058	0.097	0.114	0.120	0.083	0.062	0.107	0.082	0.102
Michigan	0.042	0.057	0.019	0.031	0.045	0.057	0.059	0.018	0.040	0.022
New York	0.038	0.075	0.037	0.032	0.042	0.070	0.077	0.030	0.062	0.035
Pennsylvania	0.029	0.075	0.037	0.025	0.033	0.066	0.076	0.030	0.063	0.032
Virginia	0.026	0.075	0.037	0.022	0.030	0.062	0.076	0.030	0.063	0.032
Washington	0.121	0.056	0.091	0.110	0.122	0.094	0.059	0.103	0.066	0.098
	JAC	KAN	LAG	LTR	LVG	LUS	MCH	MEM	MIA	MIL
California	0.099	0.083	0.028	0.092	0.035	0.104	0.138	0.097	0.137	0.097
Michigan	0.048	0.039	0.100	0.044	0.089	0.026	0.047	0.040	0.072	0.017
New York	0.060	0.055	0.118	0.057	0.107	0.037	0.029	0.052	0.067	0.040
Pennsylvania	0.052	0.052	0.116	0.053	0.107	0.034	0.030	0.048	0.057	0.041
Virginia	0.049	0.052	0.116	0.050	0.107	0.032	0.033	0.044	0.056	0.041
Washington	0.107	0.074	0.054	0.098	0.051	0.101	0.134	0.099	0.141	0.089
	MIN	MOI	NOR	NYC	NWK	OKL	OMH	PHI	PHO	POR
California	0.093	0.083	0.104	0.128	0.127	0.078	0.078	0.126	0.043	0.141
Michigan	0.036	0.032	0.055	0.042	0.041	0.050	0.038	0.040	0.089	0.049
New York	0.053	0.049	0.065	0.023	0.022	0.065	0.055	0.023	0.104	0.032
Pennsylvania	0.053	0.050	0.056	0.021	0.020	0.062	0.055	0.017	0.101	0.033
Virginia	0.054	0.050	0.053	0.023	0.023	0.062	0.056	0.021	0.101	0.036
Washington	0.075	0.079	0.114	0.123	0.123	0.086	0.075	0.122	0.063	0.136
	POT	PRO	RCH	SEA	SLC	STL	SUX	WDC	WMT	
California	0.036	0.136	0.127	0.043	0.040	0.093	0.081	0.124	0.126	
Michigan	0.104	0.045	0.041	0.096	0.075	0.030	0.037	0.038	0.040	
New York	0.122	0.027	0.028	0.119	0.092	0.045	0.060	0.024	0.023	
Pennsylvania	0.122	0.027	0.019	0.119	0.092	0.042	0.060	0.015	0.017	
Virginia	0.123	0.030	0.018	0.119	0.093	0.043	0.060	0.015	0.019	
Washington	0.019	0.132	0.123	0.017	0.040	0.091	0.068	0.120	0.122	

8. Detailed results for each policy

Note that in Table 8.2 there is no change in apple production quantities while there is reduction in CO2 emissions. The reason why there is reduction is CO2 emissions for different values of *k* parameter while apple production remains the same is because CO2 emissions due to land sparing for the same quantity of apples are different, depending on the performance of improvement in production yields. As emissions per unit decreases, total emissions also decrease given a fixed level of apple production. Likewise, in Table 8.3 there is no change in apple production quantities while there is reduction in CO2 emissions for cold storage following the same logic.

Table 8.1 Apple production quantities, CO2 emissions and consumer price under carbon tax scenario on all activities (i.e., production, storage and transportation)

k	Apple Production (Million pound)	CO2 Emissions (Metric Ton)	Consumer Price ($/pound)
0	5,562	2,239,391	1.080
0.1	5,558	2,225,322	1.080
0.2	5,554	2,220,764	1.080
0.3	5,550	2,184,994	1.080
0.4	5,545	2,181,192	1.080
0.5	5,540	2,176,907	1.080
0.6	5,536	2,172,696	1.080
0.7	5,531	2,168,595	1.080
0.8	5,527	2,164,330	1.080
0.9	5,522	2,161,788	1.080
1	5,517	2,159,448	1.080

Table 8.2 Apple production quantities, CO2 emissions and consumer price under land sparing strategy

k	Apple Production (Million Pound)	CO2 Emissions (Metric Ton)	Consumer Price ($/pound)
0	5,562	2,136,458	1.080
0.1	5,562	2,213,103	1.080
0.2	5,562	2,190,608	1.080
0.3	5,562	2,172,410	1.080
0.4	5,562	2,156,378	1.080
0.5	5,562	2,144,942	1.080
0.6	5,562	2,131,733	1.080
0.7	5,562	2,120,165	1.080
0.8	5,562	2,109,331	1.080
0.9	5,562	2,101,869	1.080
1	5,562	2,095,710	1.080

Table 8.3 Apple production quantities, CO2 emissions and consumer price under innovation in storage technologies strategies

k	Apple Production (Million Pound)	CO2 Emissions (Metric Ton)	Consumer Price ($/pound)
0	5,562	2,136,458	1.080
0.1	5,562	2,136,458	1.080
0.2	5,562	2,062,121	1.080
0.3	5,562	1,997,119	1.080
0.4	5,562	1,937,588	1.080
0.5	5,562	1,886,797	1.080
0.6	5,562	1,886,797	1.080
0.7	5,562	1,803,963	1.080
0.8	5,562	1,768,710	1.080
0.9	5,562	1,739,620	1.080
1	5,562	1,712,712	1.080

Table 8.4 Apple production quantities, CO2 emissions and consumer price under carbon tax for production activities only

Carbon Tax ($)	Apple Production (Million Pound)	CO2 Emissions (Metric Ton)	Consumer Price ($/pound)
50	5,563	2,391,420	1.080
150	5,558	2,389,825	1.080
250	5,549	2,387,435	1.080
350	5,542	2,385,404	1.080
450	5,535	2,383,268	1.080
550	5,528	2,373,137	1.080
650	5,521	2,370,920	1.080
750	5,513	2,368,753	1.080
850	5,505	2,366,238	1.080
950	5,493	2,363,130	1.080
1000	5,488	2,361,695	1.080

Table 8.5 Apple production quantities, CO2 emissions and consumer price under carbon tax for storage activities only

Carbon Tax ($)	Apple Production (Million Pound)	CO2 Emissions (Metric Ton)	Consumer Price ($/pound)
50	5,565	2,240,302	1.080
150	5,565	2,223,060	1.080
250	5,559	2,182,365	1.080
350	5,557	2,175,931	1.080
450	5,555	2,171,176	1.080
550	5,552	2,162,934	1.082
650	5,549	2,160,189	1.084
750	5,547	2,157,101	1.087
850	5,544	2,154,053	1.090
950	5,541	2,150,729	1.092
1000	5,540	2,149,067	1.094

Table 8.6 Apple production quantities, CO2 emissions and consumer price under carbon tax on all activities

Carbon Tax ($)	Apple Production (Million Pound)	CO2 Emissions (Metric Ton)	Consumer Price ($/pound)
50	5,562	2,231,924	1.080
150	5,553	2,212,757	1.080
250	5,543	2,172,472	1.080
350	5,533	2,163,297	1.080
450	5,523	2,155,461	1.080
550	5,512	2,150,469	1.082
650	5,496	2,144,073	1.084
750	5,480	2,137,454	1.087
850	5,463	2,130,525	1.090
950	5,446	2,122,998	1.093
1000	5,437	2,119,530	1.094

Table 8.7 Apple production quantities, CO2 emissions and consumer price under carbon tax for production activities only and land sparing

Carbon Tax ($)	Apple Production (Million Pound)	CO2 Emissions (Metric Ton)	Consumer Price ($/pound)
50	5,563	2,247,837	1.080
150	5,558	2,246,181	1.080
250	5,549	2,243,561	1.080
350	5,542	2,241,487	1.080
450	5,535	2,239,750	1.080
550	5,528	2,229,473	1.080
650	5,521	2,227,163	1.080
750	5,513	2,225,013	1.080
850	5,505	2,222,544	1.080
950	5,493	2,219,371	1.080
1000	5,488	2,217,856	1.080

Table 8.8 Apple production quantities, CO2 emissions and consumer price under carbon tax for storage activities only and land sparing

	Apple Production (Million Pound)	CO2 Emissions (Metric Ton)	Consumer Price ($/pound)
50	5,565	2,096,537	1.080
150	5,563	2,079,295	1.080
250	5,559	2,038,601	1.080
350	5,557	2,032,166	1.080
450	5,555	2,027,412	1.080
550	5,552	2,019,169	1.082
650	5,549	2,016,424	1.084
750	5,547	2,013,336	1.087
850	5,544	2,010,288	1.090
950	5,541	2,006,964	1.092
1000	5,540	2,005,303	1.094

Table 8.9 Apple production quantities, CO2 emissions and consumer price under carbon tax for all activities and land sparing

Carbon Tax ($)	Apple Production (Million Pound)	CO2 Emissions (Metric Ton)	Consumer Price ($/pound)
50	5,562	2,095,710	1.080
150	5,554	2,076,971	1.080
250	5,540	2,033,164	1.080
350	5,531	2,024,654	1.080
450	5,522	2,017,877	1.080
550	5,512	2,007,564	1.082
650	5,496	2,000,896	1.084
750	5,480	1,994,444	1.087
850	5,463	1,987,634	1.090
950	5,446	1,980,196	1.093
1000	5,437	1,976,864	1.094

Table 8.10 Apple production quantities, CO2 emissions and consumer price under carbon tax for production activities only and innovation in storage technologies strategies

Carbon Tax ($)	Apple Production (Million Pound)	CO2 Emissions (Metric Ton)	Consumer Price ($/pound)
50	5,563	1,782,616	1.080
150	5,558	1,781,256	1.080
250	5,549	1,779,228	1.080
350	5,541	1,777,464	1.080
450	5,535	1,775,597	1.080
550	5,528	1,774,058	1.080
650	5,521	1,772,139	1.080
750	5,513	1,770,271	1.080
850	5,505	1,768,104	1.080
950	5,493	1,765,449	1.080
1000	5,488	1,764,242	1.080

Table 8.11 Apple production quantities, CO2 emissions and consumer price under carbon tax for storage activities only and innovation in storage technologies strategies

Carbon Tax ($)	Apple Production (Million Pound)	CO2 Emissions (Metric Ton)	Consumer Price ($/pound)
50	5,566	1,714,826	1.080
150	5,565	1,709,267	1.080
250	5,564	1,704,788	1.080
350	5,562	1,688,175	1.080
450	5,561	1,686,570	1.080
550	5,559	1,684,822	1.080
650	5,558	1,682,635	1.080
750	5,557	1,680,657	1.080
850	5,555	1,678,946	1.080
950	5,554	1,678,070	1.080
1000	5,553	1,677,751	1.080

Table 8.12 Apple production quantities, CO2 emissions and consumer price under carbon tax for all activities and innovation in storage technologies strategies

Carbon Tax ($)	Apple Production (Million Pound)	CO2 Emissions (Metric Ton)	Consumer Price ($/pound)
50	5,563	1,713,926	1.080
150	5,556	1,707,101	1.080
250	5,545	1,700,581	1.080
350	5,537	1,682,003	1.080
450	5,529	1,678,517	1.080
550	5,520	1,674,883	1.080
650	5,511	1,671,066	1.080
750	5,498	1,666,119	1.080
850	5,484	1,661,515	1.080
950	5,470	1,657,739	1.080
1000	5,463	1,655,672	1.081

9. The potential of improvement of storage technologies in reducing CO2 emissions

In fact, there is no consensus in the literature about the exact potential of energy savings and CO2 emission reductions due to advancements in storage technologies. This is because energy savings in storage can be achieved by a variety of methods, techniques, technologies and/or change in storage practices. We report these estimates in selected studies:

- Garentt (2007) estimated potential energy savings between 20% and 50% through the proper specification, use and maintenance of equipment. More specifically, the study underscores that improvements can be achieved through better maintenance programs and/or the use of cleaner and more appropriate equipment to replace older ones. Furthermore, Garentt (2007) pointed out that there is vast information and guidelines to reduce GHG emissions in storage from bodies such as the Carbon Trust, the Institute of Refrigeration and the International Institute for Refrigeration.
- Suamir et al. [4] reported on experimental and theoretical investigations of the integration of CO2 refrigeration and trigeneration systems and their potential application in food refrigeration systems. The study showed that the system can offer energy savings of 30% and GHG emission savings of 43%.
- Oro et al. [5] studied energy savings and CO2 mitigation by incorporating Thermal Energy Storage (TES) and Phase Change Material (PCM) systems to cold storage and transportation systems in Europe. The compiled data on energy savings from different case studies and reported a cut down between 5% and 22% in reference to 2008 CO2 emissions in that continent.
- Liu et al. [6] proposed an innovative refrigeration system incorporating Phase Change Material (PCM) and Phase Change Thermal Storage Unit (PCTSU) for refrigerated trucks and reported 50%-80% savings in energy when using the proposed novel refrigeration system.

- James & James [3] estimated the potential for total energy saving in cold storage to be 20%-40% due to the use of new/alternative refrigeration technologies such as trigeneration and Sorption-adsorption.

Clearly, the potential of energy savings in cold-storage depends on several factors. Combining new technologies (such as PCM and TES) with optimized storage practices (such as proper maintenance) along with clean sources for generating electricity will lead to better energy savings in the cold storage sector. In our analysis we analyzed the impact of several levels of improvements in storage technologies by varying the simulation parameter k. In the three scenarios proposed, namely best case, average case and worst case, where 50%, 25% and 10% reduction in energy use correspond to each case. The value of the simulation parameter k would be 1, 0.5 and 0.2, as explained in the manuscript. From a technical perspective, one particularly promising technology is trigeneration –current trials suggest that such technologies are twice as efficient as existing ones. These systems can even use biomass as a fuel source.

10. Estimation results of the LA-ADIS model

Table 10.1 Elasticity Midwest non-harvest (Illinois, Ohio, Michigan, Missouri, Iowa, Indiana, Minnesota, Kansas, Kentucky, Nebraska, North Dakota, South Dakota, and Wisconsin).

	γ				
	gd	Gala Smith	Red delicious	Gala	Other
Gd	-0.07415	0.070151	-0.00651	0.004629	0.005879
Gala Smith	0.070151	-0.21225	0.053416	0.044719	0.04396
Red delicious	-0.00651	0.053416	-0.02001	-0.02001	-0.00689
Gala	0.004629	0.044719	-0.01586	-0.02464	-0.00885
Other	0.00588	0.04396	-0.0069	-0.0088	-0.0341
	π				
Gd	-0.00252				
Gala Smith	-0.00957				
Red delicious	-0.00547				
Gala	-0.00534				
Other	0.0229				
	σ				
Gd	0.043253				
Gala Smith	0.057504				
Red delicious	0.180598				
Gala	0.089663				
Other	0.628983				
	ϵ				
	Gd	Gala Smith	Red delicious	Gala	Other
Gd	-2.71686	1.218047	-0.03666	0.050414	0.009174
Gala Smith	1.609179	-4.70057	0.292726	0.492608	0.069016
Red delicious	-0.17336	0.911745	-1.11626	-0.23417	-0.01252
Gala	0.095955	0.769341	-0.09046	-1.28016	-0.01483
Other	0.468962	1.014964	0.041625	0.061954	-1.03132

Table 10.2 Elasticity Midwest harvest (Illinois, Ohio, Michigan, Missouri, Iowa, Indiana, Minnesota, Kansas, Kentucky, Nebraska, North Dakota, South Dakota, and Wisconsin).

	γ				
	gd	Gala Smith	Red delicious	Gala	Other
Gd	-0.01211	0.012163	0.004065	-0.00507	0.000949
Gala Smith	0.012163	-0.03319	0.001303	0.007581	0.01214
Red delicious	0.004065	0.001303	-0.00547	-0.00547	0.005563
Gala	-0.00507	0.007581	-0.0243	0.036204	-0.01442
Other	0.00095	0.01214	0.00556	-0.0144	-0.0042
	π				
gd	-0.01211				
Gala Smith	-0.01836				
Red delicious	-0.01637				
Gala	-0.02504				
Other	0.07188				
	σ				
gd	0.067111				
Gala Smith	0.065254				
Red delicious	0.168889				
Gala	0.127463				
Other	0.571284				
	ϵ				
	gd	Gala Smith	Red delicious	Gala	Other
gd	-1.19257	0.17394	0.019257	-0.04611	0.000239
Gala Smith	0.163384	-1.52693	0.000623	0.050075	0.019154
Red delicious	0.019366	-0.02241	-1.04873	-0.06457	0.004898
Gala	-0.12304	0.067249	-0.16279	-0.74101	-0.03083
other	0.626018	0.815332	0.276081	0.209047	-0.93553

Table 10.3 Elasticity Northeast non-harvest (Vermont, New York, Connecticut, New Hampshire, New Jersey, Massachusetts, Maine, Pennsylvania, and Rhode Island).

	γ				
	gd	Gala Smith	Red delicious	Gala	Other
gd	-0.0378	0.054058	-0.01068	-0.00496	-0.00061
Gala Smith	0.054058	-0.09562	0.011794	-0.006	0.035773
Red delicious	-0.01068	0.011794	-0.0015	-0.0015	0.001886
Gala	-0.00496	-0.006	-0.01393	0.031943	-0.00704
Other	-0.0006	0.03577	0.00189	-0.007	-0.03
	π				
gd	0.003215				
Gala Smith	5.86E-06				
Red delicious	-0.00655				
Gala	-0.00487				
Other	0.0082				
	σ				
gd	0.037793				
Gala Smith	0.061231				
Red delicious	0.175762				
Gala	0.110867				
Other	0.614347				
	ϵ				
	gd	Gala Smith	Red delicious	Gala	Other
gd	-1.99708	0.884834	-0.06006	-0.04368	-0.0008
Gala Smith	1.430388	-2.56162	0.067104	-0.05416	0.05823
Red delicious	-0.313	0.173816	-1.01509	-0.02392	0.001196
Gala	-0.14564	-0.10689	-0.08233	-0.71675	-0.01235
other	0.117092	0.666496	0.039389	-0.01811	-1.04064

Table 10.4 Elasticity Northeast harvest (Vermont, New York, Connecticut, New Hampshire, New Jersey, Massachusetts, Maine, Pennsylvania, and Rhode Island).

	γ				
	gd	Gala Smith	Red delicious	Gala	Other
gd	-0.0277	0.040498	-0.00806	0.000276	-0.00501
Gala Smith	0.040498	-0.16696	0.024827	0.070187	0.031444
Red delicious	-0.00806	0.024827	-0.00034	-0.00034	-0.01608
Gala	0.000276	0.070187	0.00689	-0.06848	-0.00887
Other	-0.005	0.03144	-0.0161	-0.0089	-0.0015
	π				
gd	-0.00402				
Gala Smith	-0.01404				
Red delicious	-0.01754				
Gala	-0.01579				
Other	0.05138				
	σ				
gd	0.051187				
Gala Smith	0.070649				
Red delicious	0.170787				
Gala	0.128639				
Other	0.578738				
	ϵ				
	gd	Gala Smith	Red delicious	Gala	Other
gd	-1.54518	0.570318	-0.04842	0.000548	-0.00901
Gala Smith	0.771801	-3.37721	0.13956	0.537895	0.052617
Red delicious	-0.21606	0.309021	-1.01954	-0.02594	-0.03296
Gala	-0.03429	0.964709	0.028449	-1.54814	-0.01884
other	0.483083	0.865978	0.079975	0.16221	-0.95118

Table 10.5 Elasticity South non-harvest (Georgia, Maryland, Texas, Alabama, Arkansas, Virginia, South Carolina, Mississippi, Oklahoma, Louisiana, Tennessee, West Virginia, Florida, North Carolina, Delaware, and District of Columbia).

	γ				
	gd	Gala Smith	Red delicious	Gala	Other
gd	-0.03026	0.026407	-0.00366	0.00267	0.00484
Gala Smith	0.026407	-0.06594	0.001489	-0.00571	0.043761
Red delicious	-0.00366	0.001489	0.000657	0.000657	0.000858
Gala	0.00267	-0.00571	-0.02025	0.033087	-0.00979
Other	0.00484	0.04376	0.00086	-0.0098	-0.0397
	π				
gd	-0.0028				
Gala Smith	-0.00953				
Red delicious	-0.00776				
Gala	-0.00923				
Other	0.02932				
	σ				
gd	0.042436				
Gala Smith	0.068389				
Red delicious	0.191592				
Gala	0.120696				
Other	0.576887				
	ϵ				
	gd	Gala Smith	Red delicious	Gala	Other
gd	-1.71579	0.384392	-0.01972	0.021137	0.008184
Gala Smith	0.606925	-1.97377	0.004372	-0.05274	0.074727
Red delicious	-0.12131	2.74E-05	-1.00434	-0.00688	-0.00109
Gala	0.036679	-0.09983	-0.11151	-0.73509	-0.0189
other	0.512584	0.887171	0.092747	0.058998	-1.03945

Table 10.6 Elasticity South harvest (Georgia, Maryland, Texas, Alabama, Arkansas, Virginia, South Carolina, Mississippi, Oklahoma, Louisiana, Tennessee, West Virginia, Florida, North Carolina, Delaware, and District of Columbia)).

	γ				
	gd	Gala Smith	Red delicious	Gala	Other
gd	0.001098	0.016269	0.000578	-0.0185	0.000557
Gala Smith	0.016269	-0.08091	0.011047	0.027033	0.026564
Red delicious	0.000578	0.011047	-0.00371	-0.00371	-0.0042
Gala	-0.0185	0.027033	-0.02135	0.031002	-0.01818
Other	0.00056	0.02656	-0.0042	-0.0182	-0.0047
	π				
gd	-0.01169				
Gala Smith	-0.01705				
Red delicious	-0.01992				
Gala	-0.02147				
Other	0.07014				
	σ				
gd	0.058414				
Gala Smith	0.079559				
Red delicious	0.206242				
Gala	0.16186				
Other	0.493924				
	ϵ				
	gd	Gala Smith	Red delicious	Gala	Other
gd	-0.99291	0.195905	-0.00051	-0.11853	-0.00026
Gala Smith	0.255296	-2.03408	0.046987	0.158638	0.051036
Red delicious	-0.06043	0.087211	-1.03791	-0.04831	-0.01683
Gala	-0.37624	0.296104	-0.1204	-0.82994	-0.04384
other	0.602584	0.769324	0.147582	0.101717	-0.93946

Table 10.7 Elasticity West non-harvest (California, Colorado, Oregon, Washington, Arizona, Idaho, Utah, Wyoming, Montana, Nevada, and New Mexico).

	γ				
	gd	Gala Smith	Red delicious	Gala	Other
gd	-0.05192	0.053272	-0.00046	-0.004	0.003104
Gala Smith	0.053272	-0.07482	-0.02034	0.013641	0.028247
Red delicious	-0.00046	-0.02034	0.00994	0.00994	0.000915
Gala	-0.004	0.013641	-0.01174	0.002999	-0.00091
Other	0.0031	0.02825	0.00091	-0.0009	-0.0314
	π				
gd	0.000136				
Gala Smith	-0.01134				
Red delicious	-0.00305				
Gala	-0.0062				
Other	0.02045				
	σ				
gd	0.023364				
Gala Smith	0.043901				
Red delicious	0.103363				
Gala	0.086822				
Other	0.742549				
	ϵ				
	gd	Gala Smith	Red delicious	Gala	Other
gd	-3.2222	1.213531	-0.00439	-0.046	0.004185
Gala Smith	2.258789	-2.7157	-0.20157	0.151384	0.037369
Red delicious	-0.03304	-0.47041	-0.90688	0.110856	0.000808
Gala	-0.19411	0.298473	-0.11877	-0.97165	-0.00194
other	0.782839	0.989324	0.155768	0.164482	-1.02178

Table 10.8 Elasticity West harvest (California, Colorado, Oregon, Washington, Arizona, Idaho, Utah, Wyoming, Montana, Nevada, and New Mexico).

	γ				
	gd	Gala Smith	Red delicious	Gala	Other
gd	0.011307	0.013659	-0.01551	-0.00924	-0.00022
Gala Smith	0.013659	-0.08068	0.000114	0.03962	0.027283
Red delicious	-0.01551	0.000114	0.006212	0.006212	0.002967
Gala	-0.00924	0.03962	0.001261	-0.02136	-0.01028
Other	-0.0002	0.02728	0.00297	-0.0103	-0.0198
	π				
gd	-0.00361				
Gala Smith	-0.01213				
Red delicious	-0.01607				
Gala	-0.0234				
Other	0.0552				
	σ				
gd	0.02912				
Gala Smith	0.073984				
Red delicious	0.121533				
Gala	0.149338				
Other	0.626025				
Elasticity (ϵ)					
	gd	Gala Smith	Red delicious	Gala	Other
gd	-0.61531	0.183195	-0.12845	-0.06257	-0.00052
Gala Smith	0.438239	-2.10257	-0.00644	0.259296	0.042148
Red delicious	-0.59951	-0.02485	-0.96495	0.028524	0.00162
Gala	-0.43731	0.488283	-0.01838	-1.16646	-0.022
other	1.179139	0.835866	0.30876	0.162589	-0.97635

Table 10.9 Ratio of own price elasticity to cross price elasticity of cross elasticities that are statistically significant.

Census Division	Season	Variety	Variety	Cross Elasticity	Own Elasticity	Ratio
Northeast	Non-harvest	GD	GS	0.88	2.00	2.26
Northeast	harvest	GD	GS	0.57	1.55	2.71
Northeast	harvest	GS	GD	0.77	3.38	4.38
Northeast	harvest	GS	GL	0.54	3.38	6.28
Northeast	harvest	GL	GS	0.96	1.55	1.60
Midwest	Non-harvest	GD	GS	1.22	2.72	2.23
Midwest	Non-harvest	GS	GD	1.61	4.70	2.92
Midwest	Non-harvest	GS	RD	0.29	4.70	16.06
Midwest	Non-harvest	GS	Others	0.07	4.70	68.11
Midwest	Non-harvest	RD	GS	0.91	1.12	1.22
South	Non-harvest	GD	GS	0.38	1.72	4.46
South	Non-harvest	GS	GD	0.61	1.97	3.25
South	Non-harvest	GS	Others	0.07	1.97	26.41
West	Non-harvest	GD	GS	1.21	3.22	2.66
West	Non-harvest	GS	GD	2.26	2.72	1.20
West	Non-harvest	GS	Others	0.04	2.72	72.67
West	harvest	GS	GL	0.44	2.10	4.80
West	harvest	GS	Others	0.04	2.10	49.89
West	harvest	GL	GS	0.49	1.17	2.39
Max						72.67
Min						1.20
Average						14.50

11. Temporal and Geospatial Analysis

In this section we provide temporal and geospatial analyses on the impact of a carbon tax under different strategies on consumer price, production quantities and CO2 emissions. To this end, we select the following strategies: 1) a carbon tax policy on all activities emitting CO2, 2) land sparing with a carbon tax on all activities emitting CO2, and 3) innovation in storage technologies with carbon tax on all activities emitting CO2 (i.e., strategies 3, 4 and 7 as listed in Table 1 of the main manuscript). The reason for selecting only these strategies is that they combine a carbon tax with all activities within the supply chain and will highlight the difference between carbon tax, land sparing and innovation in storage technologies. Note that the numerical results presented in section 8 of the Supplementary Material display the total apple production quantities across all production regions, total CO2 emissions due to production, storage and transportation and the average consumer price of apple across seasons and demand locations, for each scenario. Thus, the aim of

this section is to examine changes in apple production in each production region and changes in consumer prices for each consumption location for each season.

Table 11.1 presents the apple production quantities in the five production regions of the study (California, Michigan, New York, Pennsylvania, Virginia and Washington) for the base-case (column 2 i.e., no carbon taxes, production yield assumes its current levels and CO2 emissions due to storage take their current levels), carbon tax on all activities (column 3), land sparing with carbon tax on all activities emitting CO2 (column 4) and innovation in storage technologies with carbon tax on all activities emitting CO2 (column 5). The value in brackets represents the percentage change reduction with respect to the base-case scenario (column 2). We note that the biggest drop in production under a carbon tax occurs in California followed by Virginia, while only decreasing slightly in Michigan, Washington, Pennsylvania and New York. This is consistent with the fact that California is an arid state and requires higher levels of energy use relative to other states (see Section 5.1 for more discussion about CO2 emissions in production).

Table 11.1 Apple production quantities (Million pounds)[a]

	Strategy			
State	Base-case	Carbon tax	Land Sparing	Innovation in Storage Technologies
California	150.37	118.63 (21.1%)	118.63 (21.1%)	122.10 (18.80%)
Michigan	286.86	280.90 (2.08%)	280.90 (2.08%)	283.38 (1.21%)
New York	680.82	676.87 (0.58%)	676.87 (0.58%)	677.54 (0.48%)
Pennsylvania	130.06	128.74 (1.02%)	128.74 (1.02%)	128.92 (0.88%)
Virginia	32.07	30.44 (5.09%)	30.44 (5.09%)	30.85 (3.79%)

Washington	4282.38	4201.68	4201.68	4220.36
		(1.88%)	(1.88%)	(1.44%)

[a] Source: Authors' calibration based on the solution provided by GAMS

Figures 11.1-11.3 display the percentage change in apple production quantities in each region with respect to the base case.

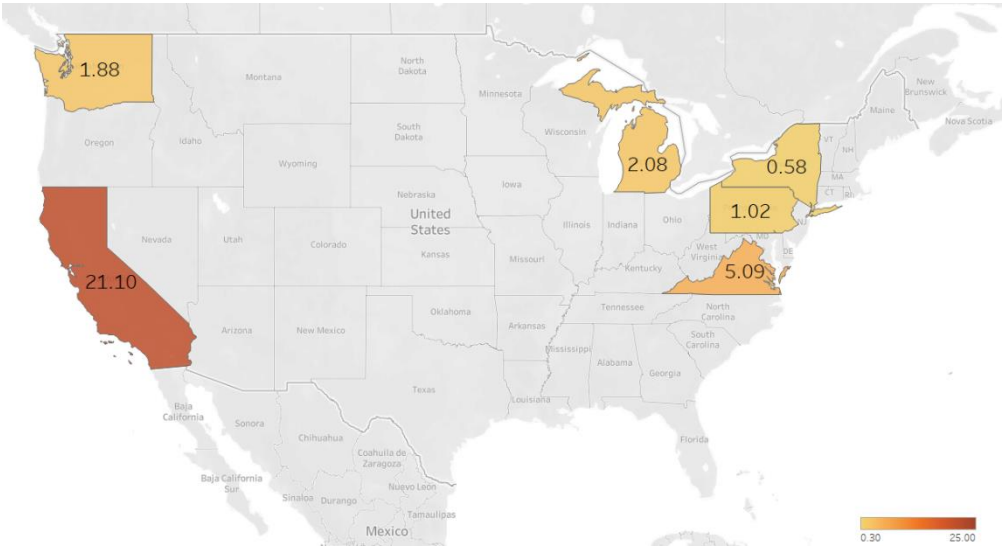

Figure 11.1 Percentage reduction in apple production in different production regions carbon tax on production, storage and transportation activities.

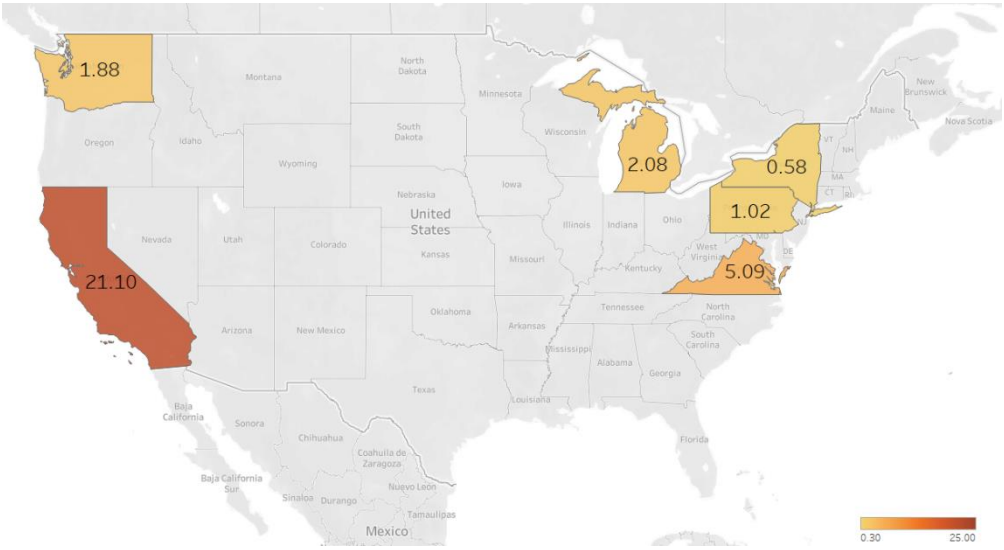

Figure 11.2 Percentage reduction in apple production in different production regions under land sparing strategy and carbon tax on production, storage and transportation activities.

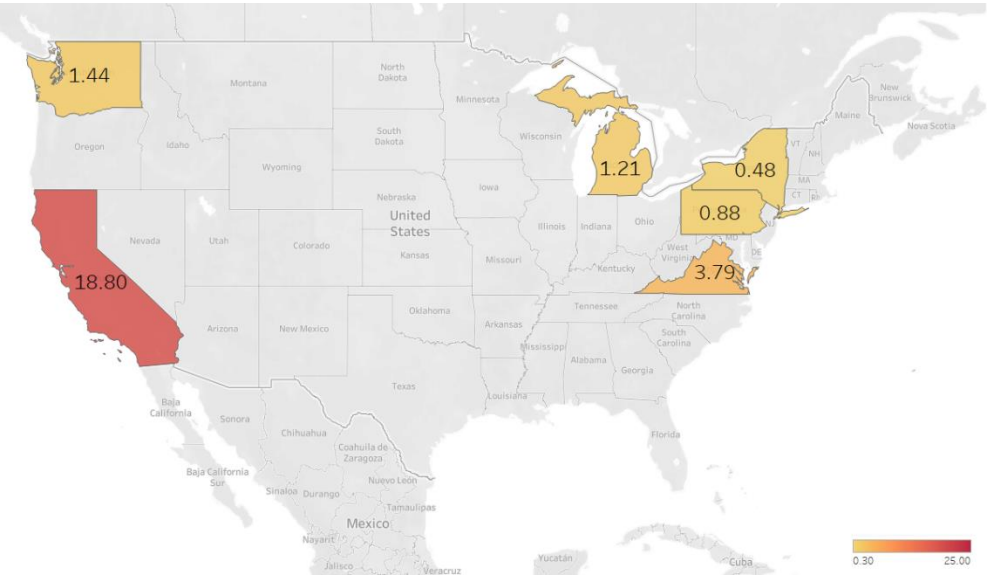

Figure 11.3 Percentage reduction in apple production in different production regions under innovation in storage technologies strategy and carbon tax on production, storage and transportation activities.

Table 11.2 presents consumer prices under different strategies for all consumption locations, both for the harvest and non-harvest seasons. We note that overall, consumer prices (i.e. the average between harvest and non-harvest seasons at the national level) increase under the carbon tax strategy. Nonetheless, this is caused by price increases in the non-harvest season, while prices during the harvest season actually drop under a carbon tax. This makes sense, because a carbon tax disproportionally increases the cost of apples sold in the non-harvest season because they must be placed in long term storage. Furthermore, as suppliers have more incentives to sell apples in the harvest season, the increased supply of apples during this season leads to further reductions in price in the harvest season."

Table 11.2: Consumer price ($/pound) across selected states under each strategy for harvest and non-harvest seasons[a]

	Base-case		Carbon Tax		Land Sparing		Storage Technologies	
State	Non-harvest	Harvest	Non-harvest	Harvest	Non-harvest	Harvest	Non-harvest	Harvest

New Mexico	0.97	0.77	0.99	0.74	0.99	0.74	0.98	0.75
Georgia	1.25	1.23	1.40	1.17	1.40	1.17	1.31	1.20
Maryland	1.25	1.24	1.41	1.18	1.41	1.18	1.32	1.21
Montana	0.96	0.76	0.99	0.74	0.99	0.74	0.97	0.75
Alabama	0.97	0.77	0.99	0.75	0.99	0.75	0.98	0.76
Massachusetts	1.04	1.25	1.17	1.19	1.17	1.19	1.09	1.22
Connecticut	0.96	0.78	0.98	0.75	0.98	0.75	0.97	0.76
Idaho	0.96	0.76	0.98	0.73	0.98	0.73	0.97	0.74
Virginia	0.96	0.78	0.97	0.75	0.97	0.75	0.96	0.76
Ohio	1.55	1.23	1.74	1.16	1.74	1.16	1.63	1.19
North Carolina	1.53	1.49	1.67	1.42	1.67	1.42	1.59	1.45
Wyoming	0.97	0.76	0.99	0.74	0.99	0.74	0.98	0.75
Illinois	1.23	1.22	1.39	1.15	1.39	1.15	1.30	1.18
South Carolina	1.00	1.20	1.08	1.13	1.08	1.13	1.03	1.16
Texas	1.53	1.22	1.66	1.15	1.66	1.15	1.58	1.18
Colorado	1.49	1.16	1.63	1.10	1.63	1.10	1.55	1.12
North Dakota	0.78	0.77	0.80	0.74	0.80	0.74	0.78	0.75
Indiana	1.19	1.18	1.26	1.12	1.26	1.12	1.21	1.14
Mississippi	0.80	0.80	0.86	0.77	0.86	0.77	0.83	0.78
Kansas	1.17	1.17	1.19	1.10	1.19	1.10	1.17	1.13

California	1.20	1.17	1.36	1.11	1.36	1.11	1.27	1.14
Arkansas	0.80	0.79	0.86	0.77	0.86	0.77	0.83	0.78
Nevada	1.16	1.14	1.18	1.08	1.18	1.08	1.16	1.11
Kentucky	1.19	1.18	1.26	1.12	1.26	1.12	1.22	1.15
New Hampshire	1.17	1.17	1.20	1.11	1.20	1.11	1.18	1.14
Tennessee	1.20	1.18	1.26	1.12	1.26	1.12	1.22	1.15
Florida	1.24	1.24	1.39	1.17	1.39	1.17	1.30	1.20
Wisconsin	1.19	0.77	1.26	0.75	1.26	0.75	1.21	0.76
Minnesota	0.78	0.77	0.79	0.74	0.79	0.74	0.78	0.75
Iowa	1.19	1.17	1.25	1.11	1.25	1.11	1.21	1.13
Louisiana	1.18	1.17	1.20	1.11	1.20	1.11	1.18	1.13
New York	1.25	1.24	1.41	1.18	1.41	1.18	1.32	1.21
New Jersey	1.25	1.24	1.41	1.18	1.41	1.18	1.32	1.21
Oklahoma	1.17	1.19	1.20	1.13	1.20	1.13	1.17	1.15
Nebraska	0.78	0.77	0.79	0.74	0.79	0.74	0.78	0.75
Pennsylvania	1.25	1.24	1.41	1.18	1.41	1.18	1.32	1.21
Arizona	1.21	1.18	1.37	1.12	1.37	1.12	1.28	1.15
Oregon	0.77	0.78	0.79	0.75	0.79	0.75	0.78	0.77
Michigan	1.15	1.13	1.17	1.07	1.17	1.07	1.15	1.10
Rhode Island	0.77	0.78	0.79	0.75	0.79	0.75	0.78	0.76
Virginia	1.20	1.20	1.26	1.13	1.26	1.13	1.22	1.16
Washington	1.44	1.42	1.52	1.34	1.52	1.34	1.47	1.37

Utah	0.77	0.76	0.79	0.74	0.79	0.74	0.78	0.75
South Dakota	1.23	1.20	1.39	1.13	1.39	1.13	1.30	1.16
West Virginia	0.79	0.77	0.86	0.74	0.86	0.74	0.82	0.75
District of Columbia	1.53	1.22	1.67	1.16	1.67	1.16	1.58	1.18
Delaware	0.77	0.78	0.79	0.75	0.79	0.75	0.78	0.76

[a] Source: Authors' calibration based on the solution provided by GAMS

References

Blundell, R., R. Pashardes, and G. Weber. 1993. "What do we learn about consumer demand patterns form micro data?", American Economic Review 83: 570-597.

Bureau of Labor Statistics. 2011. Consumer Price Indexes data base. Available at: http://www.bls.gov/.

Canals et al. 2007. "Comparing Domestic versus Imported Apples: A Focus on Energy Use", Environmental Science Pollution Resource 14: 338-344.

Deaton, A., and J. Muellbauer. 1980. "An Almost Ideal Demand System", American Economic Review 70: 312-326.

Dunn, J. W., and L. A. Garafola. 1986. "Changes in Transportation Costs and Interregional Competition in the U. S. Apple Industry", Northeastern Journal of Agricultural and Resource Economics 15: 37-44.

Heckman, J. 1978. "Dummy Endogenous Variables in a Simultaneous Equation System", Econometrica 46: 931-959.

Heien, D., and C. R. Wessells. 1990. "Demand System Estimation with Microdata: A Censored Regression Approach", Journal of Business & Economic Statistics 8: 365-371.

King et al. 2010. "Can Local Food Go Mainstream?" Choices 25(1), Available at: http://www.choicesmagazine.org/magazine/article.php?article=111.

Kroodsma, D. A., and C. B. Field. 2006. "Carbon Sequestration in California Agriculture, 1980-2000". Ecological Application 16: 1975-1985.

Lewandrowski et al. 2004. Economics of Sequestering Carbon in the U.S. Agricultural Sector, U.S. Department of Agriculture Economic Research Service, Technical Bulletin No. 1909.

Nerlove, M. 1956. "Estimates of the Elasticities of Supply of Selected Agricultural Commodities", Journal of Farm Economics 38: 496-508.

New York State Energy Research and Development Authority (UYSERDA). 2008. Energy Investments and CO2 Emissions for Fresh Produce Imported Into New York State Compared to the Same Crops Grown Locally. NYSERDA Report 08-10.

Park et al. 1996. "A Demand System Analysis of Food Commodities by U.S. Households Segmented by Income", American Journal of Agricultural Economics 78: 290-300.

Saunders, C., A. Barber, and G. Taylor. 2006. Food Miles – Comparative Energy/Emissions Performance of New Zealand's Agriculture Industry, Lincoln University, New Zealand. Agribusiness & Economics Research Unit Research Report 285.

Schotzko, R. T., and D. Granastein. 2005. A Brief Look at the Washington Apple Industry: Past and Present. School of Economic Sciences. Washington State University. SES 04-05.

Takayama, T., and G.G. Judge. 1964. "Spatial Equilibrium and Quadratic Programming", Journal of Farm Economics 46: 67-93.

U.S. Department of Agriculture Agricultural Marketing Service (USDA AMS). 2011. Fresh Fruit and Vegetable Shipments, Fruit and Vegetable Program Market News Branch, FVAS-4.

U.S Department of Agriculture Agricultural Marketing Service (USDA AMS). 2011. Agricultural Refrigerated Truck Quarterly. Transportation & Marketing Programs/Transportation Service Division.

U.S. Department of Agriculture Agricultural Marketing Service (USDA AMS). 2011. 1994-96, 1998 Continuing Survey of Food Intakes by Individuals and 1994-96 Diet and Health Knowledge Survey. Available at: http://www.ars.usda.gov/Services/docs.htm?docid=14392.

U.S. Department of Agriculture Forest Service (USDA FS). 1999. Report of the Forest Service, Fiscal Year 1998.

U.S. Department of Agriculture National Agricultural Statistics Service (USDA NASS). 2011. Noncitrus Fruits and Nuts Summary, ISSN: 1948-2698.

U.S. Department of Agriculture National Agricultural Statistics Service (USDA NASS).2008. Agricultural Chemical Usage 2007 Field Crops Summary. Ag Ch 1(08).

U.S. Environmental Protection Agency (US EPA). 2011. Mobile 6.2. Vehicle Emission Modeling Software. Available at: http://www.epa.gov/otaq/m6.htm.

U.S. Environmental Protection Agency (US EPA). 2011. Inventory of U.S. Greenhouse Gas Emissions and Sink: 1990-2009, EPA 430-R-11-005.

Weber, C. L., and H. S. Matthews. 2009. "Food-Miles and the Relative Climate Impacts of Food Choices in the United States", Environmental Science & Technology 42: 3508-3515.

James, S. J. & James, C. The food cold-chain and climate change. Food Research International 43.7, 1944–1956 (2010).

Suamir, I. N., S. A. Tassou, and D. Marriott. "Integration of CO2 refrigeration and trigeneration systems for energy and GHG emission savings in supermarkets." international journal of refrigeration 35.2 (2012): 407-417.

Oro, Eduard, et al. "Energy management and CO2 mitigation using phase change materials (PCM) for thermal energy storage (TES) in cold storage and transport." International journal of refrigeration 42 (2014): 26-35.

Liu, Ming, Wasim Saman, and Frank Bruno. "Development of a novel refrigeration system for refrigerated trucks incorporating phase change material." Applied Energy 92 (2012): 336-342.

Garnett, Tara. "Food refrigeration: What is the contribution to greenhouse gas emissions and how might emissions be reduced." Food Climate Research Network, University of Surrey (2007).

Vermeulen, Sonja J., Bruce M. Campbell, and John SI Ingram. "Climate change and food systems." Annual Review of Environment and Resources 37 (2012).

Lamb, Anthony, et al. "The potential for land sparing to offset greenhouse gas emissions from agriculture." Nature Climate Change 6.5 (2016): 488.

Jaggard, K. W., Qi, A. & Ober, E. S. Possible changes to arable crop yields by 2050. Philos. Trans. R. Soc. B Biol. Sci. 365, 2835–2851 (2010).

Ewert, F., Rounsevell, M. D. A., Reginster, I., Metzger, M. J. & Leemans, R. Future scenarios of European agricultural land use: I. Estimating changes in crop productivity. Agric. Ecosyst. Environ. 107, 101–116 (2005).

Brisson, N. et al. Why are wheat yields stagnating in Europe? A comprehensive data analysis for France. Field Crops Res. 119, 201–212 (2010).

Hall, A. J. & Richards, R. A. Prognosis for genetic improvement of yield potential and water-limited yield of major grain crops. Field Crops Res. 143, 18–33 (2013).

Berry, P. M. & Spink, J. H. A physiological analysis of oilseed rape yields: Past and future. J. Agric. Sci. 144, 381– 392 (2006).

Mackay, I. et al. Reanalyses of the historical series of UK variety trials to quantify the contributions of genetic and environmental factors to trends and variability in yield over time. Theor. Appl. Genet. 122, 225–238 (2011).

Fischer, R. A. & Edmeades, G. O. Breeding and Cereal Yield Progress. Crop Sci. 50, S–85–S–98 (2010).

Nielson HomeScan: https://catalog.data.gov/dataset/nielsen-homescan

USDA Apple Statistics: https://usda.library.cornell.edu/concern/publications/1j92g7448?locale=en

Phillips, Linda. "CSFII analysis of food intake distributions." (2003).

Cornell Cooperative Extension, Lake Ontario Fruit

program, https://lof.cce.cornell.edu/submission.php?id=270

School of Economic Sciences, Washington State University, http://ses.wsu.edu/enterprise_budgets/

Agricultural & resource Economics, University of California Davis,

https://coststudies.ucdavis.edu/en/current/commodity/apples/

BIBLIOGRAPHY

[1] Yossiri Adulyasak, Jean-François Cordeau, and Raf Jans. Formulations and branch-and-cut algorithms for multivehicle production and inventory routing problems. *INFORMS Journal on Computing*, 26(1):103–120, 2013.

[2] Yossiri Adulyasak, Jean-François Cordeau, and Raf Jans. Benders decomposition for production routing under demand uncertainty. *Operations Research*, 63(4):851–867, 2015.

[3] Renzo Akkerman, Poorya Farahani, and Martin Grunow. Quality, safety and sustainability in food distribution: A review of quantitative operations management approaches and challenges. *OR Spectrum*, 32(4):863–904, 2010.

[4] Faisal Alkaabneh, Ali Diabat, and Huaizhu Oliver Gao. Benders decomposition for the inventory vehicle routing problem with perishable products and environmental costs. *Computers & Operations Research*, 113:104751, 2020.

[5] Faisal Alkaabneh, Ali Diabat, and Huaizhu Oliver Gao. Unified framework for efficient, effective and fair resource allocation at food banks-approximate dynamic programming approach. *Omega*, Round 1 major review, 2020.

[6] Faisal Alkaabneh, Jun Lee, Miguel Gómez, and Huaizhu Oliver Gao. A systems approach to carbon policy for fruit supply chains: carbon tax, technology innovation, or land sparing? *Submitted*, 2020.

[7] Feeding America. Feeding america's foods to encourage background.

http://hungerandhealth.feedingamerica.org/wp-content/uploads/legacy/mp/files/tool_and_resources/files/f2e-background-detail.v1.pdf, 2015.

[8] Claudia Archetti, Luca Bertazzi, Gilbert Laporte, and Maria Grazia Speranza. A branch-and-cut algorithm for a vendor-managed inventory-routing problem. *Transportation Science*, 41(3):382–391, 2007.

[9] Claudia Archetti, Natashia Boland, and M. Grazia Speranza. A matheuristic for the multivehicle inventory routing problem. *INFORMS Journal on Computing*, 29(3):377–387, 2017.

[10] Burcu Balcik, Seyed Iravani, and Karen Smilowitz. Multi-vehicle sequential resource allocation for a nonprofit distribution system. *IIE Transactions*, 46(12):1279–1297, 2014.

[11] Hisham S Bamufleh, José María Ponce-Ortega, and Mahmoud M El-Halwagi. Multi-objective optimization of process cogeneration systems with economic, environmental, and social tradeoffs. *Clean Technologies and Environmental Policy*, 15(1):185–197, 2013.

[12] Chantelle Bazerghi, Fiona H McKay, and Matthew Dunn. The role of food banks in addressing food insecurity: A systematic review. *Journal of community health*, 41(4):732–740, 2016.

[13] Tolga Bektaş and Gilbert Laporte. The pollution-routing problem. *Transportation Research Part B: Methodological*, 45(8):1232–1250, 2011.

[14] Walter J. Bell, Louis M. Dalberto, Marshall L. Fisher, Arnold J. Greenfield, Ramchandran Jaikumar, Pradeep Kedia, Robert G. Mack, and Paul J. Prutzman. Improving the distribution of industrial gases with an on-line

computerized routing and scheduling optimizer. *INFORMS Journal on Applied Analytics*, 13(6):4–23, 1983.

[15] Valentin Bellassen and Sebastiaan Luyssaert. Carbon sequestration: Managing forests in uncertain times. *Nature*, 506(7487):153–155, 2014.

[16] Jacques F. Benders. Partitioning procedures for solving mixed-variables programming problems. *Numerische Mathematik*, 4(1):238–252, 1962.

[17] Seth A Berkowitz, Travis P Baggett, Deborah J Wexler, Karen W Huskey, and Christina C Wee. Food insecurity and metabolic control among u.s. adults with diabetes. *Diabetes Care*, 36(10):3093–3099, 2013.

[18] PM Berry and JH Spink. A physiological analysis of oilseed rape yields: past and future. *The Journal of Agricultural Science*, 144(5):381–392, 2006.

[19] Ali Bozorgi-Amiri, MS Jabalameli, and SMJ Mirzapour Al-e Hashem. A multi-objective robust stochastic programming model for disaster relief logistics under uncertainty. *OR Spectrum*, 35(4):905–933, 2013.

[20] Nadine Brisson, Philippe Gate, David Gouache, Gilles Charmet, François-Xavier Oury, and Frédéric Huard. Why are wheat yields stagnating in europe? a comprehensive data analysis for france. *Field Crops Research*, 119(1):201–212, 2010.

[21] Elizabeth Campbell, Karen Webb, Michelle Ross, Patricia Crawford, Heather Hudson, and Ken Hecht. *Nutrition-focused food banking*. Institute of Medicine of the National Academies, Washington, DC, 2015.

[22] Elizabeth Catherine Campbell, Michelle Ross, and Karen L Webb. Improving the nutritional quality of emergency food: A study of food bank

organizational culture, capacity, and practices. *Journal of Hunger & Environmental Nutrition*, 8(3):261–280, 2013.

[23] Annika Carlsson-Kanyama and Mireille Faist. *Energy use in the food sector: a data survey*. Swedish Environmental Protection Agency Stockolm, Sweden, 2000.

[24] Xiuli Chao, Xiting Gong, Cong Shi, and Huanan Zhang. Approximation algorithms for perishable inventory systems. *Operations Research*, 63(3):585–601, 2015.

[25] Xiuli Chao and Sean X Zhou. Optimal policy for a multiechelon inventory system with batch ordering and fixed replenishment intervals. *Operations Research*, 57(2):377–390, 2009.

[26] Marielle Christiansen. Decomposition of a combined inventory and time constrained ship routing problem. *Transportation Science*, 33(1):3–16, 1999.

[27] Leandro C. Coelho, Jean-François Cordeau, and Gilbert Laporte. Thirty years of inventory routing. *Transportation Science*, 48(1):1–19, 2013.

[28] Leandro C. Coelho and Gilbert Laporte. A branch-and-cut algorithm for the multi-product multi-vehicle inventory-routing problem. *International Journal of Production Research*, 51(23-24):7156–7169, 2013.

[29] Leandro C. Coelho and Gilbert Laporte. The exact solution of several classes of inventory-routing problems. *Computers & Operations Research*, 40(2):558–565, 2013.

[30] Leandro C. Coelho and Gilbert Laporte. Optimal joint replenishment, delivery and inventory management policies for perishable products. *Computers & Operations Research*, 47:42–52, 2014.

[31] A Coleman-Jensen and C Gregory. Definitions of food security. united states department of agriculture economic research service. web, 2014.

[32] Ivan Contreras, Jean-François Cordeau, and Gilbert Laporte. Benders decomposition for large-scale uncapacitated hub location. *Operations Research*, 59(6):1477–1490, 2011.

[33] John T Cook and Ana Paula Poblacion. Estimating the health-related costs of food insecurity and hunger. *The Nourishing Effect: Ending Hunger, Improving Health, Reducing Inequality (2016 Hunger Report). Washington, DC: Bread for the World Institute*, 2016.

[34] Jean-François Cordeau, François Soumis, and Jacques Desrosiers. Simultaneous assignment of locomotives and cars to passenger trains. *Operations Research*, 49(4):531–548, 2001.

[35] Jean-François Côté, Mauro Dell'Amico, and Manuel Iori. Combinatorial Benders' cuts for the Strip Packing Problem. *Operations Research*, 62(3):643–661, 2014.

[36] D Coulomb. Refrigeration and cold chain serving the global food industry and creating a better future: two key iir challenges for improved health and environment. *Trends in food science & technology*, 19(8):413–417, 2008.

[37] Ana L. Custódio and Rui C. Oliveira. Redesigning distribution operations: a case study on integrating inventory management and vehicle routes design. *International Journal of Logistics: Research and Applications*, 9(2):169–187, 2006.

[38] Beth Osborne Daponte, Gordon H Lewis, Seth Sanders, and Lowell Tay-

lor. Food pantry use among low-income households in allegheny county, pennsylvania. *Journal of Nutrition Education*, 30(1):50–57, 1998.

[39] Maryam Darvish, Claudia Archetti, and Leandro C. Coelho. Minimizing emissions in integrated distribution problems. Technical Report CIRRELT-2017-41, Interuniversity Research Centre on Enterprise Networks, Logistics, and Transportation, July 2017.

[40] Lauren B Davis, Irem Sengul, Julie S Ivy, Luther G Brock III, and Lastella Miles. Scheduling food bank collections and deliveries to ensure food safety and improve access. *Socio-Economic Planning Sciences*, 48(3):175–188, 2014.

[41] Emrah Demir, Tolga Bektaş, and Gilbert Laporte. An adaptive large neighborhood search heuristic for the pollution-routing problem. *European Journal of Operational Research*, 223(2):346–359, 2012.

[42] Guy Desaulniers, Jørgen G Rakke, and Leandro C. Coelho. A branch-price-and-cut algorithm for the inventory-routing problem. *Transportation Science*, 50(3):1060–1076, 2015.

[43] Gopalakrishnan Easwaran and Halit Üster. Tabu Search and Benders Decomposition Approaches for a Capacitated Closed-Loop Supply Chain Network Design Problem. *Transportation Science*, 43(3):301–320, 2009.

[44] Ohad Eisenhandler and Michal Tzur. The humanitarian pickup and distribution problem. *Operations Research*, 67(1):10–32, 2018.

[45] F Ewert, MDA Rounsevell, I Reginster, MJ Metzger, and R Leemans. Future scenarios of european agricultural land use: I. estimating changes

in crop productivity. *Agriculture, Ecosystems & Environment*, 107(2-3):101–116, 2005.

[46] Thomas A. Feo and Mauricio G.C. Resende. A probabilistic heuristic for a computationally difficult set covering problem. *Operations Research Letters*, 8(2):67–71, 1989.

[47] Paola Festa and Mauricio G.C. Resende. GRASP: basic components and enhancements. *Telecommunication Systems*, 46(3):253–271, 2011.

[48] Sefakor Fianu and Lauren B Davis. A markov decision process model for equitable distribution of supplies under uncertainty. *European Journal of Operational Research*, 264(3):1101–1115, 2018.

[49] RA Fischer and Gregory O Edmeades. Breeding and cereal yield progress. 2010.

[50] Guangtao Fu, Zoran Kapelan, and Patrick Reed. Reducing the complexity of multiobjective water distribution system optimization through global sensitivity analysis. *Journal of Water Resources Planning and Management*, 138(3):196–207, 2012.

[51] Tara Garnett. Food refrigeration: What is the contribution to greenhouse gas emissions and how might emissions be reduced. *Food Climate Research Network, University of Surrey*, 2007.

[52] Tara Garnett, Michael C Appleby, Andrew Balmford, Ian J Bateman, Tim G Benton, Phil Bloomer, Barbara Burlingame, Marian Dawkins, Liam Dolan, David Fraser, et al. Sustainable intensification in agriculture: premises and policies. *Science*, 341(6141):33–34, 2013.

[53] Miguel I Gómez, Jun Lee, Julia Koerner, et al. Do retail coffee prices rise faster than they fall? asymmetric price transmission in france, germany and the united states. *Journal of International Agricultural Trade and Development*, 6(2):175–196, 2010.

[54] Miguel I Gómez, Edward W McLaughlin, and Kristen S Park. 3 apple case studies in the syracuse msa. *Growing Local: Case Studies on Local Food Supply Chains*, page 35, 2014.

[55] David Hadka and Patrick Reed. Borg: An auto-adaptive many-objective evolutionary computing framework. *Evolutionary computation*, 21(2):231–259, 2013.

[56] Antonio J Hall and Richard A Richards. Prognosis for genetic improvement of yield potential and water-limited yield of major grain crops. *Field Crops Research*, 143:18–33, 2013.

[57] Ken Hambleton. *Conquering Complexity: Lessons for defence systems acquisition*. The Stationery Office, 2005.

[58] Becky Handforth, Monique Hennink, and Marlene B Schwartz. A qualitative study of nutrition-based initiatives at selected food banks in the feeding america network. *Journal of the Academy of Nutrition and Dietetics*, 113(3):411–415, 2013.

[59] Brent R Heard and Shelie A Miller. Critical research needed to examine the environmental impacts of expanded refrigeration on the food system. *Environmental science & technology*, 50(22):12060–12071, 2016.

[60] Vera Hemmelmayr, Karl F. Doerner, Richard F. Hartl, and Martin W.P. Savelsbergh. Vendor managed inventory for environments with stochas-

tic product usage. *European Journal of Operational Research*, 202(3):686–695, 2010.

[61] Mario Herrero, Philip K Thornton, Pierre Gerber, and Robin S Reid. Livestock, livelihoods and the environment: understanding the trade-offs. *Current Opinion in Environmental Sustainability*, 1(2):111–120, 2009.

[62] Helen Hicks. Balancing nature and agriculture, 2012.

[63] John N. Hooker. Planning and scheduling by logic-based benders decomposition. *Operations Research*, 55(3):588–602, 2007.

[64] Leo Horrigan, Robert S Lawrence, and Polly Walker. How sustainable agriculture can address the environmental and human health harms of industrial agriculture. *Environmental health perspectives*, 110(5):445–456, 2002.

[65] Patricia Houlihan. How food banks came to love the free market. *Chicago Booth Magazine*, pages 34–39, 2006.

[66] Y. Anny Huang, Christopher L. Weber, and H. Scott Matthews. Categorization of scope 3 emissions for streamlined enterprise carbon footprinting. *Environmental Science & Technology*, 43(22):8509–8515, 2009.

[67] Keith W Jaggard, Aiming Qi, and Eric S Ober. Possible changes to arable crop yields by 2050. *Philosophical Transactions of the Royal Society B: Biological Sciences*, 365(1554):2835–2851, 2010.

[68] SJ James and C James. The food cold-chain and climate change. *Food Research International*, 43(7):1944–1956, 2010.

[69] Robert Jandl, Marcus Lindner, Lars Vesterdal, Bram Bauwens, Rainer Baritz, Frank Hagedorn, Dale W Johnson, Kari Minkkinen, and Kenneth A Byrne. How strongly can forest management influence soil carbon sequestration? *Geoderma*, 137(3-4):253–268, 2007.

[70] Leah R Kicinski. Characteristics of short and long-term food pantry users. *Michigan Sociological Review*, 26, 2012.

[71] Sharon I Kirkpatrick and Valerie Tarasuk. Assessing the relevance of neighbourhood characteristics to the household food security of low-income toronto families. *Public health nutrition*, 13(7):1139–1148, 2010.

[72] Anthony Lamb, Rhys Green, Ian Bateman, Mark Broadmeadow, Toby Bruce, Jennifer Burney, Pete Carey, David Chadwick, Ellie Crane, Rob Field, et al. The potential for land sparing to offset greenhouse gas emissions from agriculture. *Nature Climate Change*, 6(5):488–492, 2016.

[73] Tung Le, Ali Diabat, Jean-Philippe Richard, and Yuehwern Yih. A column generation-based heuristic algorithm for an inventory routing problem with perishable goods. *Optimization Letters*, 7(7):1481–1502, 2013.

[74] Deishin Lee, Erkut Sönmez, Miguel I Gómez, and Xiaoli Fan. Combining two wrongs to make two rights: Mitigating food insecurity and food waste through gleaning operations. *Food policy*, 68:40–52, 2017.

[75] Hau Leung Lee and W. Seungjin. The whose, where and how of inventory control design. *Supply Chain Management Review*, 12(8):22–29, 2008.

[76] Fang-Fang Li and Jun Qiu. Multi-objective optimization for integrated hydro–photovoltaic power system. *Applied Energy*, 167:377–384, 2016.

[77] Robert W Lien, Seyed MR Iravani, and Karen R Smilowitz. Sequential resource allocation for nonprofit operations. *Operations Research*, 62(2):301–317, 2014.

[78] Ming Liu, Wasim Saman, and Frank Bruno. Development of a novel refrigeration system for refrigerated trucks incorporating phase change material. *Applied Energy*, 92:336–342, 2012.

[79] Rachel Loopstra and Valerie Tarasuk. The relationship between food banks and household food insecurity among low-income toronto families. *Canadian Public Policy*, 38(4):497–514, 2012.

[80] Brian J Lunday and Matthew J Robbins. Collaboratively-developed vaccine pricing and stable profit sharing mechanisms. *Omega*, 84:102–113, 2019.

[81] I Mackay, A Horwell, J Garner, J White, J McKee, and H Philpott. Reanalyses of the historical series of uk variety trials to quantify the contributions of genetic and environmental factors to trends and variability in yield over time. *Theoretical and Applied Genetics*, 122(1):225–238, 2011.

[82] Thomas L. Magnanti and Richard T. Wong. Accelerating Benders Decomposition: Algorithmic Enhancement and Model Selection Criteria. *Operations Research*, 29(3):464–484, 1981.

[83] Katie S Martin, Michele Wolff, Kate Callahan, and Marlene B Schwartz. Supporting wellness at pantries: Development of a nutrition stoplight system for food banks and food pantries. *Journal of the Academy of Nutrition and Dietetics*, 119(4):559, 2019.

[84] Alan Matthews. Greening agricultural payments in the eu's common agricultural policy. *Bio-based and Applied Economics*, 2(1):1–27, 2013.

[85] Matthew S Maxwell, Mateo Restrepo, Shane G Henderson, and Huseyin Topaloglu. Approximate dynamic programming for ambulance redeployment. *INFORMS Journal on Computing*, 22(2):266–281, 2010.

[86] Fiona H McKay and Matthew Dunn. Food security among asylum seekers in melbourne. *Australian and New Zealand journal of public health*, 39(4):344–349, 2015.

[87] Bert Metz, Ogunlade R Davidson, Peter R Bosch, Rutu Dave, and Leo A Meyer. Contribution of working group iii to the fourth assessment report of the intergovernmental panel on climate change. 2007.

[88] Alan S. Minkoff. A markov decision model and decomposition heuristic for dynamic vehicle dispatching. *Operations Research*, 41(1):77–90, 1993.

[89] MOVES. *Motor Vehicle Emissions Simulator*. United States Environmental Protection Agency, 2018. `https://www.epa.gov/moves/latest-version-motor-vehicle-emission-simulator-moves`.

[90] Anna Nagurney, Amir H Masoumi, and Min Yu. Supply chain network operations management of a blood banking system with cost and risk minimization. *Computational Management Science*, 9(2):205–231, 2012.

[91] Amir Ali Nasrollahzadeh, Amin Khademi, and Maria E Mayorga. Real-time ambulance dispatching and relocation. *Manufacturing & Service Operations Management*, 20(3):467–480, 2018.

[92] William D Nordhaus. *A question of balance: Weighing the options on global warming policies*. Yale University Press, 2014.

[93] Irem Sengul Orgut, Julie Ivy, Reha Uzsoy, and James R Wilson. Modeling for the equitable and effective distribution of donated food under capacity constraints. *IIE Transactions*, 48(3):252–266, 2016.

[94] Irem Sengul Orgut, Julie S Ivy, Reha Uzsoy, and Charlie Hale. Robust optimization approaches for the equitable and effective distribution of donated food. *European Journal of Operational Research*, 269(2):516–531, 2018.

[95] Eduard Oró, Laia Miró, Mohammed M Farid, Viktoria Martin, and Luisa F Cabeza. Energy management and co2 mitigation using phase change materials (pcm) for thermal energy storage (tes) in cold storage and transport. *International journal of refrigeration*, 42:26–35, 2014.

[96] Vildan Özkır and Hüseyin Başlıgil. Multi-objective optimization of closed-loop supply chains in uncertain environment. *Journal of Cleaner Production*, 41:114–125, 2013.

[97] Noel Pérez-Rodríguez and José Holguín-Veras. Inventory-allocation distribution models for postdisaster humanitarian logistics with explicit consideration of deprivation costs. *Transportation Science*, 50(4):1261–1285, 2015.

[98] Tobias Plieninger, Christian Schleyer, Harald Schaich, Bettina Ohnesorge, Holger Gerdes, Mónica Hernández-Morcillo, and Claudia Bieling. Mainstreaming ecosystem services through reformed european agricultural policies. *Conservation Letters*, 5(4):281–288, 2012.

[99] Richard Price, Simeon Thornton, and Stephen Nelson. The Social Cost of Carbon and the Shadow Price of Carbon: what they are, and how to use them in economic appraisal in the UK. Technical report, Economics

Group, Department for Environment, Food, and Rural Affairs, London, 2007.

[100] Wendy W. Qu, James H Bookbinder, and Paul Iyogun. An integrated inventory–transportation system with modified periodic policy for multiple products. *European Journal of Operational Research*, 115(2):254–269, 1999.

[101] Ragheb Rahmaniani, Teodor Gabriel Crainic, Michel Gendreau, and Walter Rei. The Benders Decomposition Algorithm: A Literature Review. *European Journal of Operational Research*, 259(3):801–817, 2017.

[102] Andre MN Renzaho and David Mellor. Food security measurement in cultural pluralism: Missing the point or conceptual misunderstanding? *Nutrition*, 26(1):1–9, 2010.

[103] Christophe Rizet, Michael Browne, Eric Cornelis, and Jacques Leonardi. Assessing carbon footprint and energy efficiency in competing supply chains: review–case studies and benchmarking. *Transportation Research Part D: Transport and Environment*, 17(4):293–300, 2012.

[104] Matthew J Robbins, Phillip R Jenkins, Nathaniel D Bastian, and Brian J Lunday. Approximate dynamic programming for the aeromedical evacuation dispatching problem: Value function approximation utilizing multiple level aggregation. *Omega*, 91:102020, 2020.

[105] Michelle Ross, Elizabeth Catherine Campbell, and Karen L Webb. Recent trends in the nutritional quality of food banks' food and beverage inventory: case studies of six california food banks. *Journal of hunger & environmental nutrition*, 8(3):294–309, 2013.

[106] Beate Rottkemper, Kathrin Fischer, and Alexander Blecken. A transshipment model for distribution and inventory relocation under uncertainty in humanitarian operations. *Socio-Economic Planning Sciences*, 46(1):98–109, 2012.

[107] Tjendera Santoso, Shabbir Ahmed, Marc Goetschalckx, and Alexander Shapiro. A stochastic programming approach for supply chain network design under uncertainty. *European Journal of Operational Research*, 167(1):96–115, 2005.

[108] Emanuel S Savas. On equity in providing public services. *Management Science*, 24(8):800–808, 1978.

[109] Abdelkader Sbihi and Richard W. Eglese. The relationship between vehicle routing and scheduling and green logistics – a literature survey. Technical report, The Department of Management Science, Lancaster University Management School, 2007.

[110] Kellie Schneider and Sarah G Nurre. A multi-criteria vehicle routing approach to improve the compliance audit schedule for food banks. *Omega*, 84:127–140, 2019.

[111] Kristine Siefert, Colleen M Heflin, Mary E Corcoran, and David R Williams. Food insufficiency and physical and mental health in a longitudinal survey of welfare recipients. *Journal of health and social behavior*, 45(2):171–186, 2004.

[112] Thiago AO Silva and Mauricio C de Souza. Surgical scheduling under uncertainty by approximate dynamic programming. *Omega*, page 102066, 2019.

[113] Pete Smith, Helmut Haberl, Alexander Popp, Karl-heinz Erb, Christian Lauk, Richard Harper, Francesco N Tubiello, Alexandre Siqueira Pinto, Mostafa Jafari, Saran Sohi, et al. How much land-based greenhouse gas mitigation can be achieved without compromising food security and environmental goals? *Global Change Biology*, 19(8):2285–2302, 2013.

[114] Senay Solak, Christina Scherrer, and Ahmed Ghoniem. The stop-and-drop problem in nonprofit food distribution networks. *Annals of Operations Research*, 221(1):407–426, 2014.

[115] Oğuz Solyalı and Haldun Süral. A branch-and-cut algorithm using a strong formulation and an a priori tour-based heuristic for an inventory-routing problem. *Transportation Science*, 45(3):335–345, 2011.

[116] Mehmet Soysal, Jacqueline M. Bloemhof-Ruwaard, Rene Haijema, and Jack G.A.J. van der Vorst. Modeling a green inventory routing problem for perishable products with horizontal collaboration. *Computers & Operations Research*, 89:168–182, 2018.

[117] Maria Grazia Speranza and Walter Ukovich. Minimizing transportation and inventory costs for several products on a single link. *Operations Research*, 42(5):879–894, 1994.

[118] Commodity Procurement Staff. United states department of agriculture agricultural marketing service. 2016.

[119] Linda Jacobs Starkey, Harriet V Kuhnlein, and Katherine Gray-Donald. Food bank users: sociodemographic and nutritional characteristics. *Cmaj*, 158(9):1143–1149, 1998.

[120] Henning Steinfeld, Pierre Gerber, TD Wassenaar, Vincent Castel, Mauricio Rosales, Mauricio Rosales, and Cees de Haan. *Livestock's long shadow: environmental issues and options*. Food & Agriculture Org., 2006.

[121] Franziska Stoessel, Ronnie Juraske, Stephan Pfister, and Stefanie Hellweg. Life cycle inventory and carbon and water foodprint of fruits and vegetables: application to a swiss retailer. *Environmental science & technology*, 46(6):3253–3262, 2012.

[122] IN Suamir, SA Tassou, and D Marriott. Integration of co2 refrigeration and trigeneration systems for energy and ghg emission savings in supermarkets. *International journal of refrigeration*, 35(2):407–417, 2012.

[123] Takashi Takayama and George G Judge. Spatial equilibrium and quadratic programming. *American Journal of Agricultural Economics*, 46(1):67–93, 1964.

[124] S Tofighi, S Ali Torabi, and S Afshin Mansouri. Humanitarian logistics network design under mixed uncertainty. *European Journal of Operational Research*, 250(1):239–250, 2016.

[125] HHS USDA. 2015—2020 dietary guidelines for americans. `https://health.gov/dietaryguidelines/2015/resources/2015-2020_Dietary_Guidelines.pdf`, 2015.

[126] Sonja J. Vermeulen, Bruce M. Campbell, and John S.I. Ingram. Climate change and food systems. *Annual Review of Environment and Resources*, 37(1):195, 2012.

[127] Fan Wang, Xiaofan Lai, and Ning Shi. A multi-objective optimization for

green supply chain network design. *Decision support systems*, 51(2):262–269, 2011.

[128] Karen L Webb. Introduction–food banks of the future: organizations dedicated to improving food security and protecting the health of the people they serve. *Journal of Hunger & Environmental Nutrition*, 8(3):257–260, 2013.

[129] Paul Wentges. Accelerating Benders' decomposition for the capacitated facility location problem. *Mathematical Methods of Operations Research*, 44(2):267–290, 1996.

[130] Henk Westhoek, Jan Peter Lesschen, Trudy Rood, Susanne Wagner, Alessandra De Marco, Donal Murphy-Bokern, Adrian Leip, Hans van Grinsven, Mark A Sutton, and Oene Oenema. Food choices, health and environment: effects of cutting europe's meat and dairy intake. *Global Environmental Change*, 26:196–205, 2014.

[131] Seunghee Wie and Kathryn Giebler. Nonfood-related challenges and resources affect functioning of food banks. *Journal of foodservice business research*, 16(1):76–84, 2013.

[132] Stefan Wirsenius, Fredrik Hedenus, and Kristina Mohlin. Greenhouse gas taxes on animal food products: rationale, tax scheme and climate mitigation effects. *Climatic change*, 108(1-2):159–184, 2011.

[133] Tang Xifeng, Zhang Ji, and Xu Peng. A multi-objective optimization model for sustainable logistics facility location. *Transportation Research Part D: Transport and Environment*, 22:45–48, 2013.

[134] Wei-Chang Yeh and Mei-Chi Chuang. Using multi-objective genetic algo-

rithm for partner selection in green supply chain problems. *Expert Systems with applications*, 38(4):4244–4253, 2011.

[135] Min Yu and Anna Nagurney. Competitive food supply chain networks with application to fresh produce. *European Journal of Operational Research*, 224(2):273–282, 2013.

[136] Huanan Zhang, Cong Shi, and Xiuli Chao. Approximation algorithms for perishable inventory systems with setup costs. *Operations Research*, 64(2):432–440, 2016.